Copy 93

~~RESTRICTED~~

RM A50D04

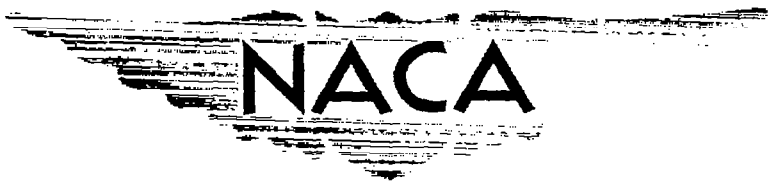

RESEARCH MEMORANDUM

EFFECTS OF LEADING-EDGE RADIUS AND MAXIMUM THICKNESS-CHORD RATIO ON THE VARIATION WITH MACH NUMBER OF THE AERODYNAMIC CHARACTERISTICS OF SEVERAL THIN NACA AIRFOIL SECTIONS

By Robert E. Berggren and Donald J. Graham

Ames Aeronautical Laboratory
Moffett Field, Calif.

NATIONAL ADVISORY COMMITTEE FOR AERONAUTICS

WASHINGTON
July 3, 1950

~~RESTRICTED~~

National Aeronautics and
Space Administration

Langley Research Center
Hampton, Virginia
23665

NASA

Reply to Attn of 139A

JUN 1 6 1983

TO: Distribution

FROM: 180A/Security Classification Officer

SUBJECT: Authority to Declassify NACA/NASA Documents Dated Prior to January 1, 1960

Effective this date, all material (informal, correspondence) classified by this Center prior to January 1, 1960, is declassified. This action does not include material derivatively classified at the Center upon instructions from other Agencies.

Immediate re-marking is not required; however, until material is re-marked by lining through the classification and annotating with the following statement, it must continue to be protected as if classified:

> "Declassified by authority of LaRC Security Classification Officer (SCO) letter dated June 16, 1983," and the signature of person performing the re-marking.

If re-marking a large amount of material is desirable, but unduly burdensome, custodians may follow the instructions contained in NHB 1640.4, subpart F, section 1203.604, paragraph (h).

This declassification action complements earlier actions by the National Archives and Records Service (NARS) and by the NASA Security Classification Officer (SCO). In Declassification Review Program 807008, NARS declassified the Center's "Research Authorization" files, which contain reports, Research Authorizations, correspondence, photographs, and other documentation. Earlier, in a 1971 letter, the NASA SCO declassified all NACA/NASA formal series documents with the exception of the following reports, which must remain classified:

Document No.	First Author
E-51A30	Nagey
E-53G20	Francisco
E-53G21	Johnson
E-53K18	Spooner
SL-54J21a	Westphal
E-55C16	Fox
E-56H23a	Himmel

NATIONAL ADVISORY COMMITTEE FOR AERONAUTICS

RESEARCH MEMORANDUM

EFFECTS OF LEADING-EDGE RADIUS AND MAXIMUM THICKNESS-CHORD RATIO ON THE VARIATION WITH MACH NUMBER OF THE AERODYNAMIC CHARACTERISTICS OF SEVERAL THIN NACA AIRFOIL SECTIONS

By Robert E. Berggren and Donald J. Graham

SUMMARY

A wind-tunnel investigation has been made to determine the effects of leading-edge radius and maximum thickness-chord ratio on the variation with Mach number of the aerodynamic characteristics of several thin symmetrical NACA 4-digit-series airfoil sections. The Mach number range of the investigation was from 0.3 to approximately 0.9 and the corresponding Reynolds number range from approximately 1×10^6 to 2×10^6.

The variations with Mach number of the lift, drag, and pitching moment for a 4-percent-chord-thick airfoil section are not significantly affected by a change of leading-edge radius from 0.18 to 0.53 percent of the chord. A similar conclusion can be drawn for a leading-edge-radius variation from 0.10- to 0.40-percent chord on a 6-percent-chord-thick section.

Progressive improvement of the variation of lift-curve slope with Mach number, the lift and drag-divergence characteristics, and the maximum section lift characteristics at Mach numbers above 0.6 results from reduction of the maximum thickness-chord ratio from 10 to 4 percent. Section pitching-moment characteristics are not greatly affected by variation of the maximum thickness-chord ratio.

INTRODUCTION

To investigate the influence of airfoil leading-edge radius on the variation with Mach number of the aerodynamic characteristics of thin

airfoil sections, a series of airfoil tests was conducted in the Ames 1- by 3-1/2-foot high-speed wind tunnel. The results of the investigation for a thickness-chord ratio of 10 percent have been reported in reference 1. The results for thickness-chord ratios of 6 and 4 percent are reported in the present paper. The basic thickness form of the airfoils investigated was the NACA 4-digit series (see reference 2) with maximum thickness at 40 percent of the airfoil chord.

In addition to the leading-edge-radius study, the investigation permitted further analysis of the effects of thickness-chord-ratio variation on the characteristics of airfoil sections at high subsonic Mach numbers. This analysis is also contained in the present report.

NOTATION

a_o section lift-curve slope, per degree

c airfoil chord, feet

c_d section drag coefficient

c_l section lift coefficient

$c_{l_{max}}$ maximum section lift coefficient

$c_{m_{c/4}}$ section pitching-moment coefficient about the quarter-chord point

M free-stream Mach number

M_d Mach number for drag divergence, defined as the Mach number at which $\left(\frac{dc_d}{dM}\right)_{\alpha_o = \text{constant}} = 0.1$

M_l Mach number for lift divergence, defined as the Mach number at which $\left(\frac{d^2c_l}{dM^2}\right)_{\alpha_o = \text{constant}} = 0$

V free-stream velocity, feet per second

v local velocity, feet per second

Δv_a increment in local velocity corresponding to additional type of load distribution, feet per second

x distance along chord from leading edge, fraction of chord

y distance perpendicular to chord, fraction of chord

α_o section angle of attack, degrees

DESCRIPTION OF AIRFOILS

The airfoil sections of the present study are:

NACA airfoil designation		Leading-edge radius (percent chord)
0004 – 1.10	40/1.575	0.18
0004 – 3.30	40/1.575	.53
0006 – 1.10	40/1.575	.40
0006 – .70	40/1.575	.25
0006 – .27	40/1.575	.10
0008 – 1.10	40/1.575	.70
0010 – 1.10	40/1.575	1.10

The first digit of the airfoil designation indicates the camber in percent of the chord; the second, the position of the camber in tenths of the chord from the leading edge; and the third and fourth, the maximum thickness in percent of the chord. The decimal number following the dash is the leading-edge-radius index; the leading-edge radius as a fraction of the airfoil chord is given by the product of the radius index and the square of the thickness-chord ratio. A radius index of 1.10 is standard for the NACA 4-digit-series airfoil sections. The two digits immediately preceding the slant represent the position of maximum thickness in percent of the chord from the leading edge. The last decimal number is the trailing-edge-angle index, the angle being twice the arc tangent of the product of the angle index and the thickness-chord ratio.

The coordinates of the airfoils investigated are given in tables I to VII. The profiles are illustrated in figure 1 and the theoretical low-speed pressure distributions, determined by the method of reference 3, in figure 2.

APPARATUS AND TESTS

The tests were made in the Ames 1- by 3-1/2-foot high-speed wind tunnel, a low-turbulence two-dimensional-flow wind tunnel.

The airfoil models, constructed of aluminum alloy, were of 6-inch chord and completely spanned the 1-foot dimension of the wind-tunnel test section. End leakage was prevented by means of contoured sponge-rubber gaskets compressed between the model ends and the tunnel walls.

Measurements of lift, drag, and pitching moment were made at Mach numbers from 0.3 to as high as 0.9 for each of the airfoils at angles of attack increasing by 1° or 2° increments from -2° to a maximum of 12°. This range of angles of attack was sufficient to encompass the lift stall up to Mach numbers of the order of 0.8. The Reynolds number of the tests ranged from approximately 1×10^6 at the minimum Mach number to approximately 2×10^6 at the highest Mach numbers.

Lift and pitching moments were evaluated by a method similar to that described in reference 4 from integrations of the pressure reactions on the tunnel walls produced by the airfoil models. Drag measurements were made by means of wake surveys using a rake of total-head tubes.

RESULTS AND DISCUSSION

Section lift, drag, and quarter-chord pitching-moment coefficients for the airfoil sections investigated are presented as functions of Mach number at constant angles of attack in figures 3, 4, and 5, respectively. The characteristics for the 10-percent-thickness-chord ratio are taken from reference 2. The angles of attack indicated in the figures represent but nominal values, being subject to a maximum experimental error in setting of 0.15°. The characteristics have been corrected for tunnel-wall interference by the methods of reference 5. Dashed lines have been used in the figures to indicate the region of possible influence of wind-tunnel choking effects on the results.

Leading-Edge Radius

Within the limits of the present investigation, the leading-edge radius does not significantly influence the variation with Mach number of the aerodynamic characteristics of 4- and 6-percent-chord-thick airfoil sections. A small superiority in the maximum section lift coefficient at Mach numbers from 0.4 to 0.75 is indicated in figures 6 and 7 for the 4-percent-thick airfoil with the very large nose radius. For the

6-percent-thick sections no important differences exist. No important effect of nose radius change on the lift-curve-slope variation with Mach number is indicated in figure 8 for either thickness-chord ratio. The minimum drag coefficient is noted from a study of figure 9 (illustrating the variation of section drag coefficient with section lift coefficient at constant Mach number) to be lower at all Mach numbers for the 4-percent-thick section with the standard leading-edge radius; but, at moderate to large lift coefficients for Mach numbers up to 0.7, the drag coefficients are lower for the profile with the larger nose radius. The latter trend can also be noted from this figure for the 6-percent-thickness-chord ratio. No real differences are observed in the variations of section pitching-moment coefficient with section lift coefficient at constant Mach number (fig. 10) for the sections with the various leading-edge radii.

Maximum Thickness-Chord Ratio

A progressive improvement in airfoil-section lift characteristics results from reduction of the airfoil maximum thickness-chord ratio from 10 to 4 percent. From figure 11, the lift-divergence Mach number is observed to increase nearly linearly with thickness reduction. Figure 12 illustrates the gain in maximum section lift coefficient with decrease in maximum thickness at Mach numbers above 0.6. The values at Mach numbers below about 0.6 are subject to question because of the low scale. However, the results of the investigation of reference 6 indicate that at the higher Mach numbers the values are not much influenced by the relatively low test Reynolds numbers (approximately 2×10^6). The effects of maximum thickness-chord-ratio variation on the section lift-curve slope, illustrated in figure 13, are what should be expected in that each successive reduction of thickness increases the Mach number at which the lift-curve slope breaks.

The effect of reduction of thickness-chord ratio on the Mach number for drag divergence (fig. 14) is to increase markedly the value of this parameter at zero lift. With increasing lift coefficient this favorable effect diminishes, becoming very small at a lift coefficient of 0.5.

At Mach numbers below 0.7, the variation of section drag coefficient with section lift coefficient (fig. 9) is adversely affected by reduction of the maximum thickness; for Mach numbers greater than 0.75, the converse is true. The minimum drag coefficient is progressively decreased with maximum thickness reduction at all Mach numbers.

Maximum thickness-chord ratio, within the limits of the present investigation, has no important influence on airfoil-section pitching-moment characteristics.

CONCLUSIONS

From the results of a high-speed wind-tunnel investigation of the effects of leading-edge radius and maximum thickness-chord ratio on the variation with Mach number of the aerodynamic characteristics of several thin symmetrical NACA 4-digit-series airfoil sections, it is concluded:

1. The variations with Mach number of the lift, drag, and pitching moment for a 4-percent-chord-thick airfoil section are not significantly affected by a change of the leading-edge radius from 0.18 to 0.53 percent of the chord. The same is true for a leading-edge-radius variation from 0.10- to 0.40-percent chord on a 6-percent-chord-thick section.

2. Reduction of the maximum thickness-chord ratio from 10 to 4 percent progressively improves the variation of lift-curve slope with Mach number, the lift and drag-divergence characteristics, and the maximum section lift characteristics at Mach numbers above 0.6.

3. Section pitching-moment characteristics are not greatly affected by variation of the maximum thickness-chord ratio.

Ames Aeronautical Laboratory,
National Advisory Committee for Aeronautics,
Moffett Field, Calif.

REFERENCES

1. Summers, James L., and Graham, Donald J.: Effects of Systematic Changes of Trailing-Edge Angle and Leading-Edge Radius on the Variation with Mach Number of the Aerodynamic Characteristics of a 10-Percent-Chord-Thick NACA Airfoil Section. NACA RM A9G18, 1949.

2. Stack, John, and von Doenhoff, Albert E.: Tests of 16 Related Airfoils at High Speeds. NACA Rep. 492, 1934.

3. Theodorsen, Theodore: Theory of Wing Sections of Arbitrary Shape. NACA Rep. 411, 1931.

4. Abbott, Ira H., von Doenhoff, Albert E., and Stivers, Louis S., Jr.: Summary of Airfoil Data. NACA Rep. 824, 1945.

5. Allen, H. Julian, and Vincenti, Walter G.: Wall Interference in a Two-Dimensional-Flow Wind Tunnel, With Consideration of the Effect of Compressibility. NACA Rep. 782, 1944.

6. Spreiter, John R., and Steffen, Paul J.: Effect of Mach and Reynolds Numbers on Maximum Lift Coefficient. NACA TN 1044, 1946.

TABLE I. — COORDINATES AND THEORETICAL PRESSURE DISTRIBUTIONS FOR THE NACA 0004–1.10 40/1.575 AIRFOIL

x (percent c)	y (percent c)	$(v/V)^2$	v/V	$\Delta v_a/V$
0	0	0	0	5.565
1.25	.605	1.125	1.061	1.427
2.5	.818	1.130	1.063	1.010
5.0	1.090	1.123	1.060	.705
7.5	1.270	1.115	1.056	.566
10	1.413	1.108	1.053	.483
15	1.620	1.099	1.048	.382
20	1.765	1.097	1.048	.320
30	1.940	1.093	1.046	.243
40	2.000	1.088	1.043	.195
50	1.940	1.085	1.042	.156
60	1.773	1.082	1.040	.125
70	1.493	1.061	1.030	.096
80	1.106	1.032	1.016	.069
90	.622	.994	.997	.037
95	.342	.940	.970	.013
100	.040	0	0	0

L. E. radius: 0.18 percent c.

TABLE II. – COORDINATES AND THEORETICAL PRESSURE DISTRIBUTIONS FOR THE NACA 0004–3.30 40/1.575 AIRFOIL

x (percent c)	y (percent c)	$(v/V)^2$	v/V	$\Delta v_a/V$
0	0	0	0	3.515
1.25	.931	1.328	1.153	1.199
2.5	1.196	1.317	1.148	.994
5.0	1.468	1.214	1.102	.685
7.5	1.611	1.182	1.087	.549
10	1.717	1.153	1.074	.466
15	1.799	1.112	1.054	.366
20	1.862	1.091	1.045	.306
30	1.955	1.078	1.038	.234
40	2.000	1.082	1.040	.189
50	1.940	1.083	1.041	.154
60	1.773	1.079	1.039	.126
70	1.493	1.059	1.029	.099
80	1.106	1.033	1.016	.075
90	.622	.994	.997	.049
95	.342	.935	.967	.033
100	.040	0	0	0

L. E. radius: 0.53 percent c.

TABLE III. — COORDINATES AND THEORETICAL PRESSURE DISTRIBUTIONS FOR THE NACA 0006–1.10 40/1.575 AIRFOIL

x (percent c)	y (percent c)	$(v/V)^2$	v/V	$\Delta v_a/V$
0	0	0	0	3.781
1.25	.907	1.149	1.072	1.361
2.5	1.228	1.174	1.084	.974
5.0	1.633	1.174	1.084	.684
7.5	1.908	1.164	1.080	.551
10	2.120	1.158	1.076	.470
15	2.433	1.145	1.070	.372
20	2.645	1.141	1.068	.312
30	2.915	1.143	1.069	.239
40	3.000	1.141	1.068	.189
50	2.915	1.128	1.062	.154
60	2.660	1.115	1.056	.125
70	2.240	1.088	1.043	.098
80	1.660	1.053	1.026	.072
90	.934	1.002	1.001	.045
95	.514	.915	.957	.027
100	.060	0	0	0

L. E. radius: 0.40 percent c.

TABLE IV. — COORDINATES AND THEORETICAL PRESSURE DISTRIBUTIONS FOR THE NACA 0006–0.70 40/1.575 AIRFOIL

x (percent c)	y (percent c)	$(v/V)^2$	v/V	$\Delta v_a/V$
0	0	0	0	4.520
1.25	.766	1.083	1.041	1.365
2.5	1.067	1.123	1.060	.977
5.0	1.473	1.138	1.067	.687
7.5	1.767	1.142	1.069	.555
10	1.989	1.144	1.069	.474
15	2.354	1.148	1.072	.377
20	2.607	1.152	1.073	.317
30	2.908	1.148	1.072	.241
40	3.000	1.145	1.070	.193
50	2.915	1.136	1.066	.156
60	2.660	1.117	1.057	.126
70	2.240	1.095	1.046	.099
80	1.660	1.056	1.028	.074
90	.934	.997	.999	.047
95	.514	.924	.961	.030
100	.060	0	0	0

L. E. radius: 0.25 percent c.

NACA

TABLE V. — COORDINATES AND THEORETICAL PRESSURE DISTRIBUTIONS FOR THE NACA 0006-0.27 40/1.575 AIRFOIL

x (percent c)	y (percent c)	$(v/V)^2$	v/V	$\Delta v_a/V$
0	0	0	0	6.893
1.25	.566	.962	.981	1.349
2.5	.840	1.029	1.015	.974
5.0	1.247	1.077	1.038	.689
7.5	1.567	1.097	1.047	.558
10	1.826	1.119	1.058	.480
15	2.246	1.140	1.068	.383
20	2.546	1.154	1.074	.322
30	2.900	1.160	1.077	.245
40	3.000	1.148	1.071	.194
50	2.914	1.134	1.065	.157
60	2.660	1.120	1.058	.127
70	2.240	1.097	1.047	.099
80	1.660	1.058	1.029	.073
90	.934	.999	.999	.046
95	.514	.920	.959	.028
100	.060	0	0	0

L. E. radius: 0.10 percent c.

TABLE VI. — COORDINATES AND THEORETICAL PRESSURE DISTRIBUTIONS FOR THE NACA 0008–1.10 40/1.575 AIRFOIL

x (percent c)	y (percent c)	$(v/V)^2$	v/V	$\Delta v_a/V$
0	0	0	0	2.923
1.25	1.210	1.138	1.067	1.329
2.5	1.636	1.228	1.108	.974
5.0	2.179	1.236	1.112	.686
7.5	2.540	1.223	1.106	.552
10	2.825	1.217	1.103	.471
15	3.240	1.206	1.098	.374
20	3.530	1.199	1.095	.314
30	3.889	1.194	1.093	.239
40	4.000	1.191	1.092	.191
50	3.889	1.182	1.087	.155
60	3.545	1.160	1.077	.125
70	2.985	1.123	1.060	.098
80	2.212	1.075	1.037	.072
90	1.243	.994	.997	.045
95	.684	.919	.958	.029
100	.080	0	0	0
L. E. radius: 0.70 percent c.				

TABLE VII. – COORDINATES AND THEORETICAL PRESSURE DISTRIBUTIONS FOR THE NACA 0010–1.10 40/1.575 AIRFOIL

x (percent c)	y (percent c)	$(v/V)^2$	v/V	$\Delta v_a/V$
0	0	0	0	2.324
1.25	1.511	1.108	1.053	1.286
2.5	2.044	1.245	1.116	.966
5.0	2.722	1.286	1.134	.690
7.5	3.178	1.277	1.130	.556
10	3.533	1.269	1.127	.475
15	4.056	1.261	1.123	.377
20	4.411	1.248	1.117	.316
30	4.856	1.244	1.116	.241
40	5.000	1.242	1.115	.193
50	4.856	1.231	1.110	.155
60	4.433	1.211	1.101	.126
70	3.733	1.155	1.074	.098
80	2.767	1.089	1.043	.072
90	1.556	.980	.990	.045
95	.856	.912	.955	.030
100	.100	0	0	0

L. E. radius: 1.10 percent c.

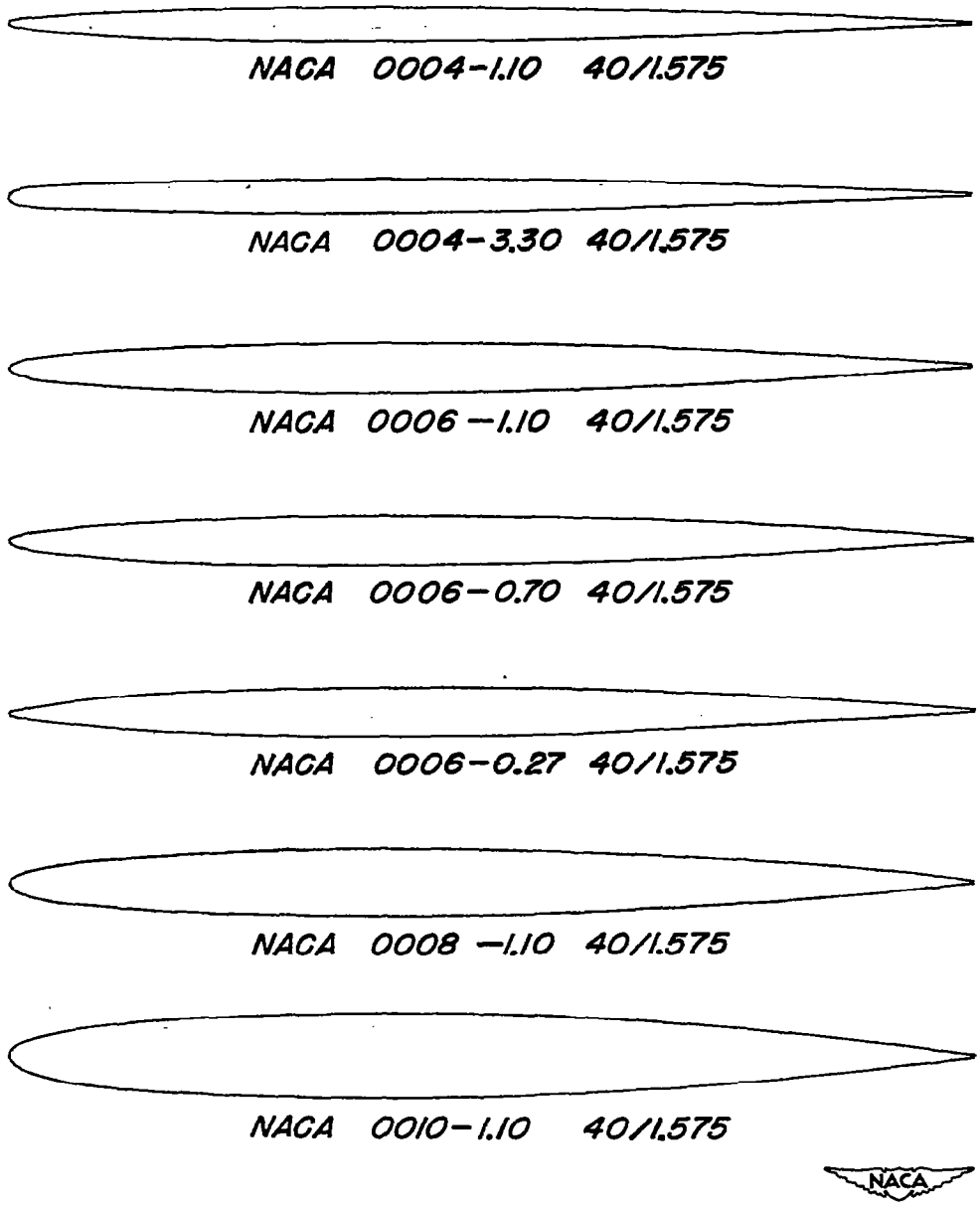

Figure 1.- NACA airfoil profiles investigated.

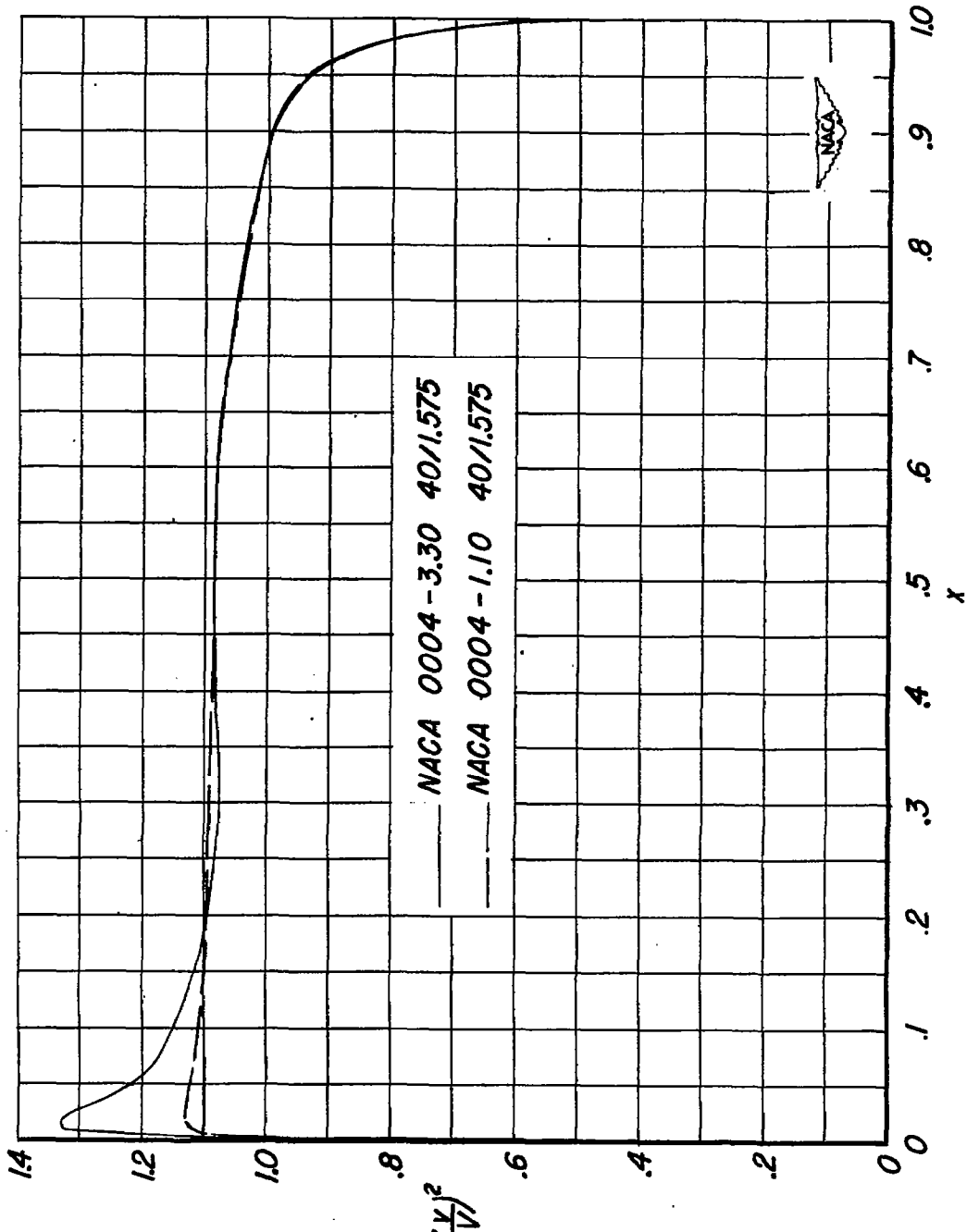

(a) Maximum thickness-chord ratio of 0.04.

Figure 2.- Theoretical pressure distributions showing the effect of change of maximum thickness-chord ratio and leading-edge radius. c_l, 0; M, 0.

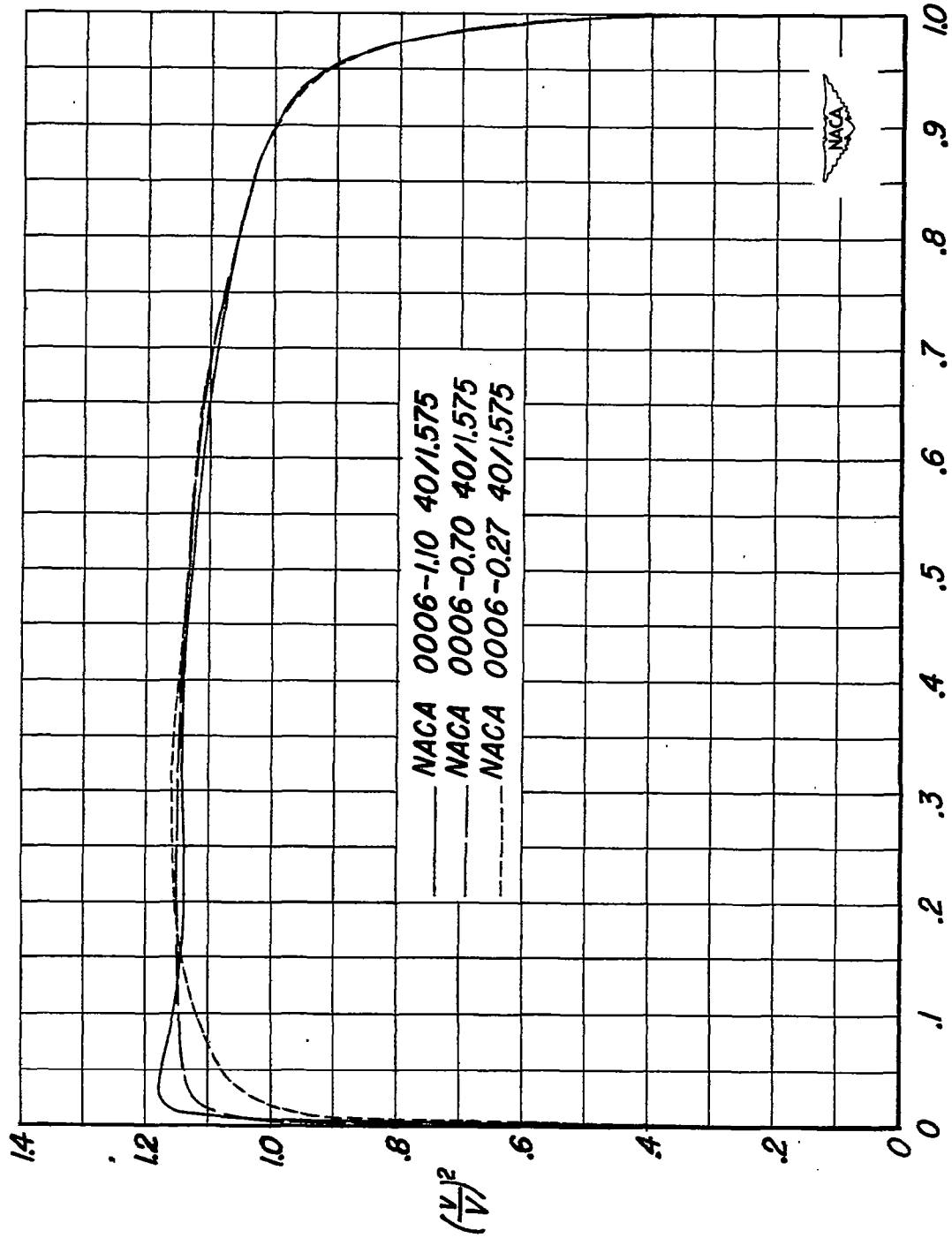

(b) Maximum thickness - chord ratio of 0.06.

Figure 2.- Continued.

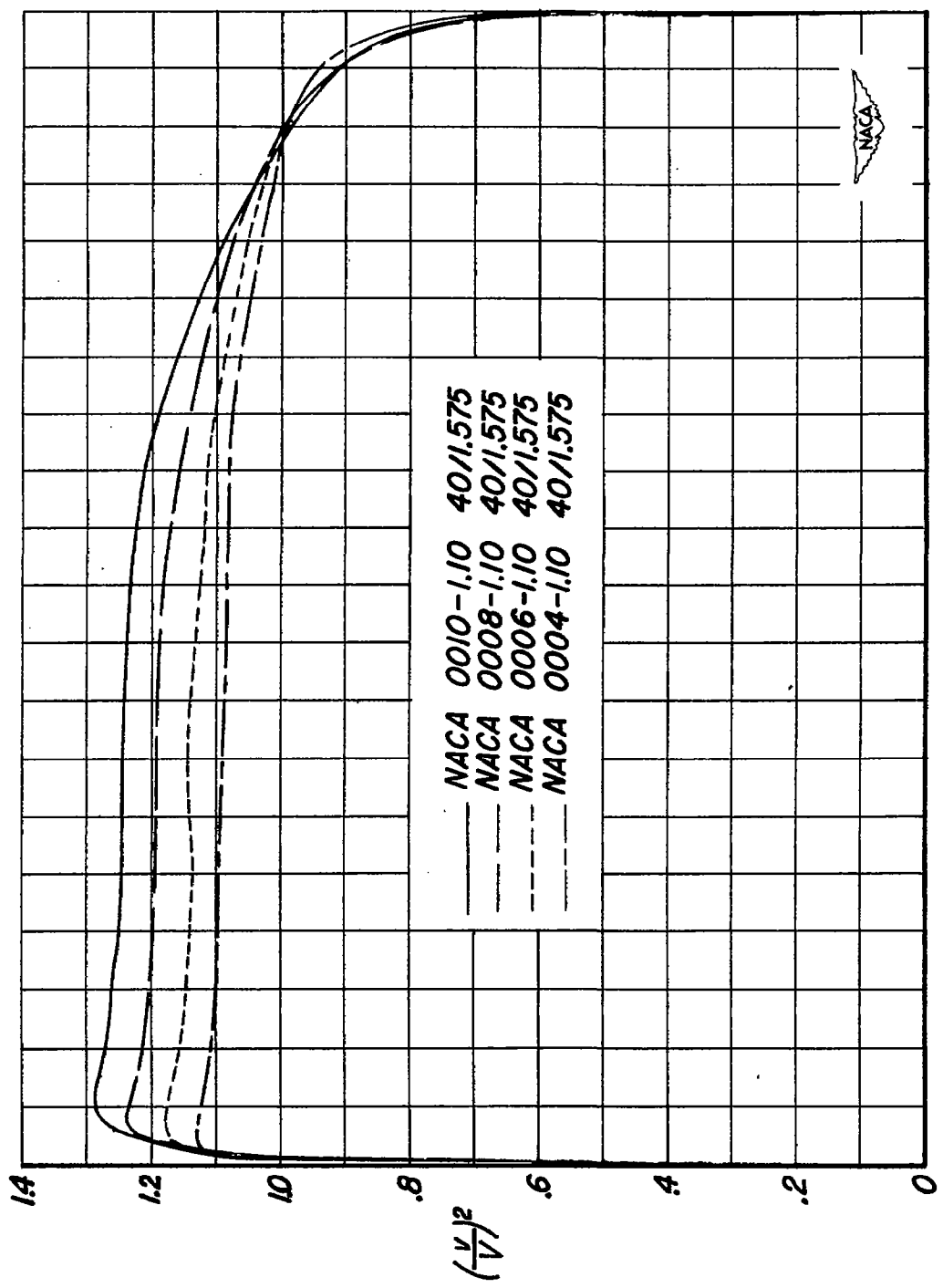

(c) Variation of maximum thickness-chord ratio.

Figure 2.- Concluded.

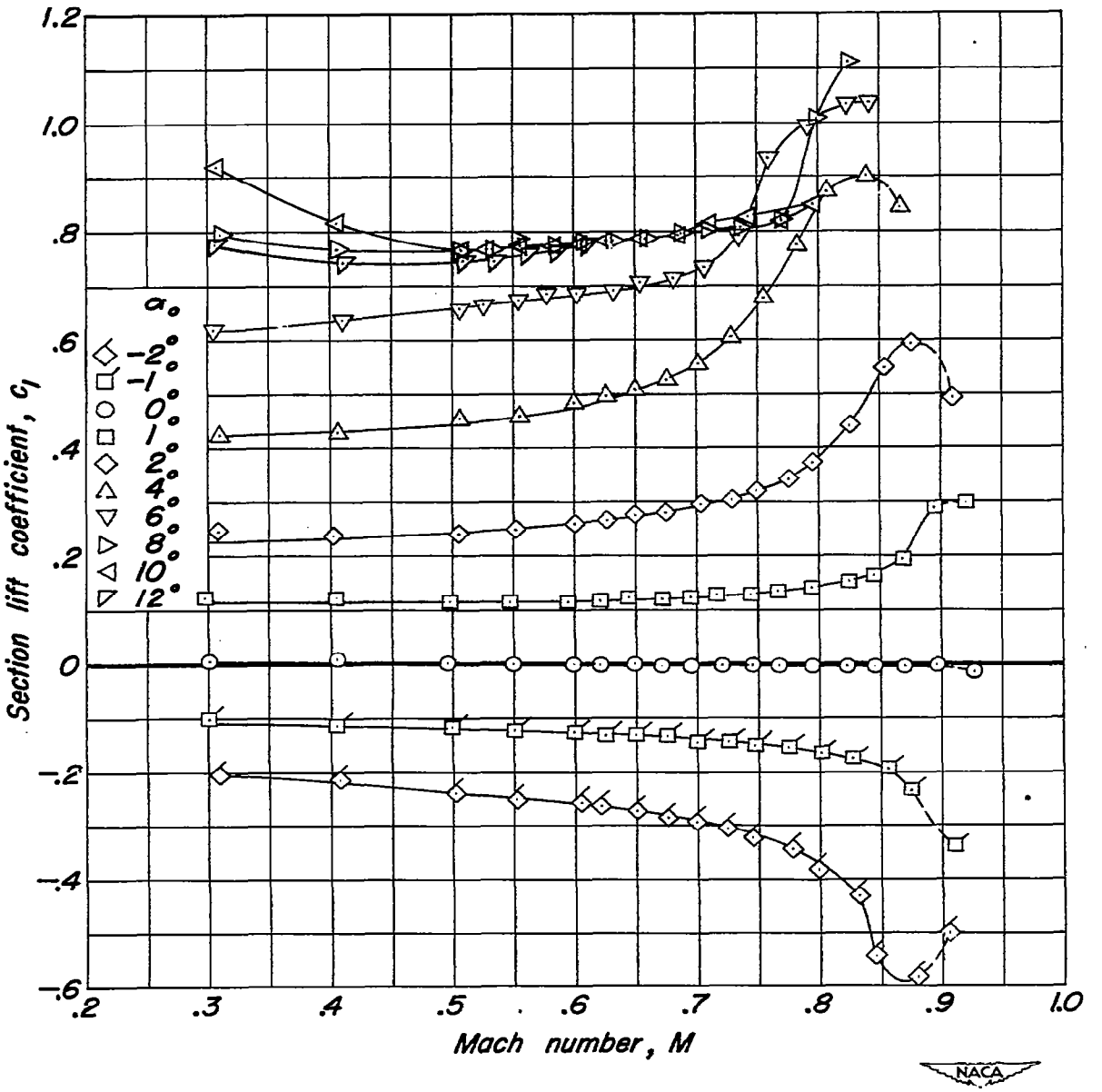

(a) NACA 0004-1.10 40/1.575 Airfoil.

Figure 3.- Variation of section lift coefficient with Mach number at constant angles of attack.

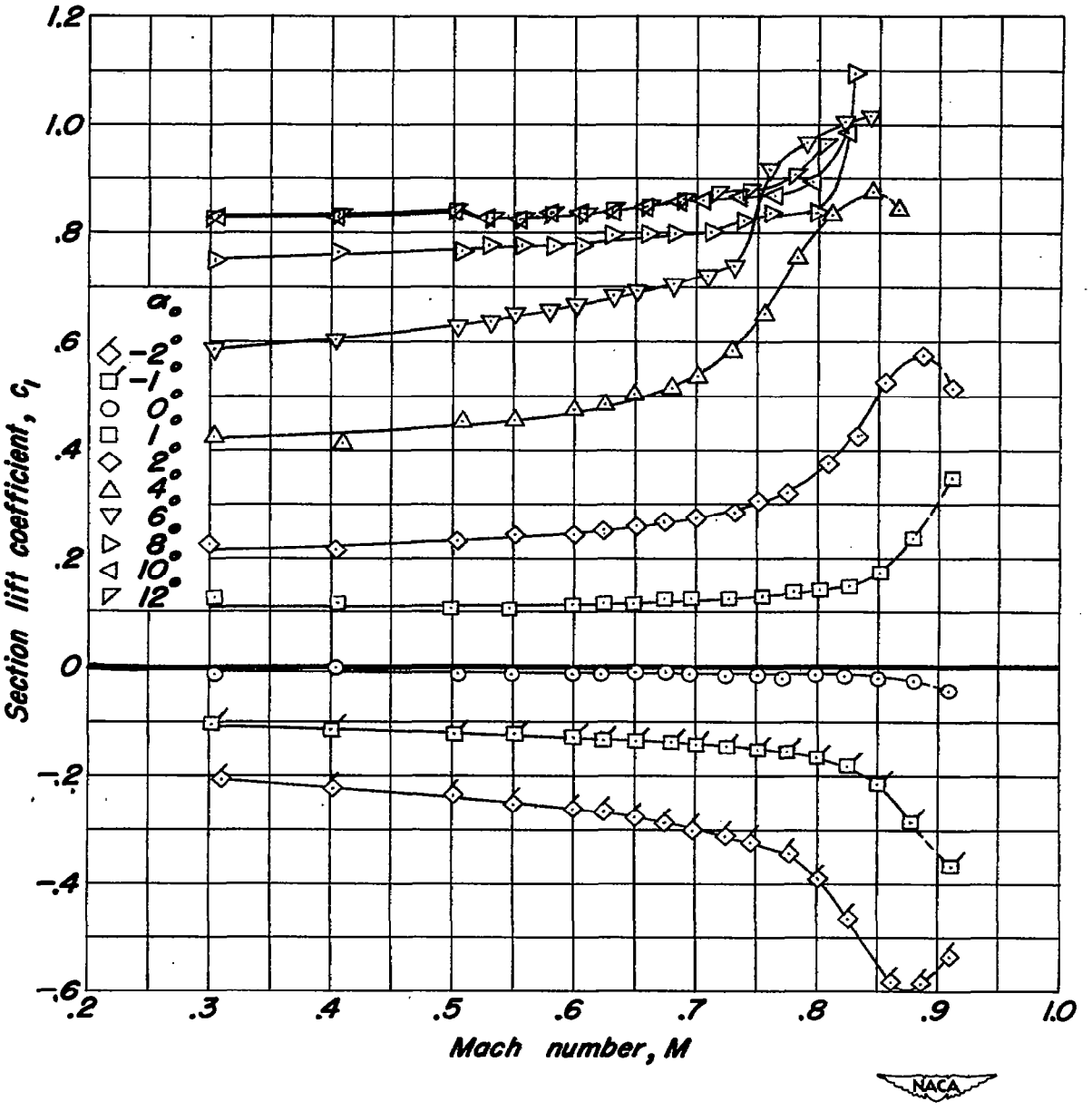

(b) NACA 0004-3.30 40/1.575 Airfoil.

Figure 3.- Continued.

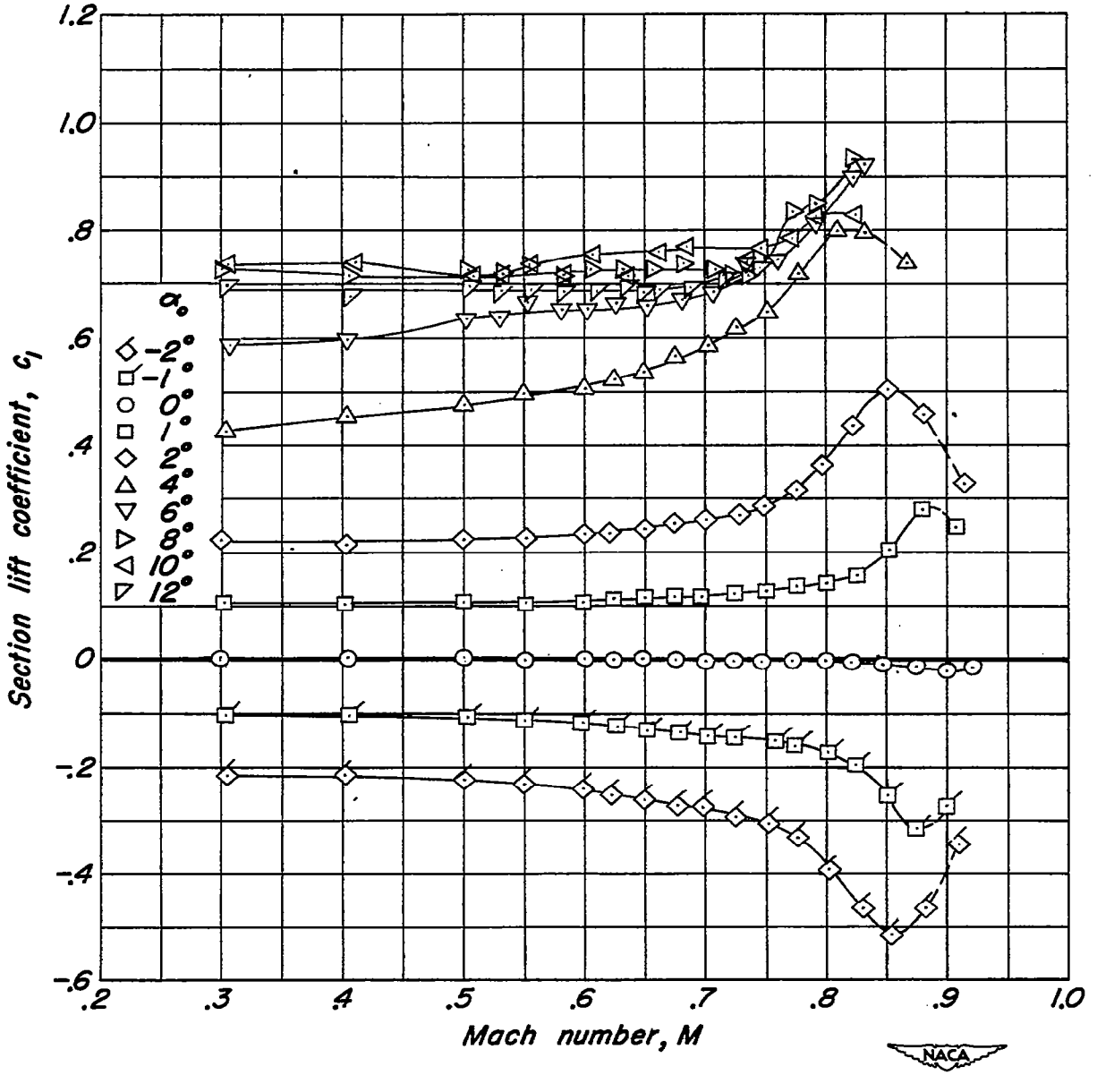

(c) NACA 0006-1.10 40/1.575 Airfoil.

Figure 3.- Continued.

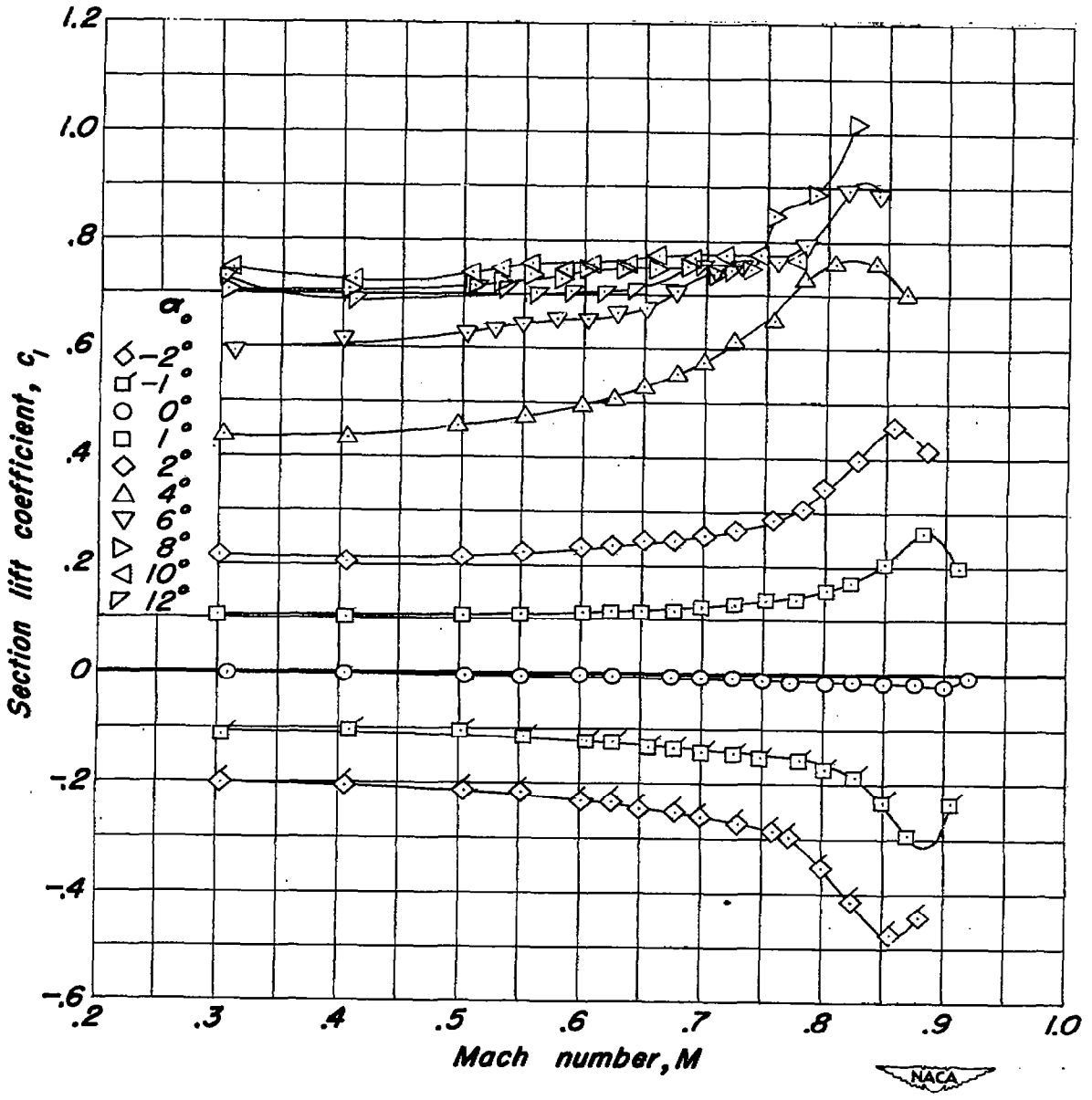

(d) NACA 0006-0.70 40/1.575 Airfoil.

Figure 3.- Continued.

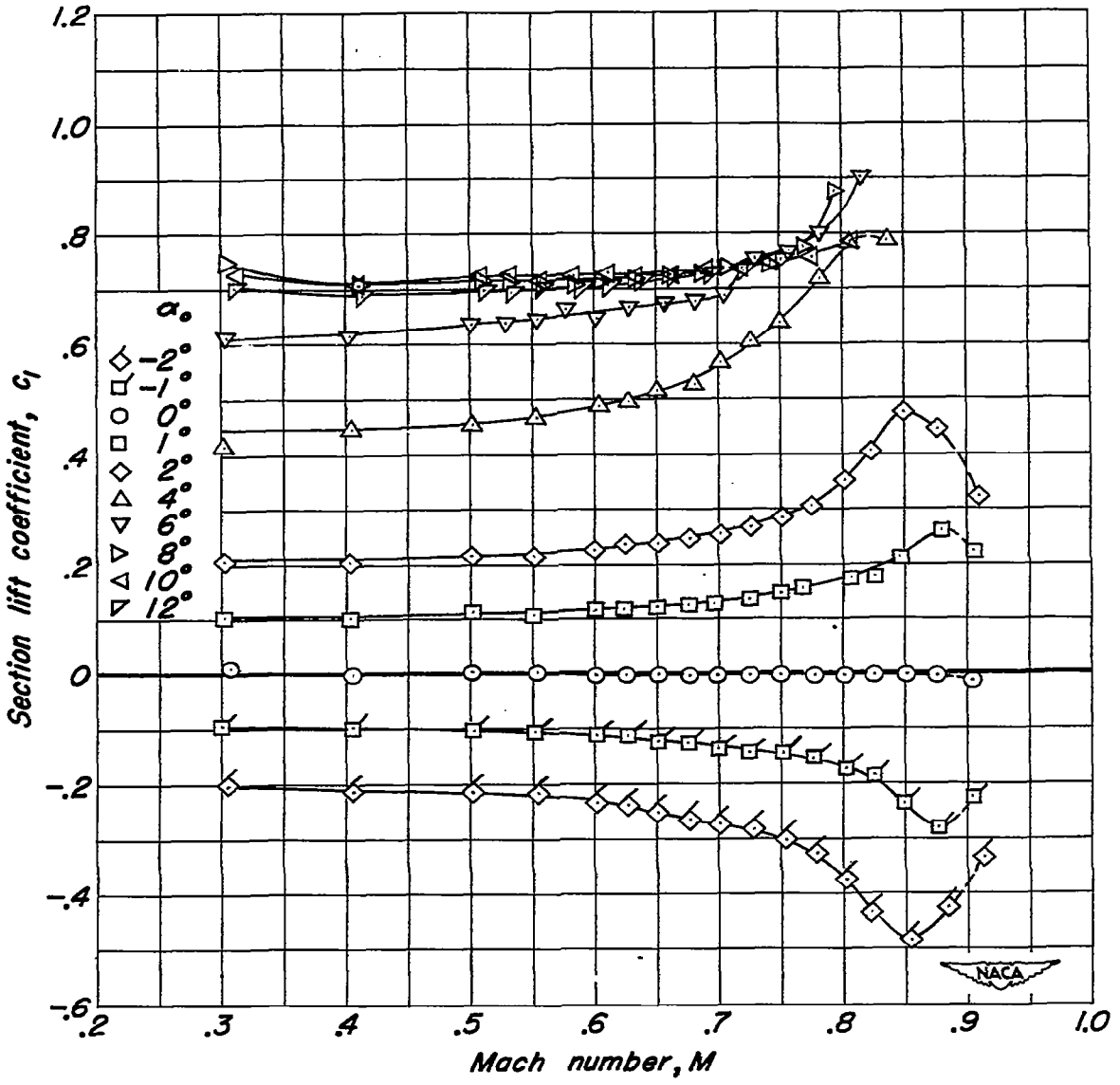

(e) NACA 0006-0.27 40/1.575 Airfoil.

Figure 3.- Continued.

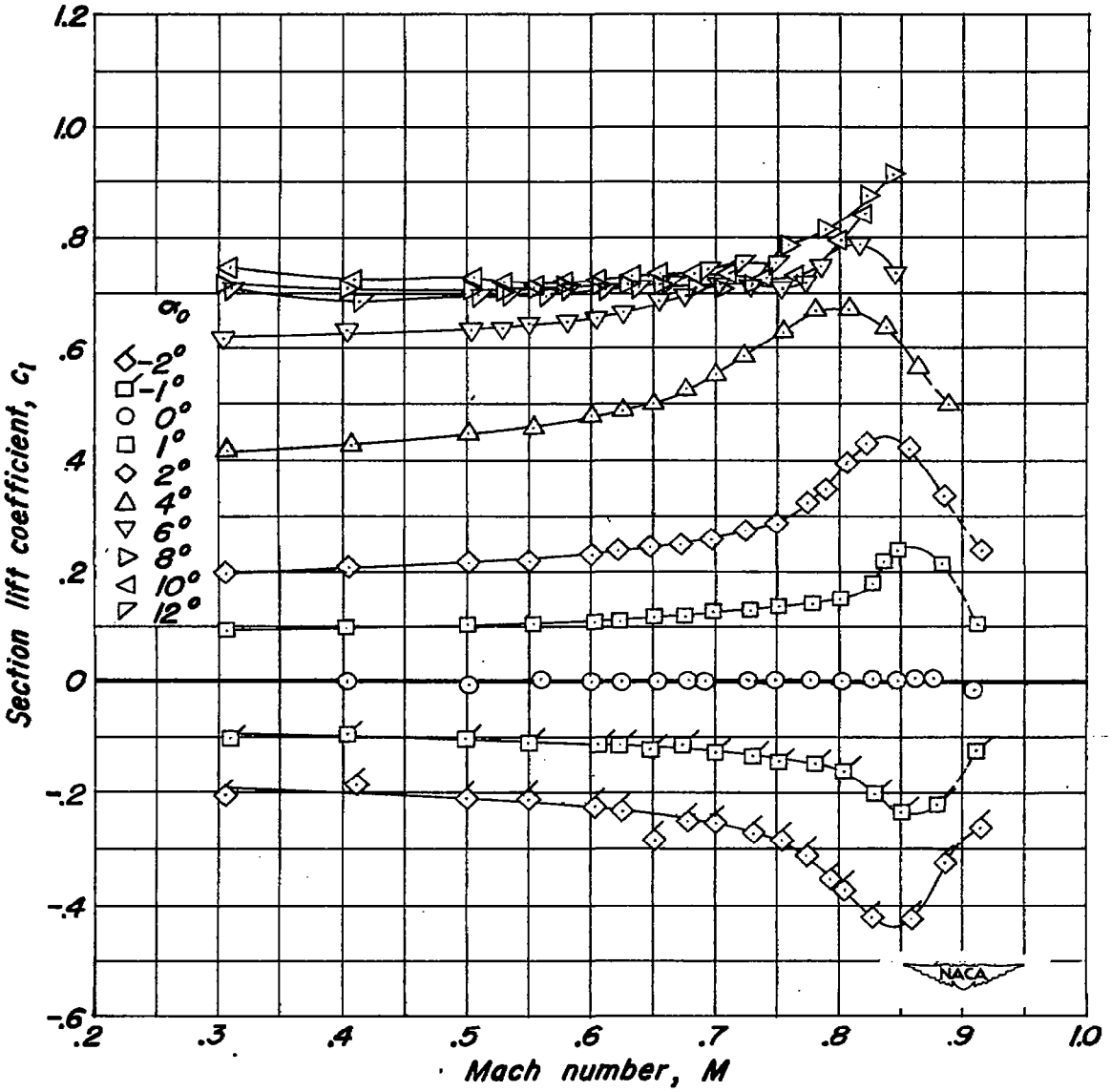

(f) NACA 0008-1.10 40/1.575 Airfoil.

Figure 3.- Continued.

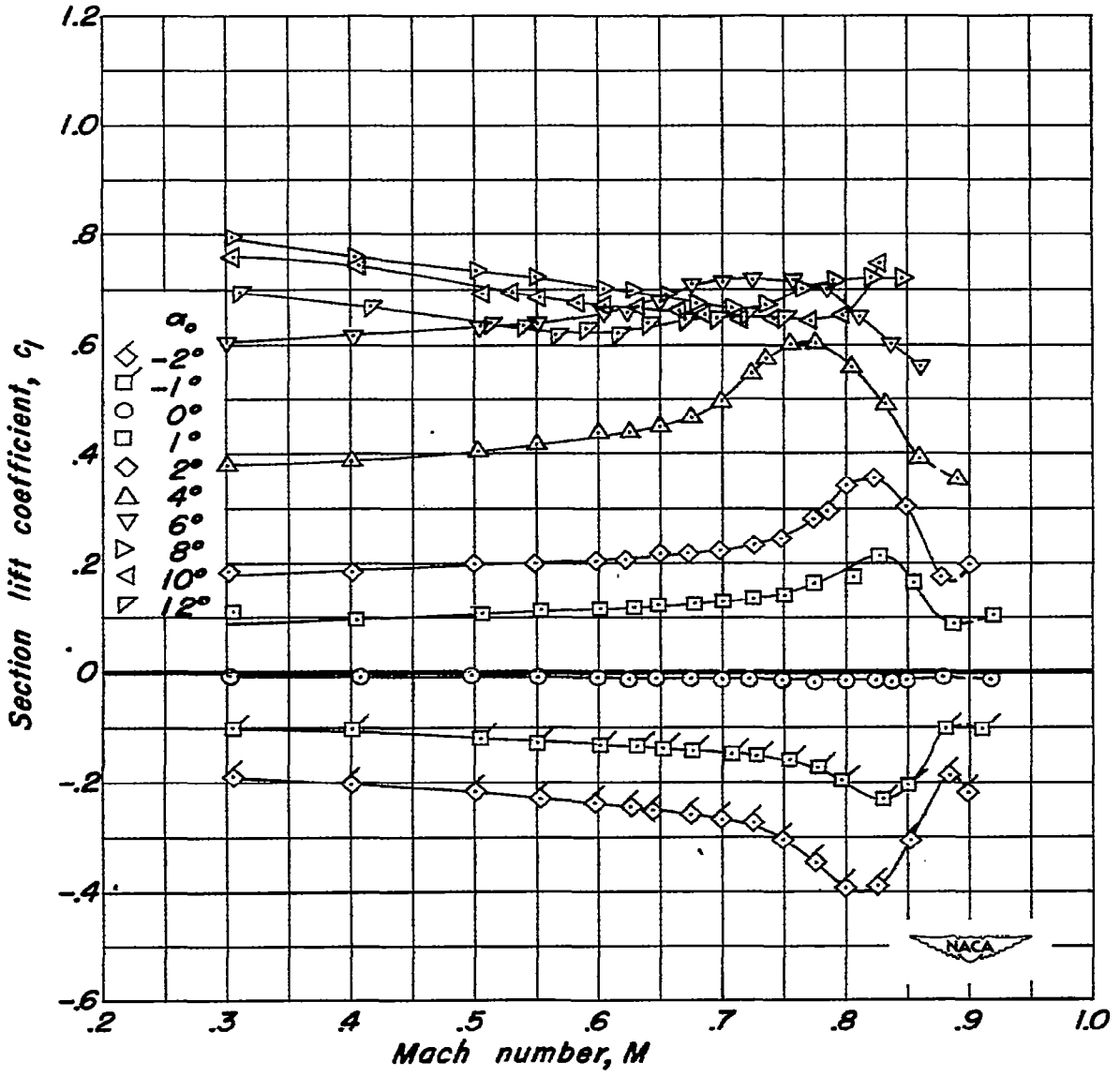

(g) NACA 0010-1.10 40/1.575 Airfoil.

Figure 3.- Concluded.

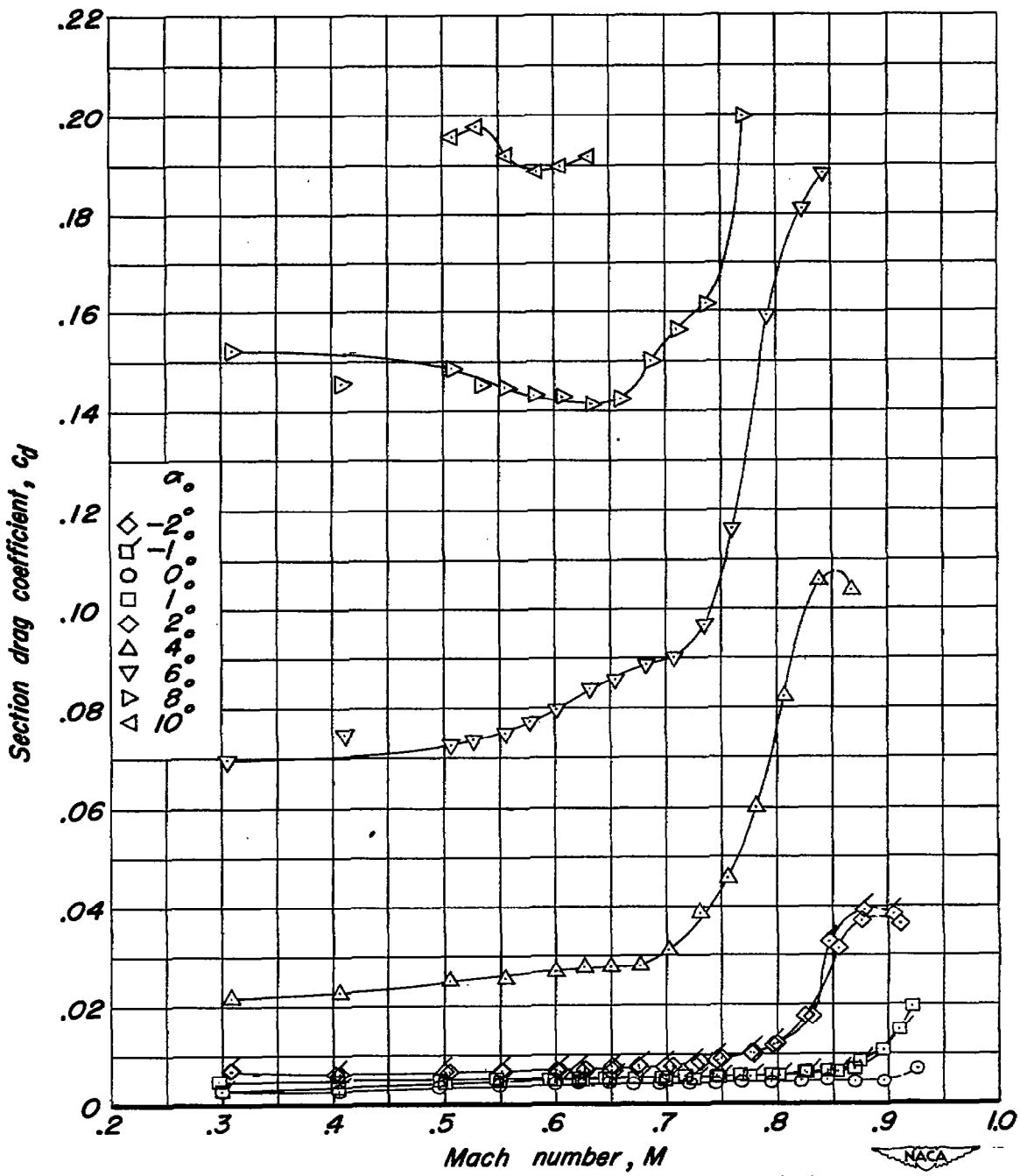

(a) NACA 0004-1.10 40/1.575 Airfoil.

Figure 4.- Variation of section drag coefficient with Mach number at constant angles of attack.

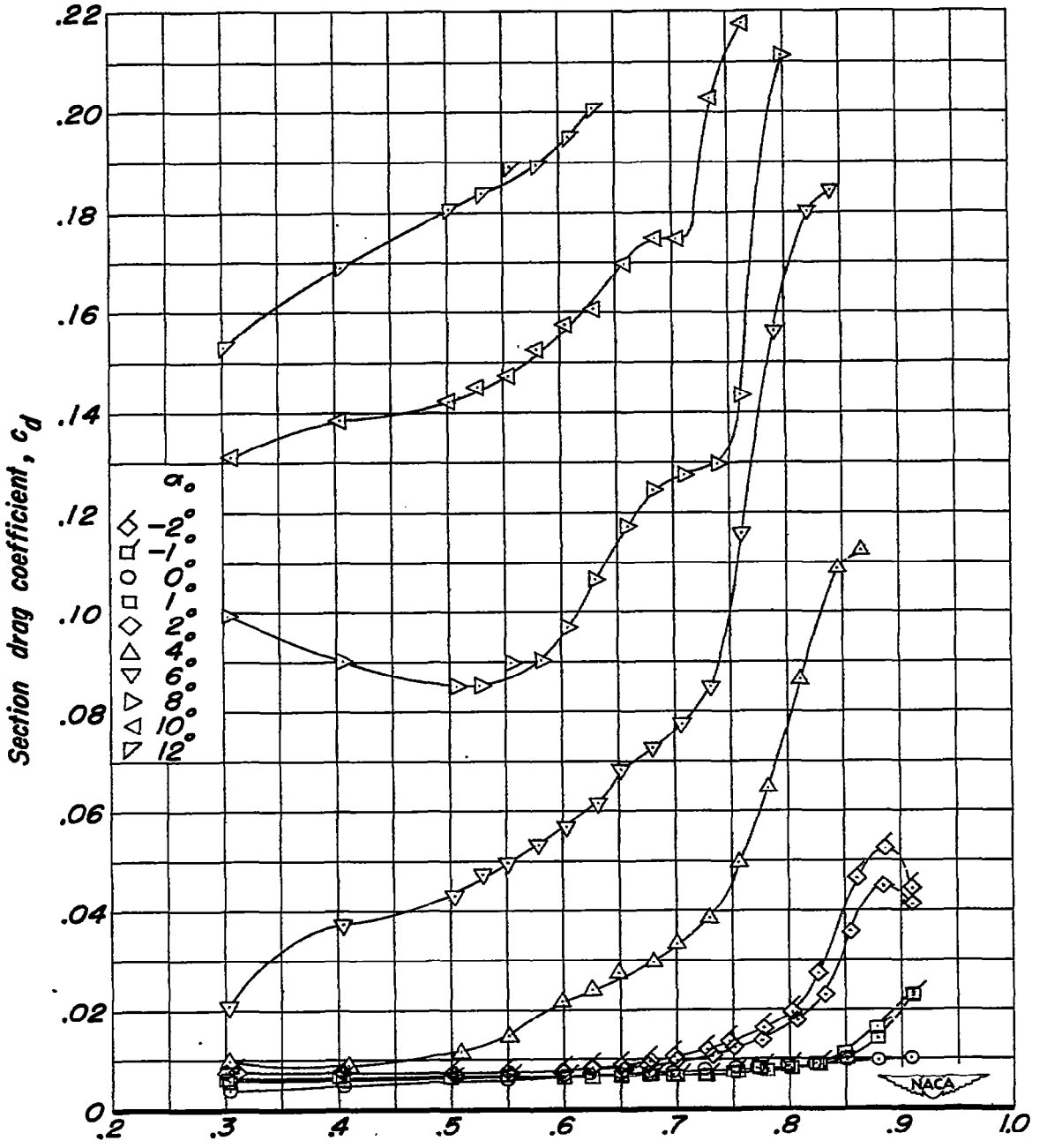

(b) NACA 0004-3.30 40/1.575 Airfoil.

Figure 4.- Continued.

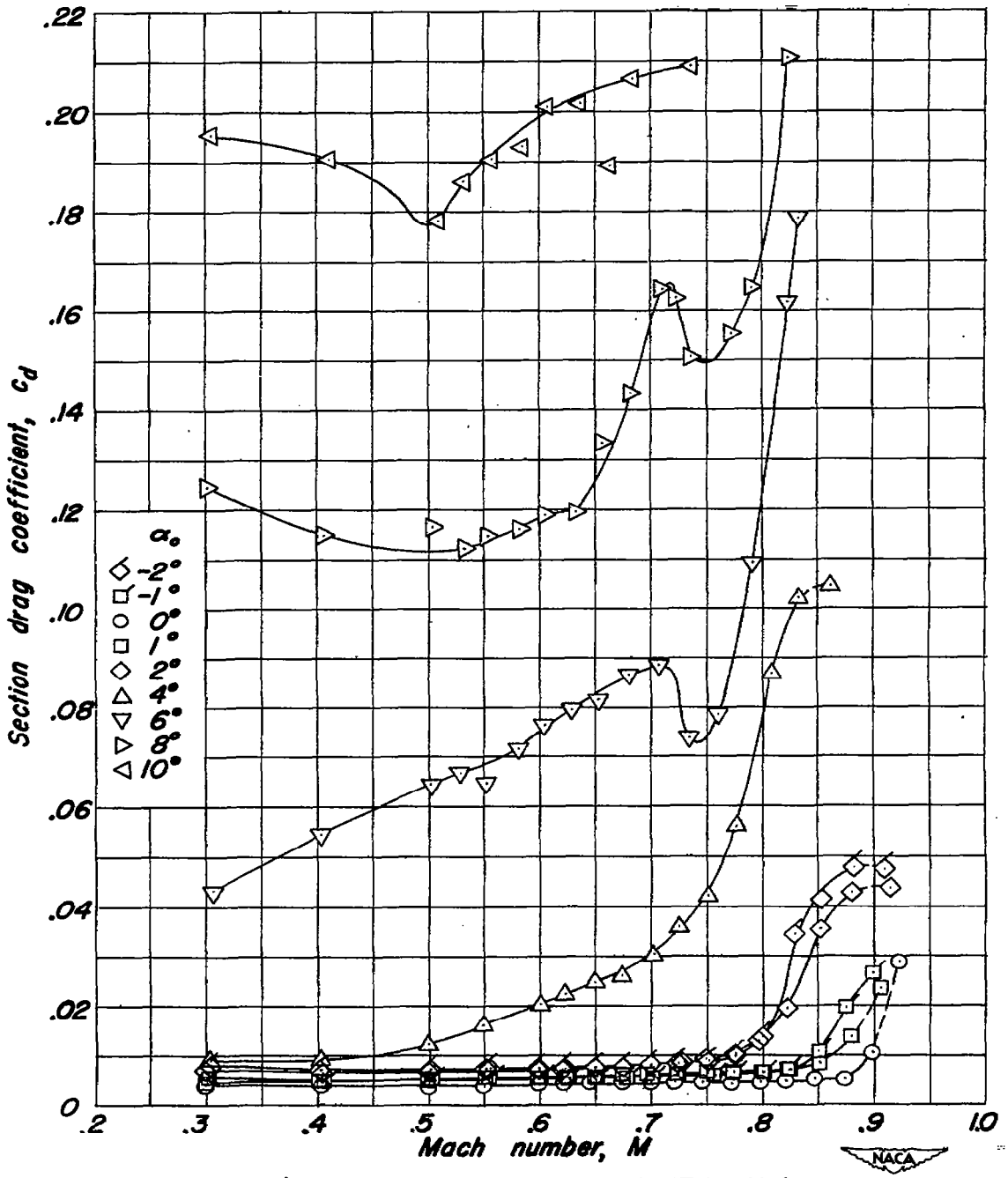

(c) NACA 0006-1.10 40/1.575 Airfoil.

Figure 4.- Continued.

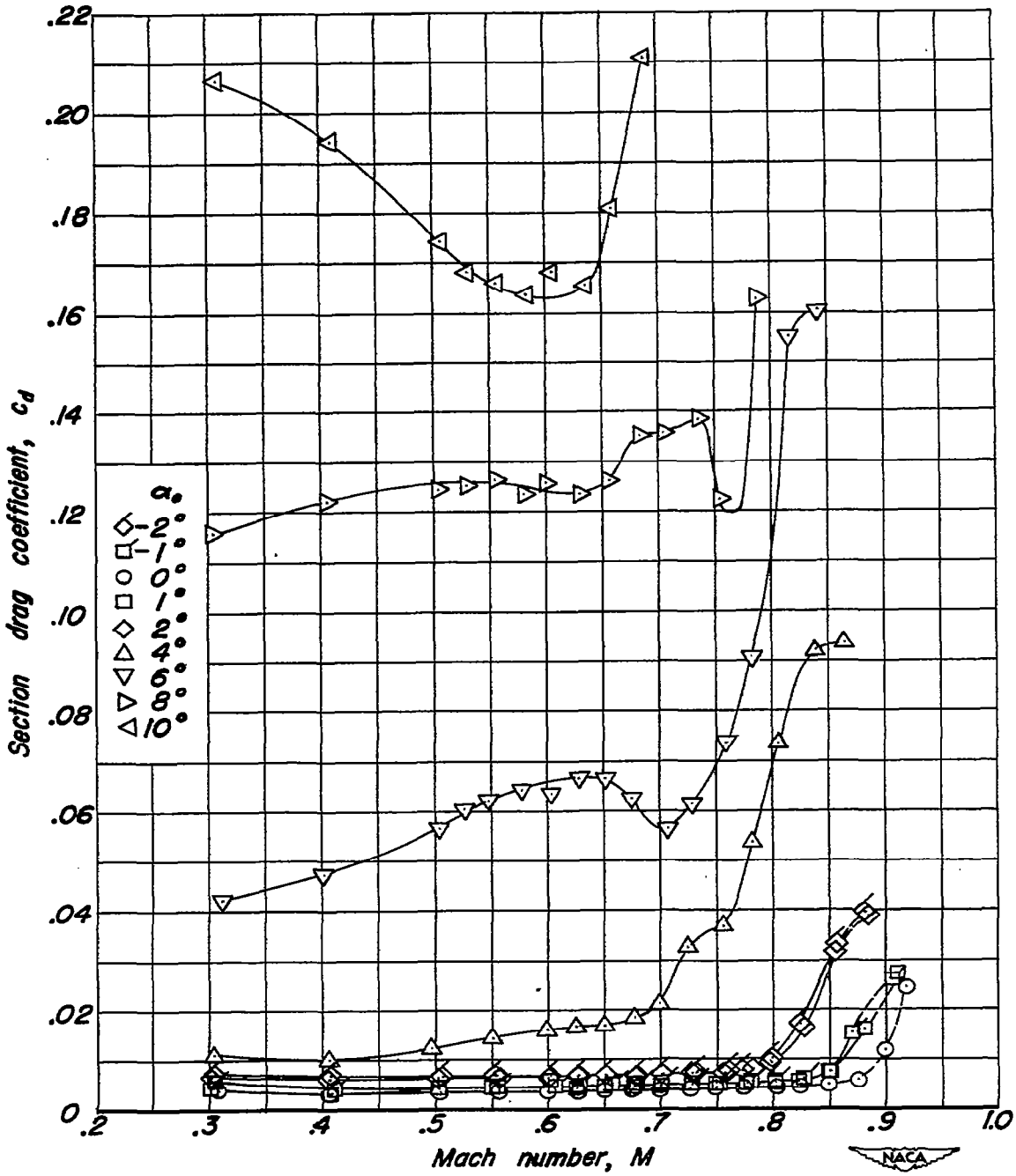

(d) NACA 0006-0.70 40/1.575 Airfoil.

Figure 4.- Continued.

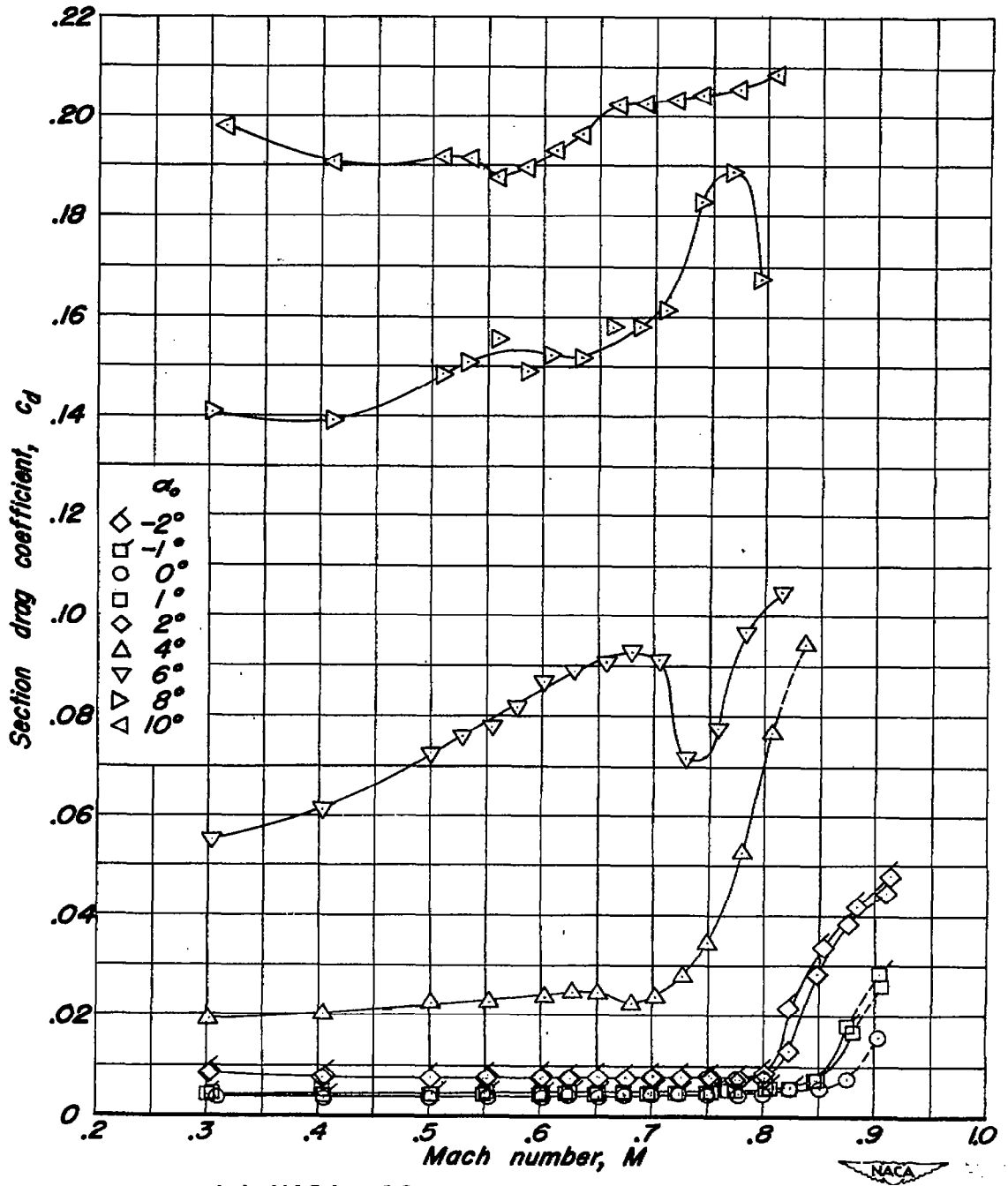

(e) NACA 0006-0.27 40/1.575 Airfoil.

Figure 4.- Continued.

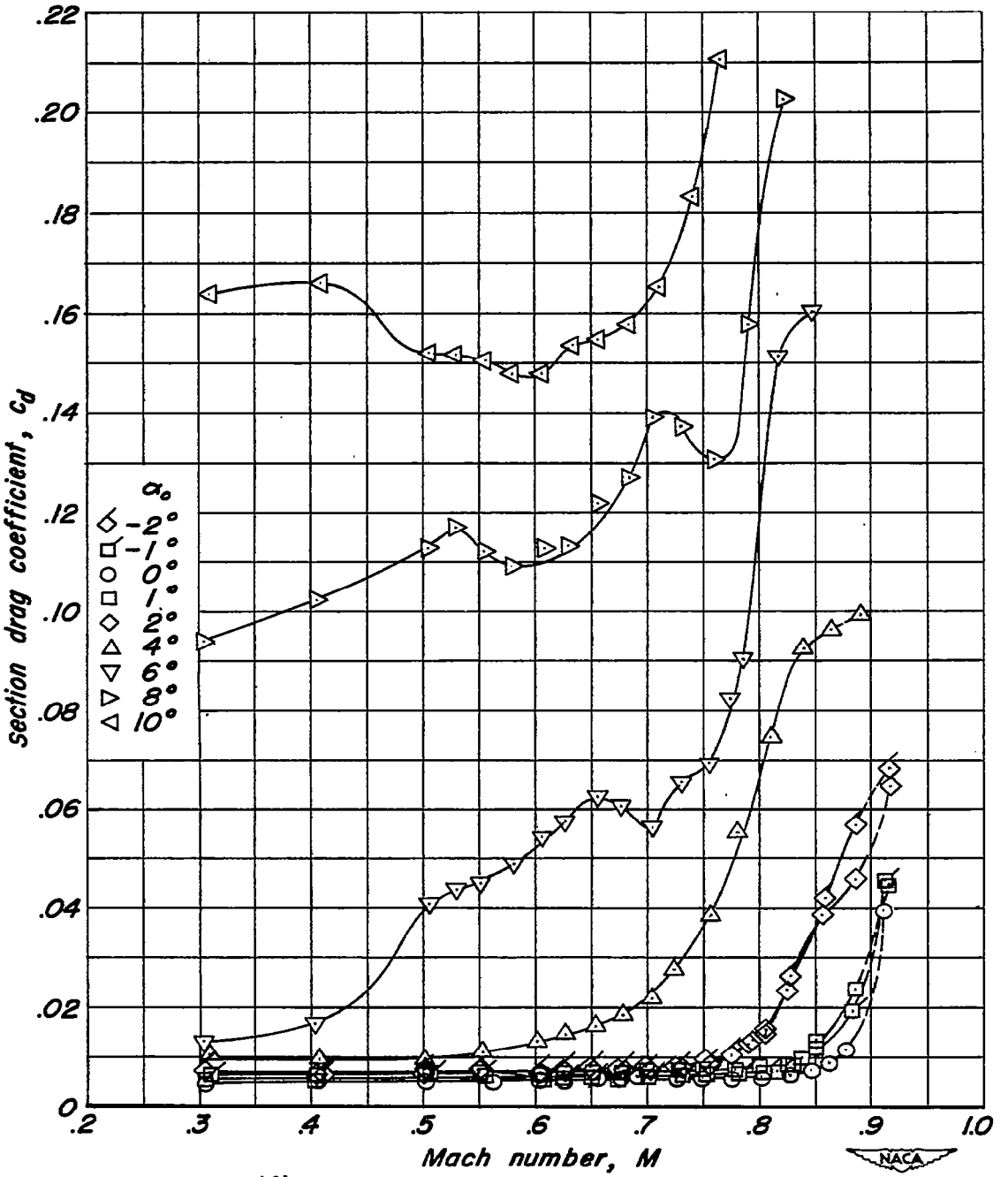

(f) NACA 0008-1.10 40/1.575 Airfoil.

Figure 4.- Continued.

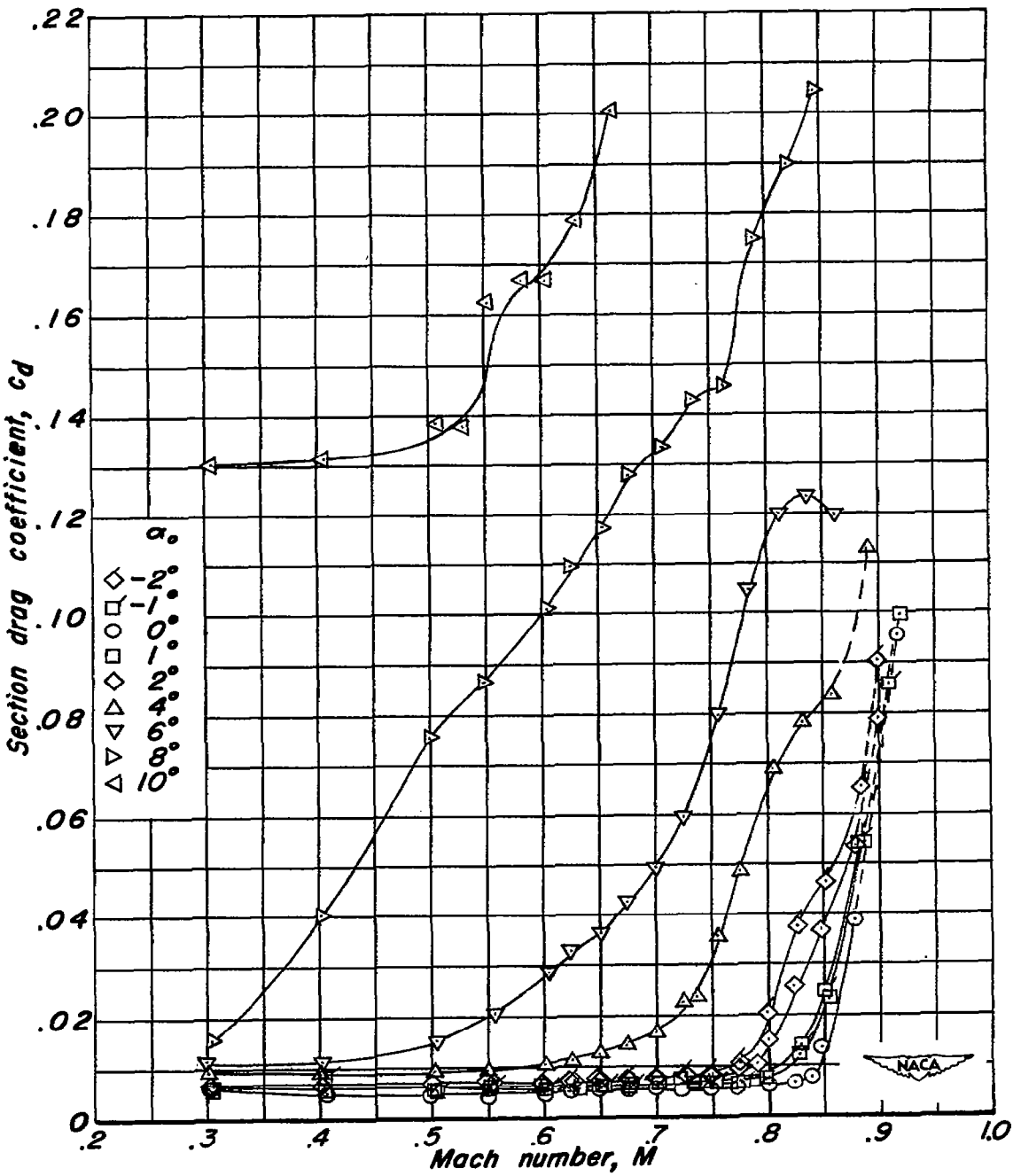

(g) NACA 0010-1.10 40/1.575 Airfoil.

Figure 4.- Concluded.

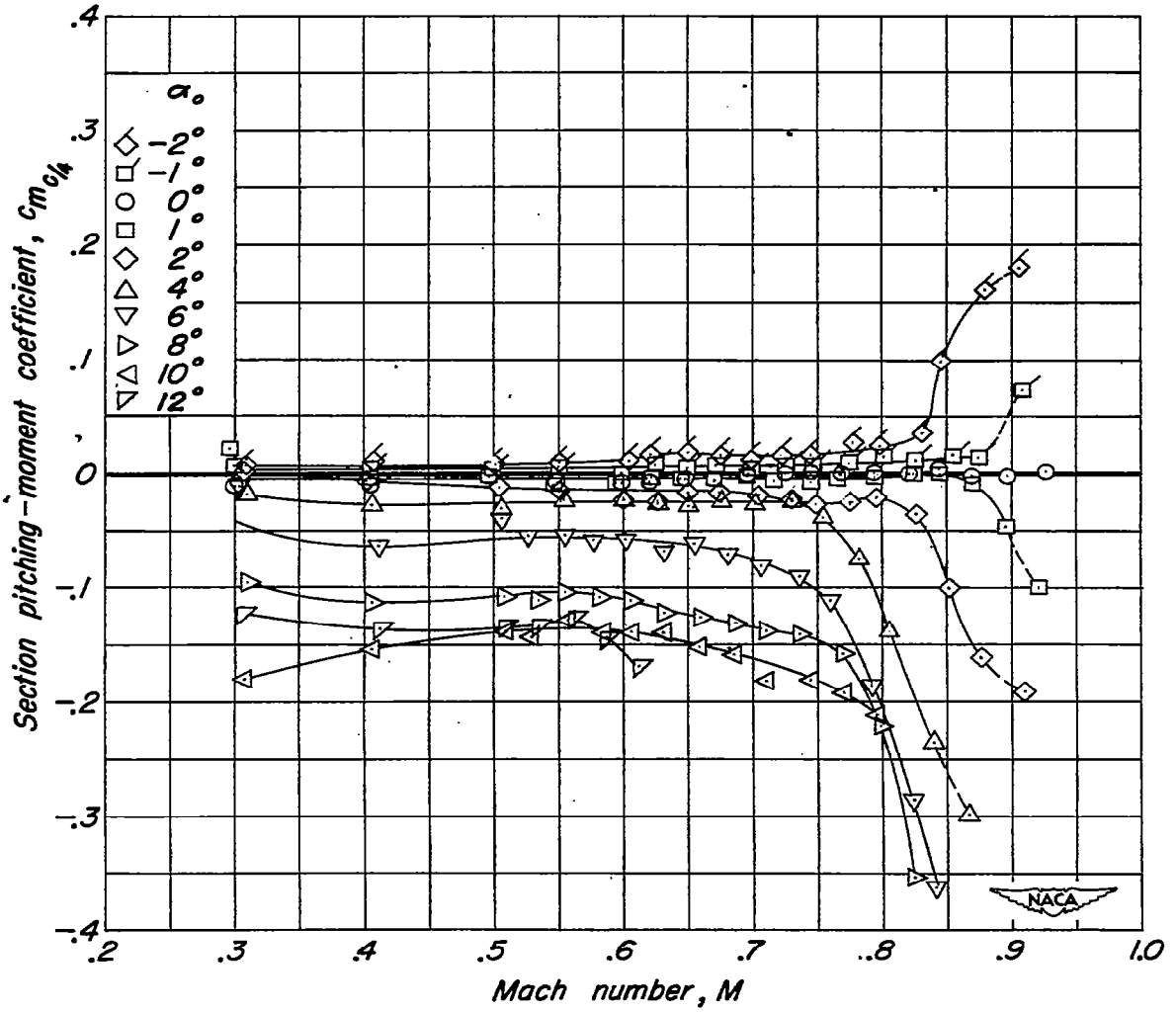

(a) NACA 0004-1.10 40/1.575 Airfoil.

Figure 5.- Variation of section pitching-moment coefficient with Mach number at constant angles of attack.

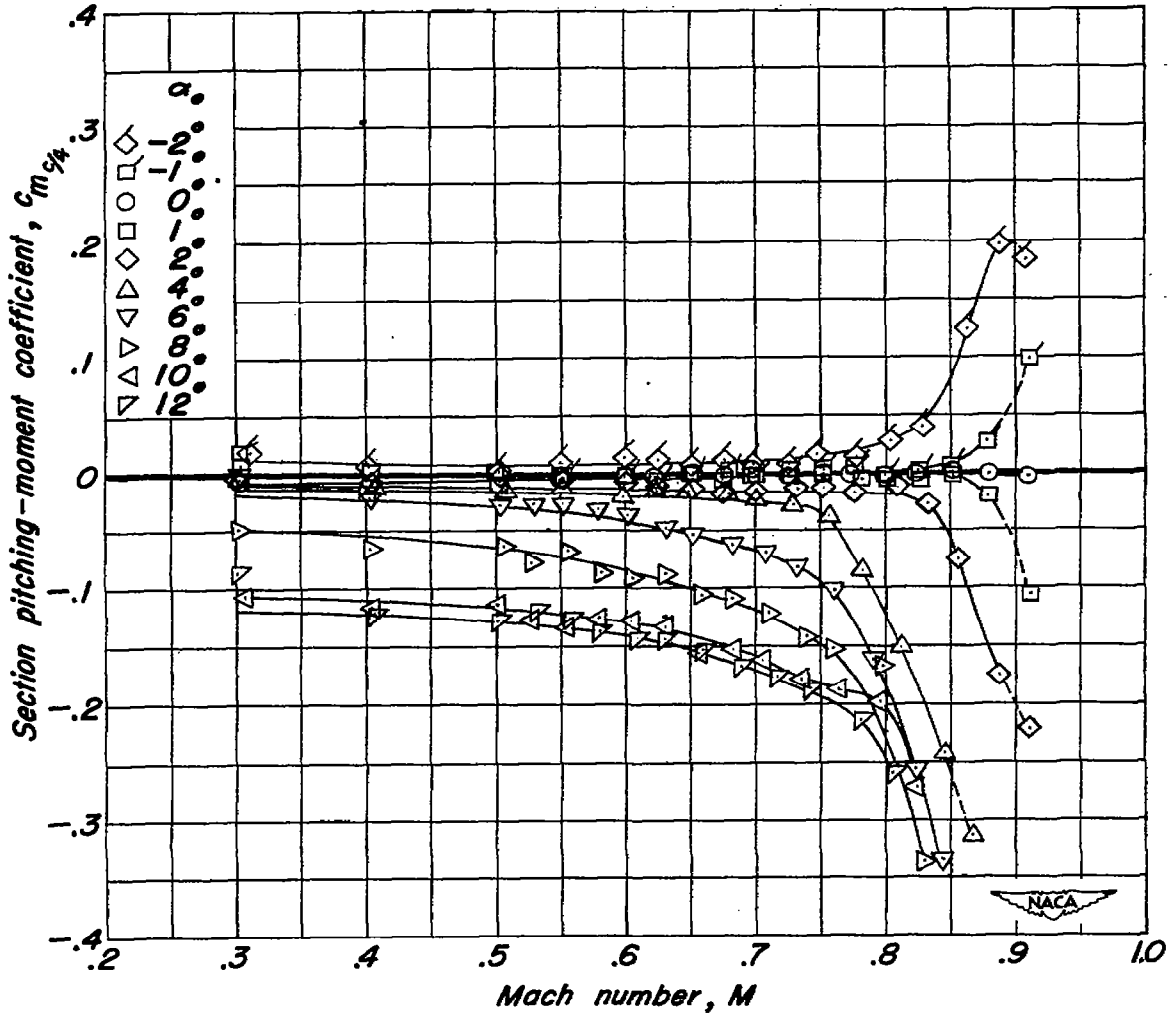

(b) NACA 0004-3.30 40/1.575 Airfoil.

Figure 5.- Continued.

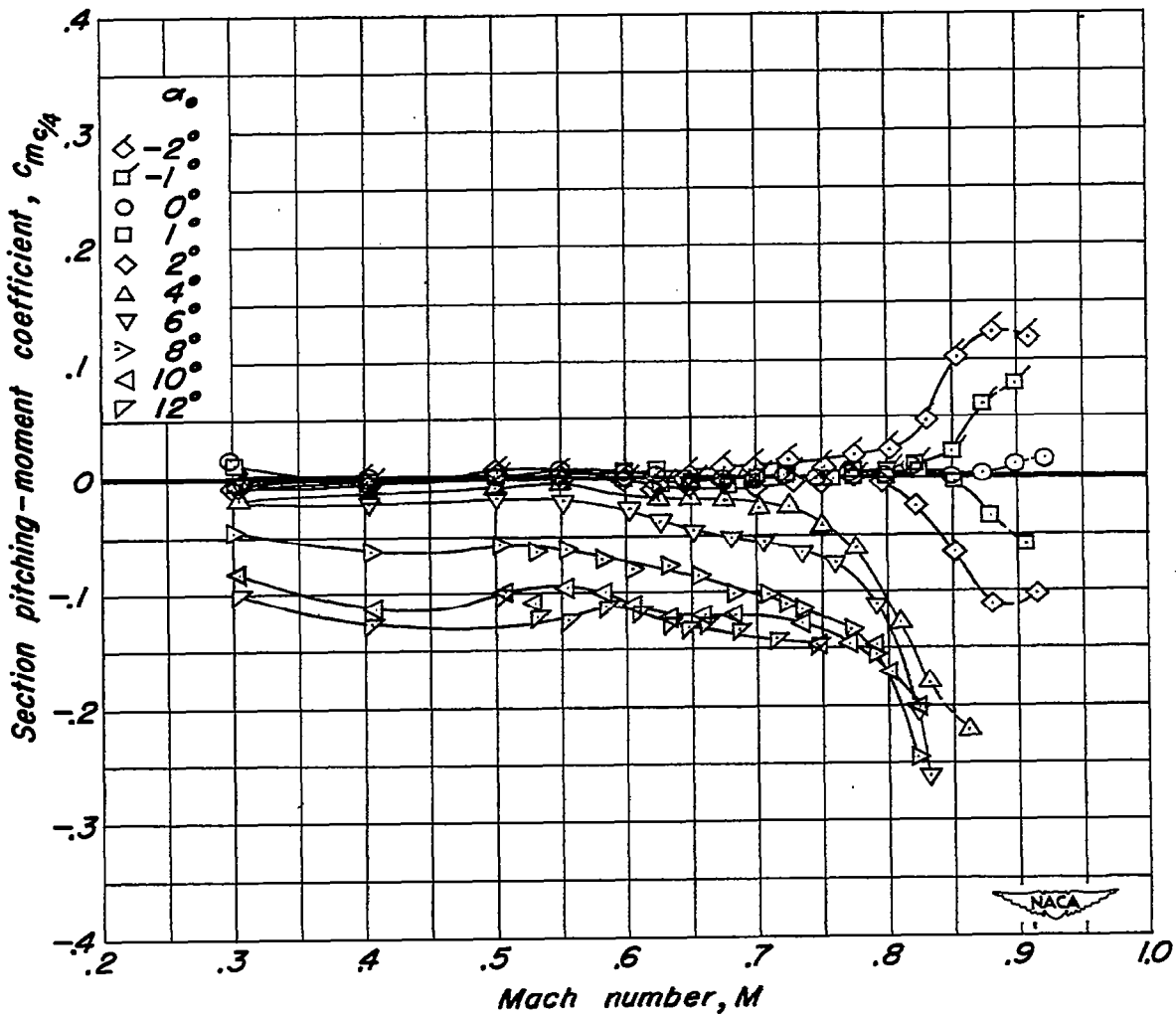

(c) NACA 0006-1.10 40/1.575 Airfoil.

Figure 5.- Continued.

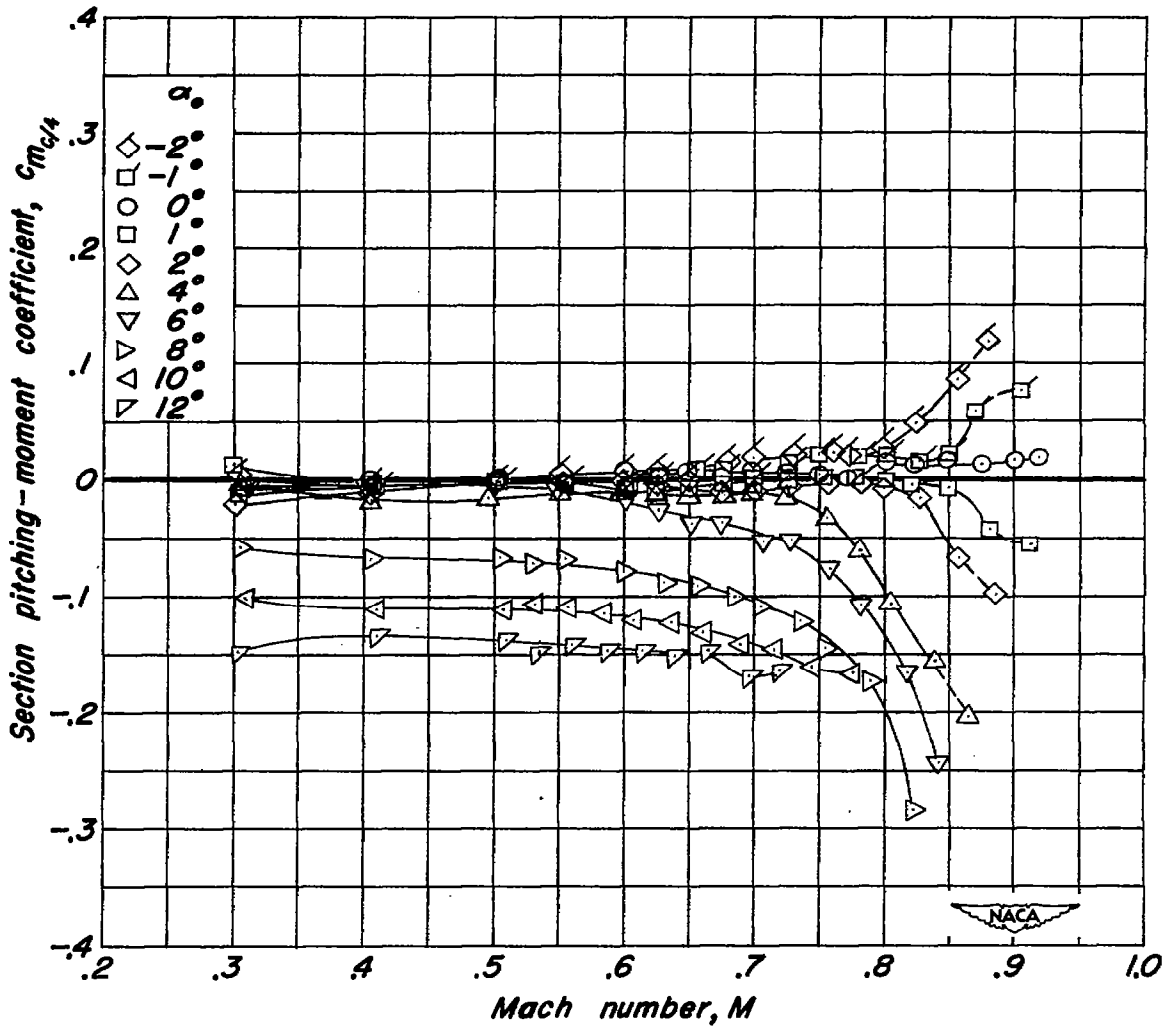

(d) NACA 0006-0.70 40/1.575 Airfoil.

Figure 5.- Continued.

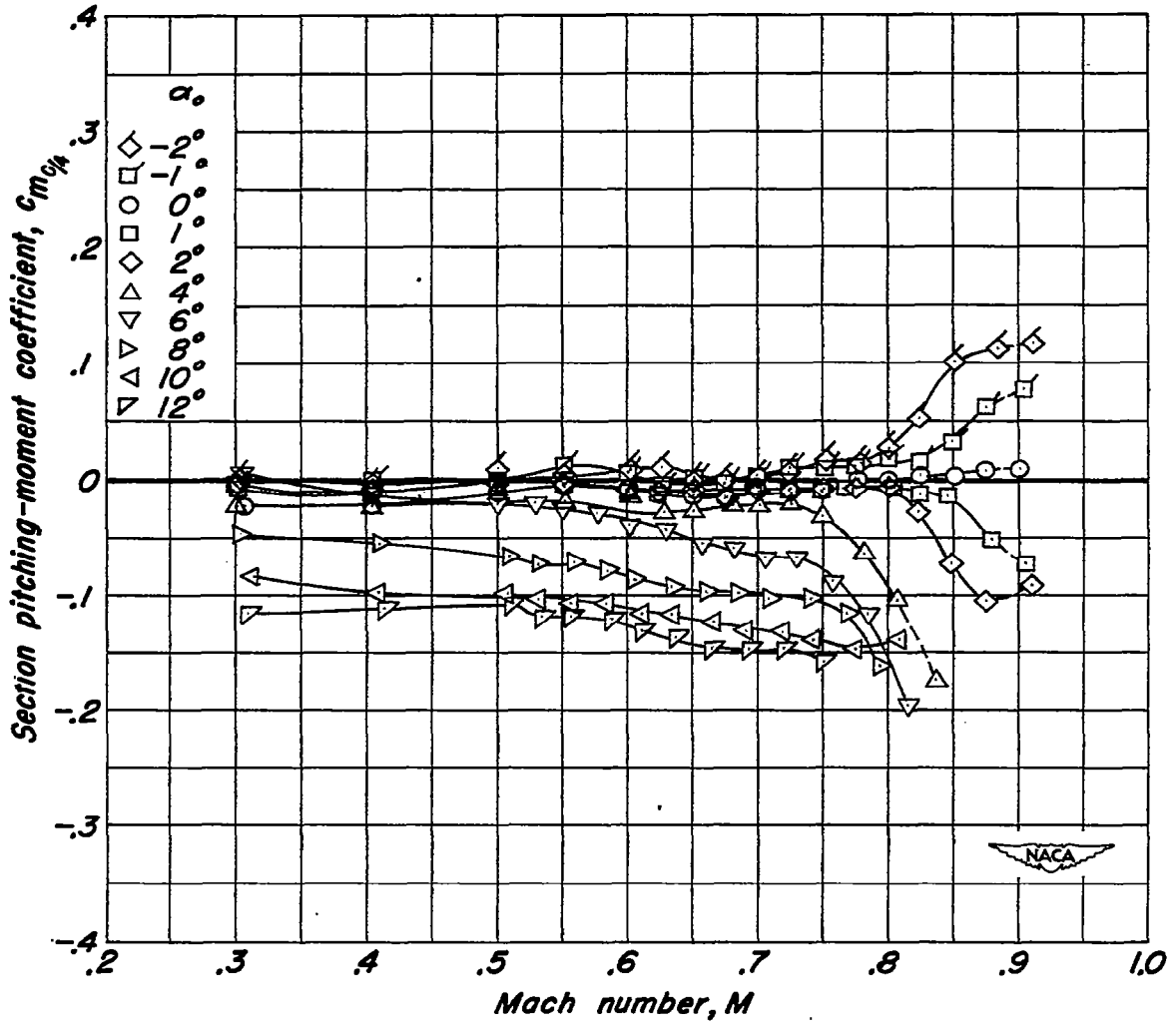

(e) NACA 0006-0.27 40/1.575 Airfoil.

Figure 5.- Continued.

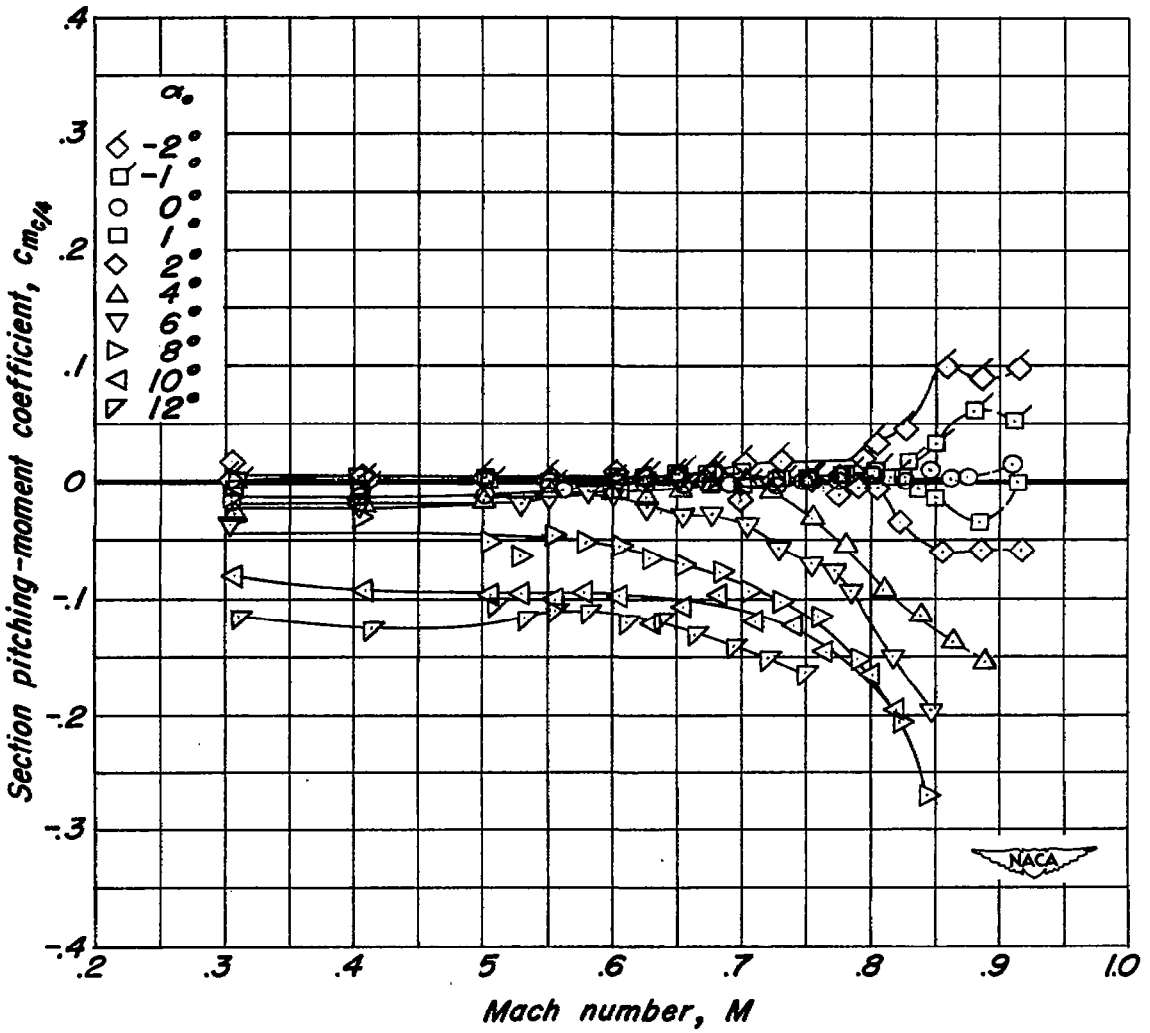

(f) NACA 0008-1.10 40/1.575 Airfoil.

Figure 5.- Continued.

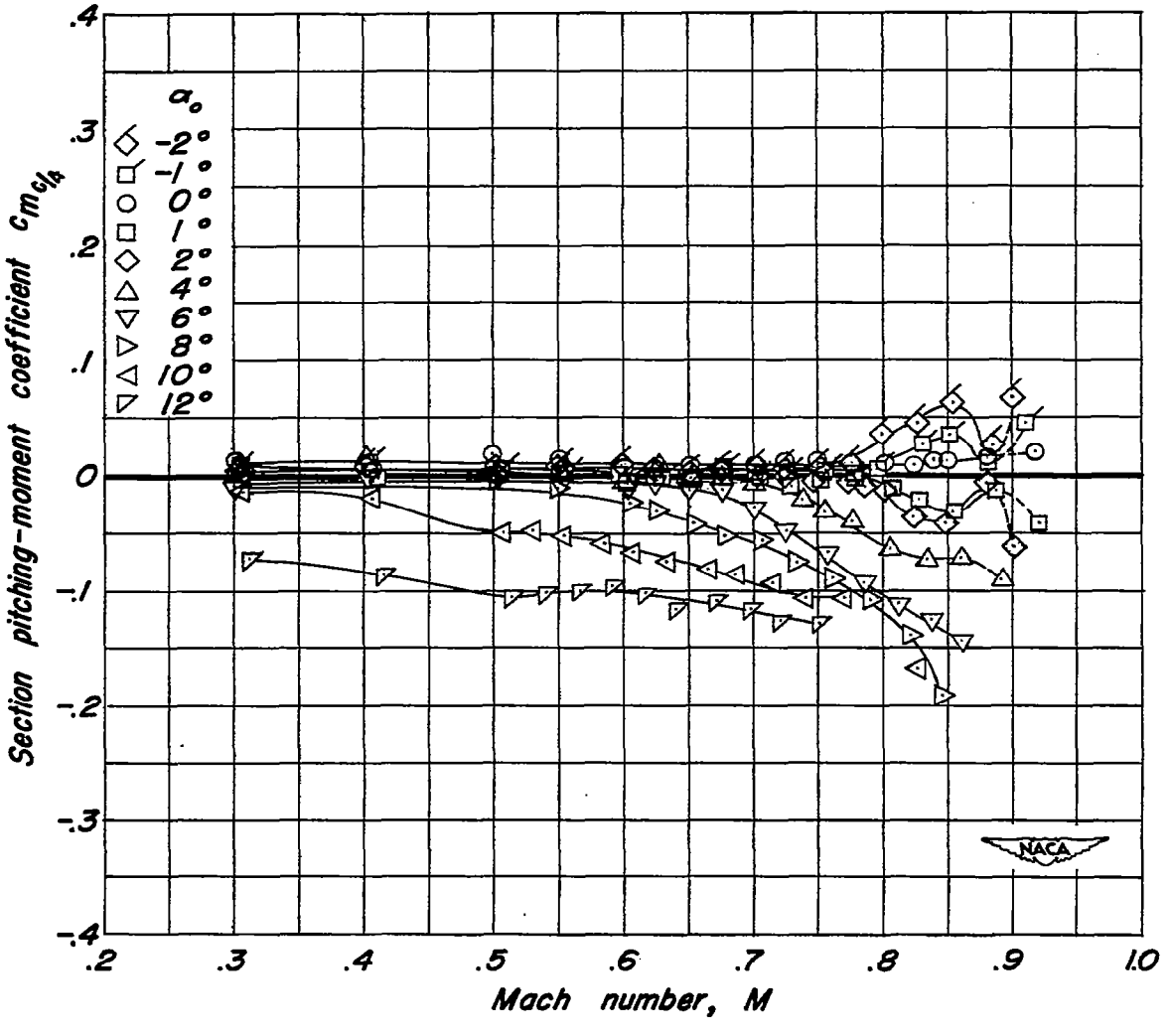

(g) NACA 0010-1.10 40/1.575 Airfoil.

Figure 5.- Concluded.

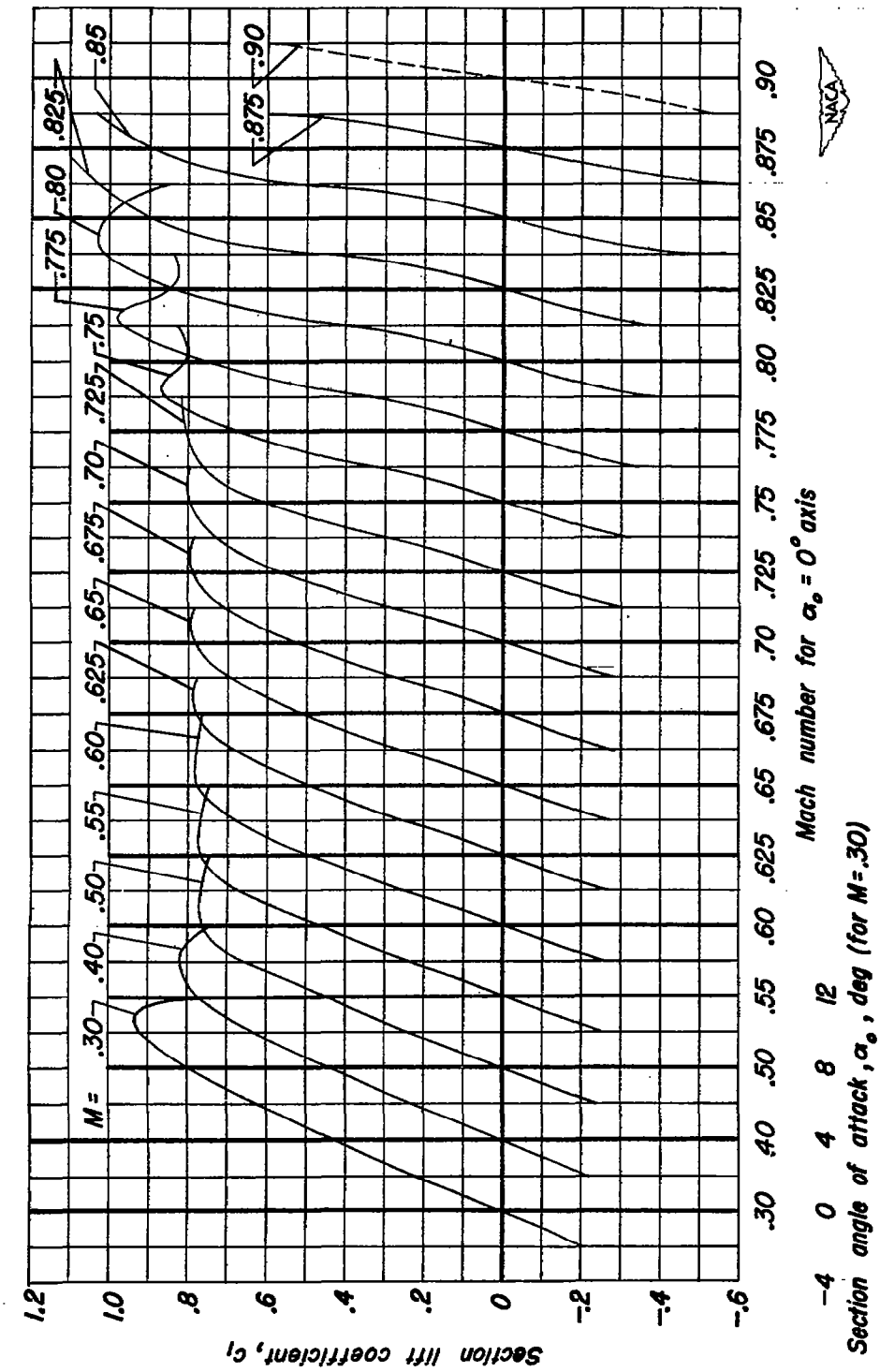

(a) NACA 0004-1.10 40/1.575 Airfoil.

Figure 6.- Variation of section lift coefficient with angle of attack at constant Mach numbers.

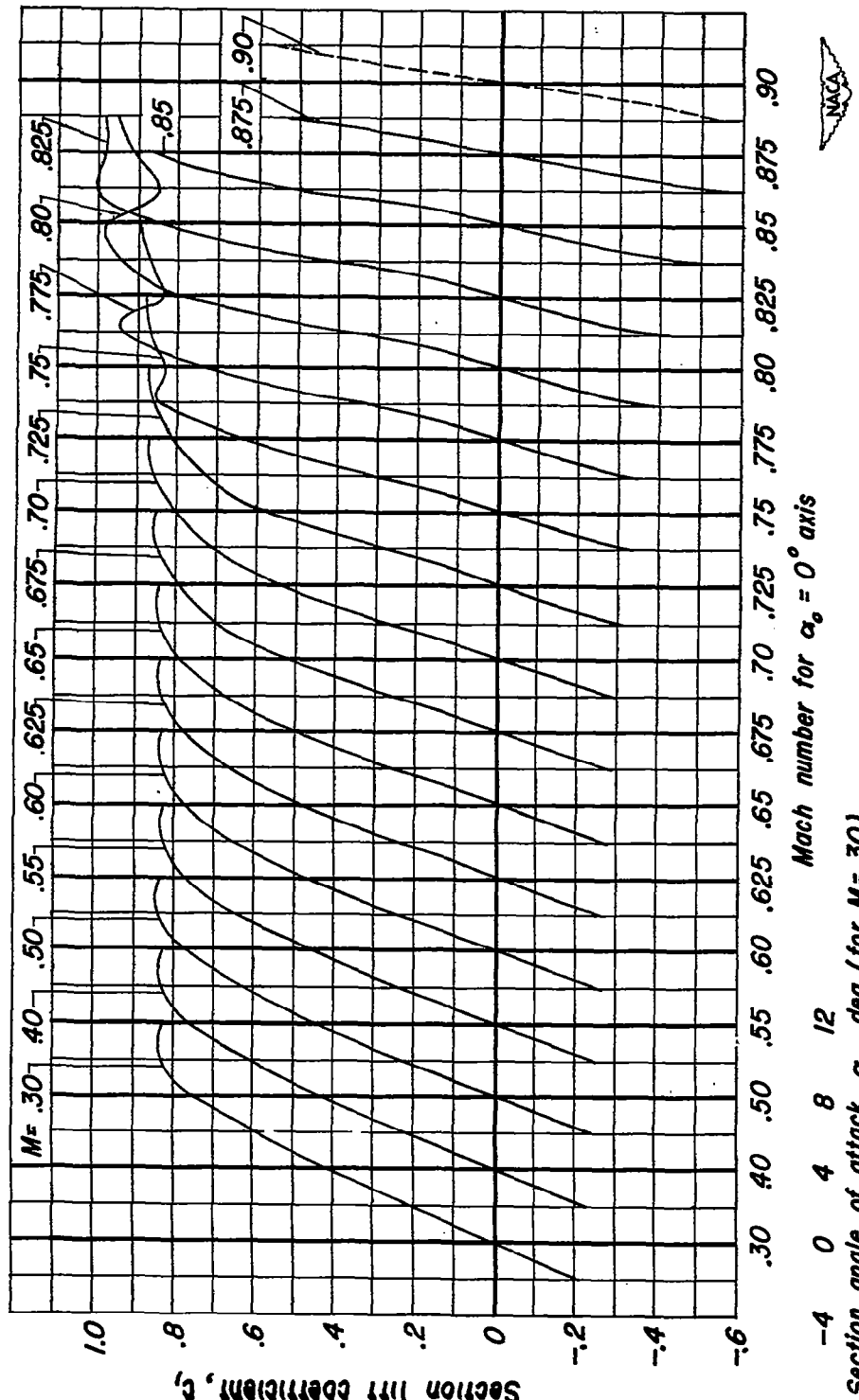

(b) NACA 0004-3.30 40/1.575 Airfoil.

Figure 6.- Continued.

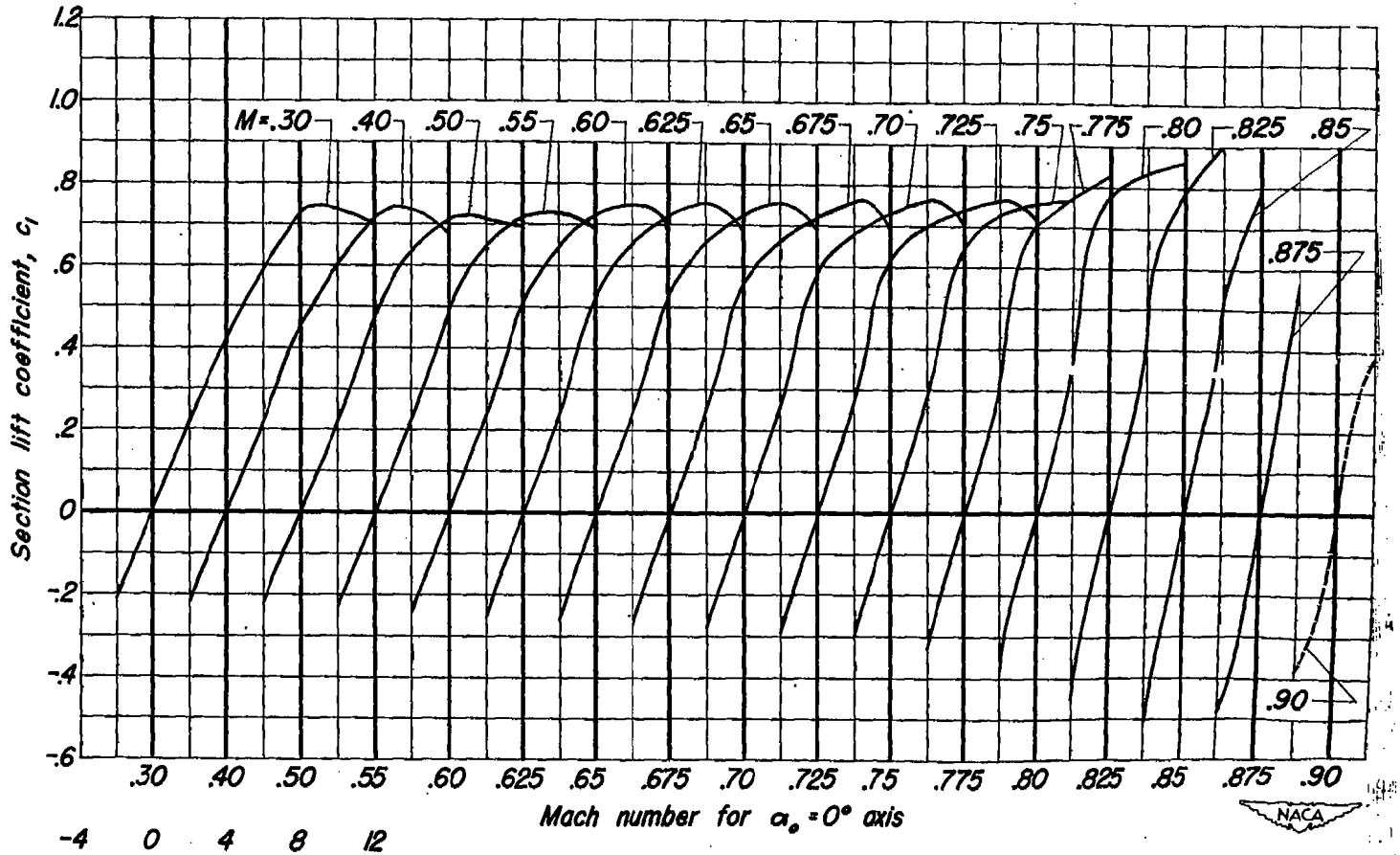

(c) NACA 0006-1.10 40/1.575 Airfoil.

Figure 6.- Continued.

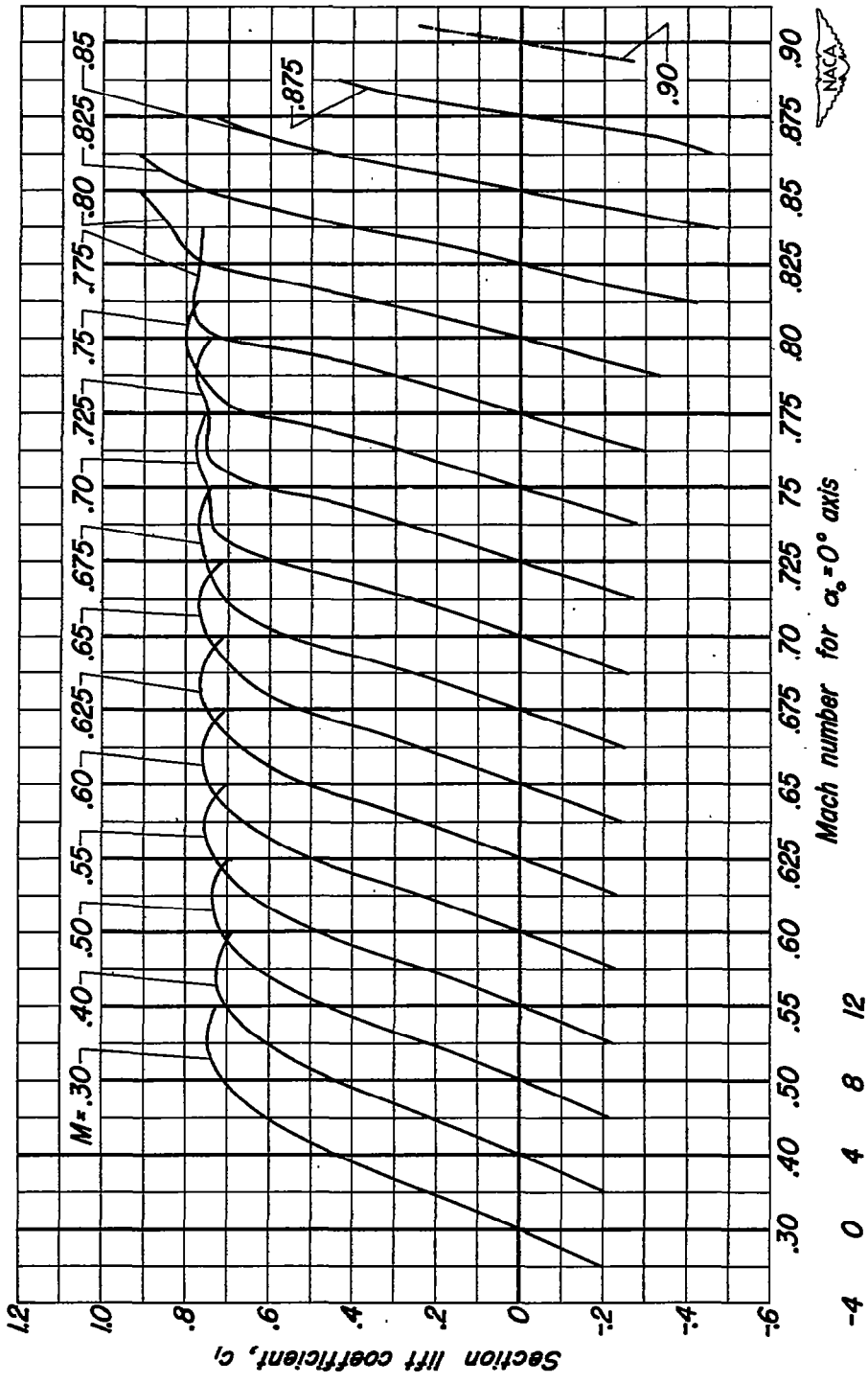

(d) NACA 0006-0.70 40/1.575 Airfoil.

Figure 6.- Continued.

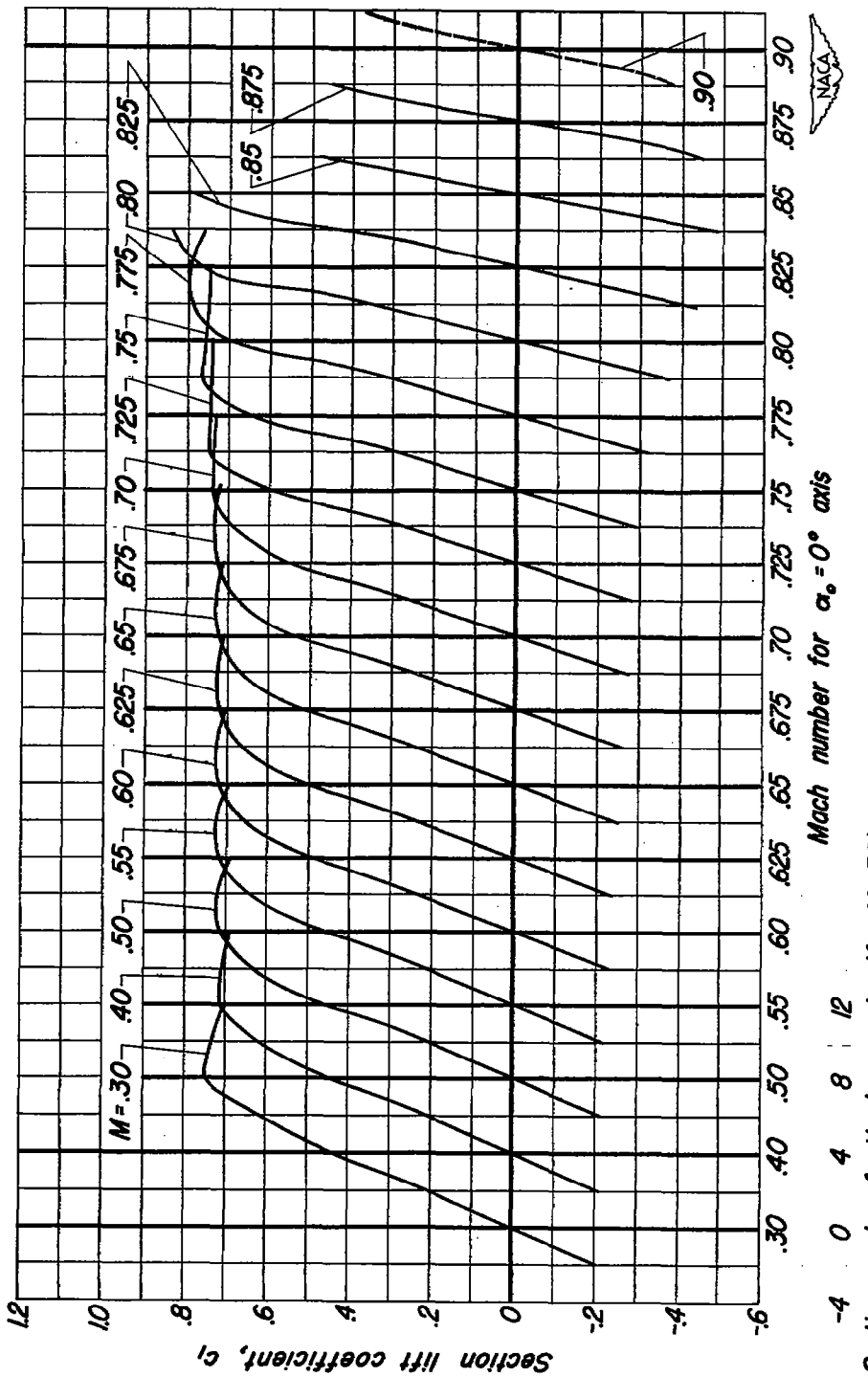

(e) NACA 0006-0.27 40/1.575 Airfoil.

Figure 6.- Continued.

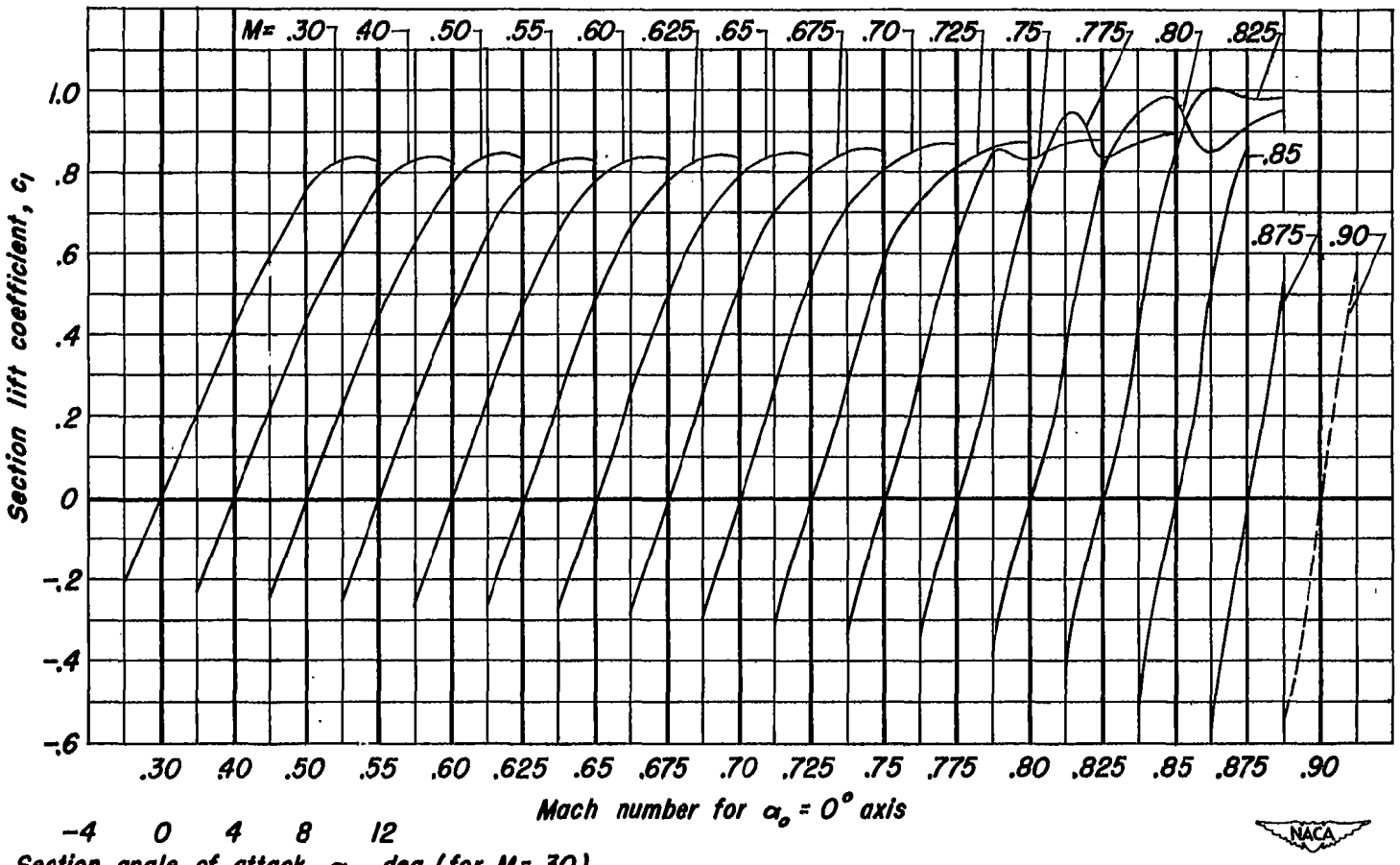

(b) NACA 0004-3.30 40/1.575 Airfoil.

Figure 6.- Continued.

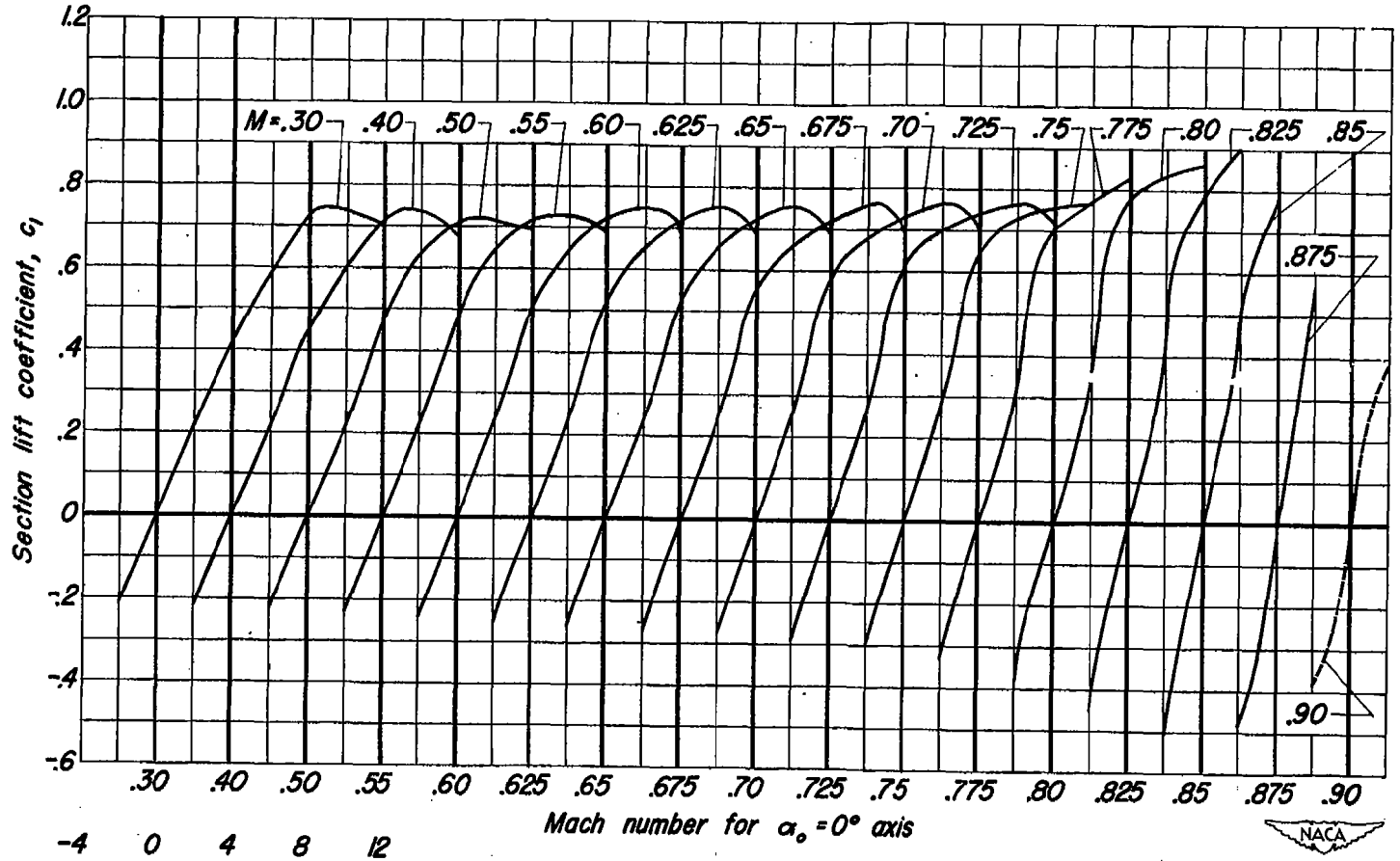

(c) NACA 0006-1.10 40/1.575 Airfoil.

Figure 6.- Continued.

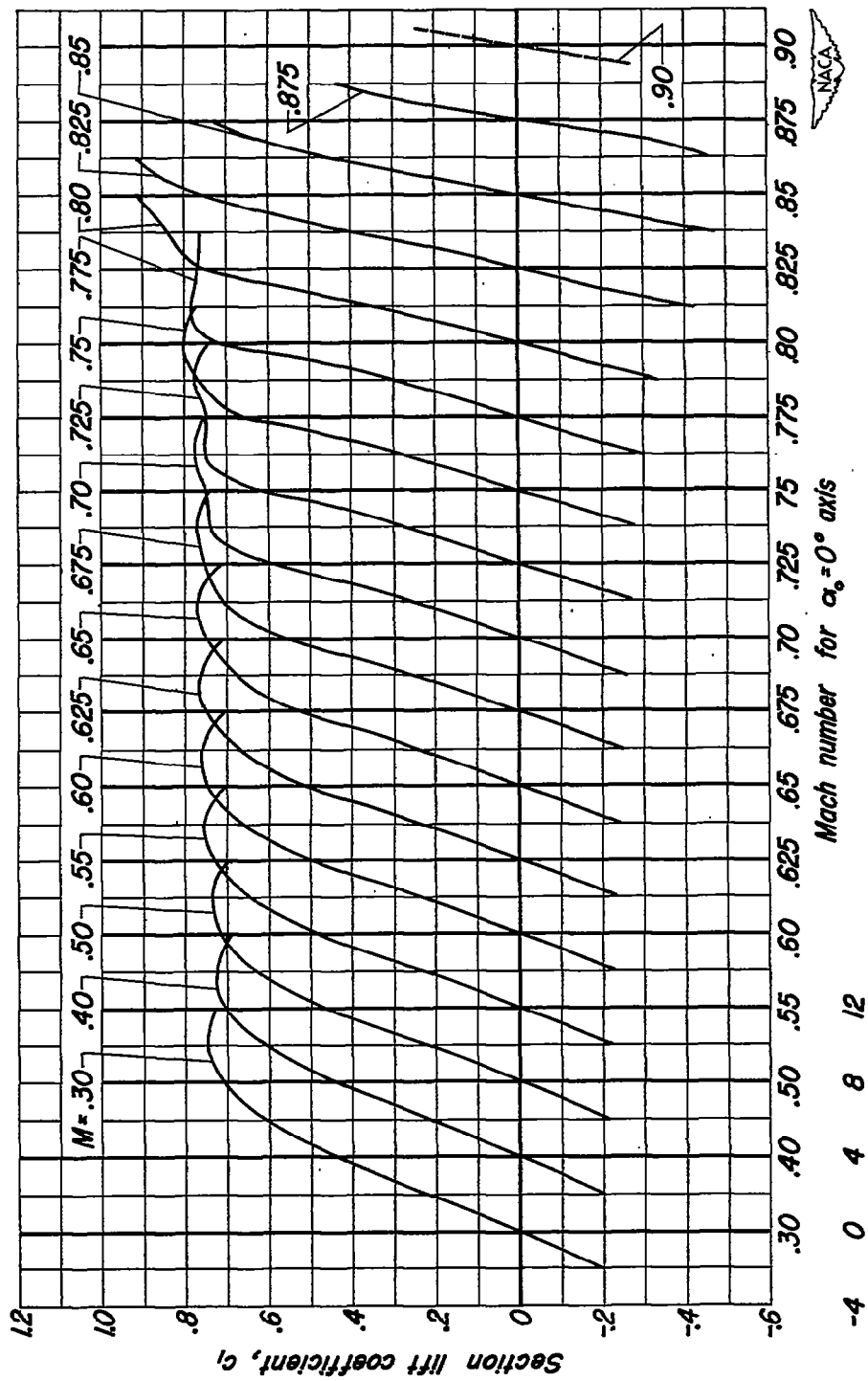

(d) NACA 0006-0.70 40/1.575 Airfoil.

Figure 6.- Continued.

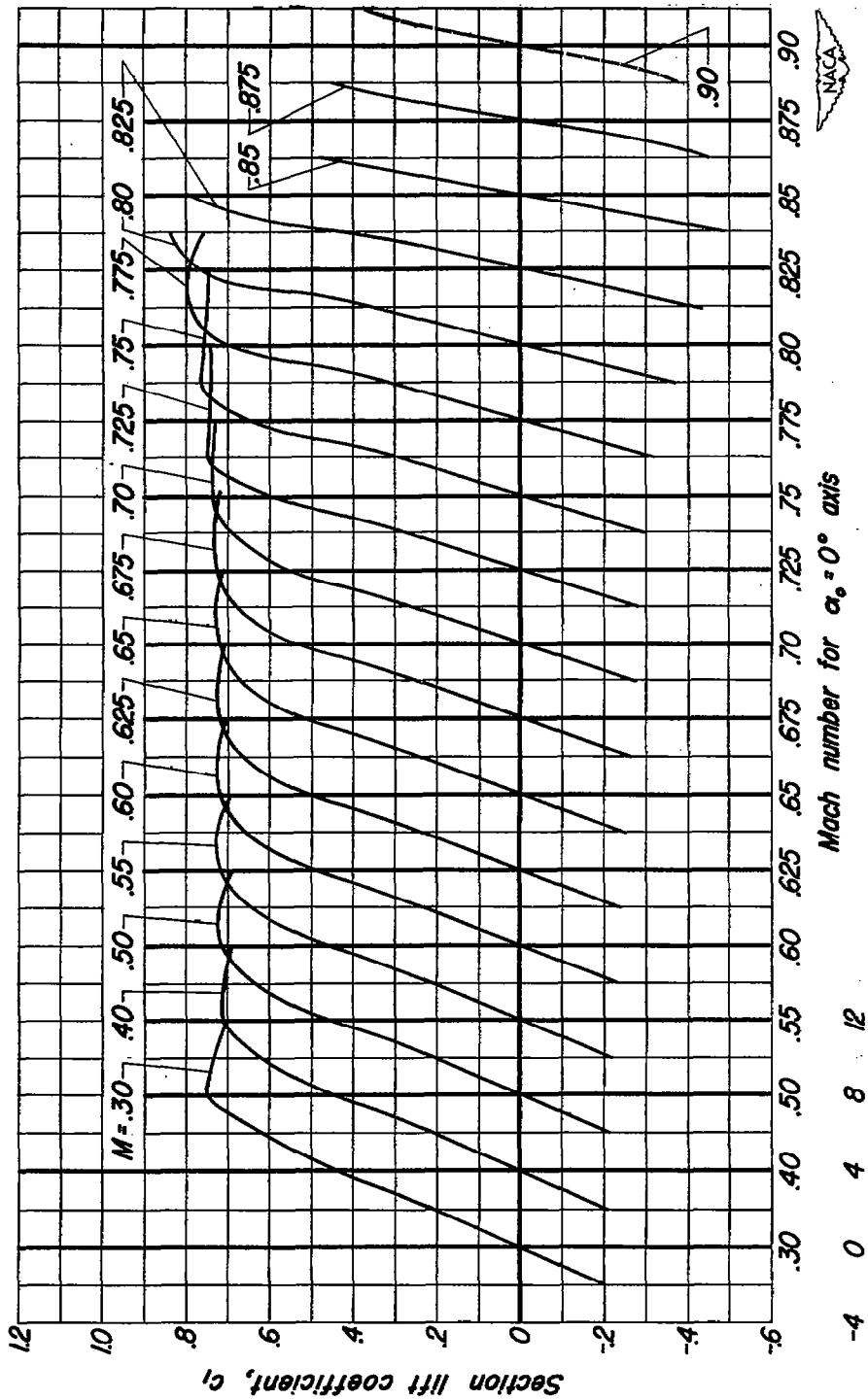

(e) NACA 0006-0.27 40/1.575 Airfoil.

Figure 6.- Continued.

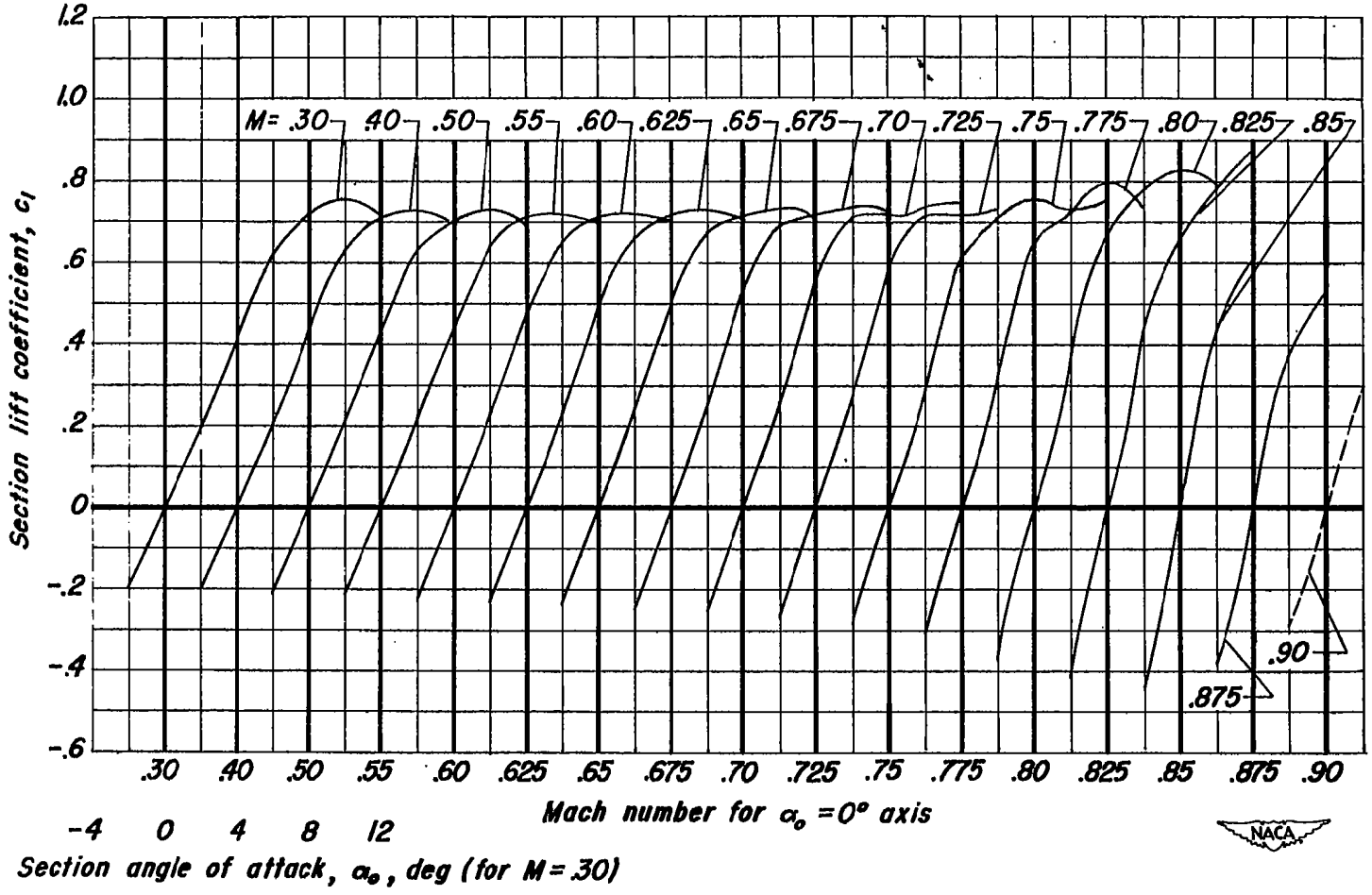

(f) NACA 0008-1.10 40/1.575 Airfoil.

Figure 6.- Continued.

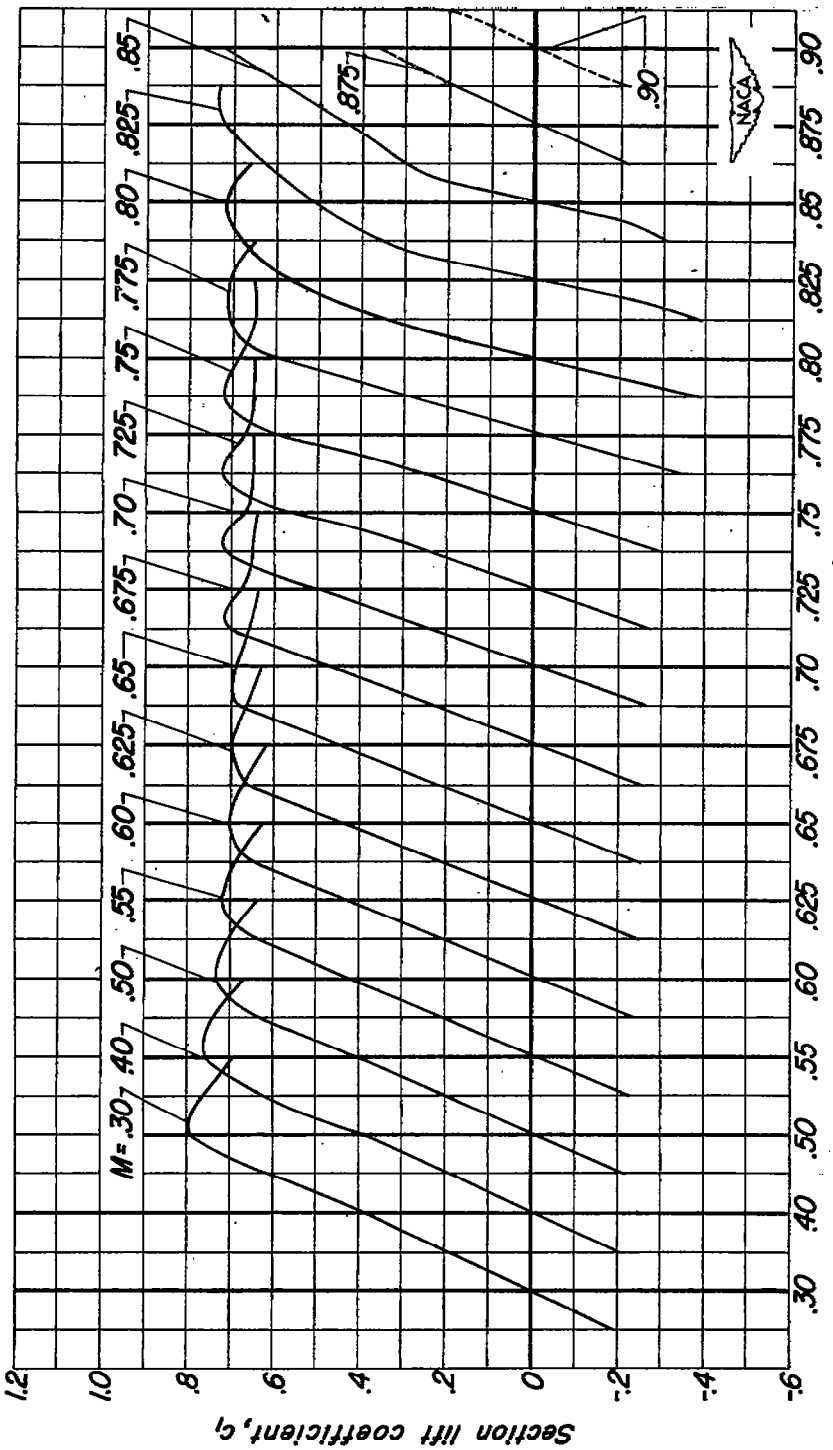

(g) NACA 0010-1.10 40/1.575 airfoil section.

Figure 6.- Concluded.

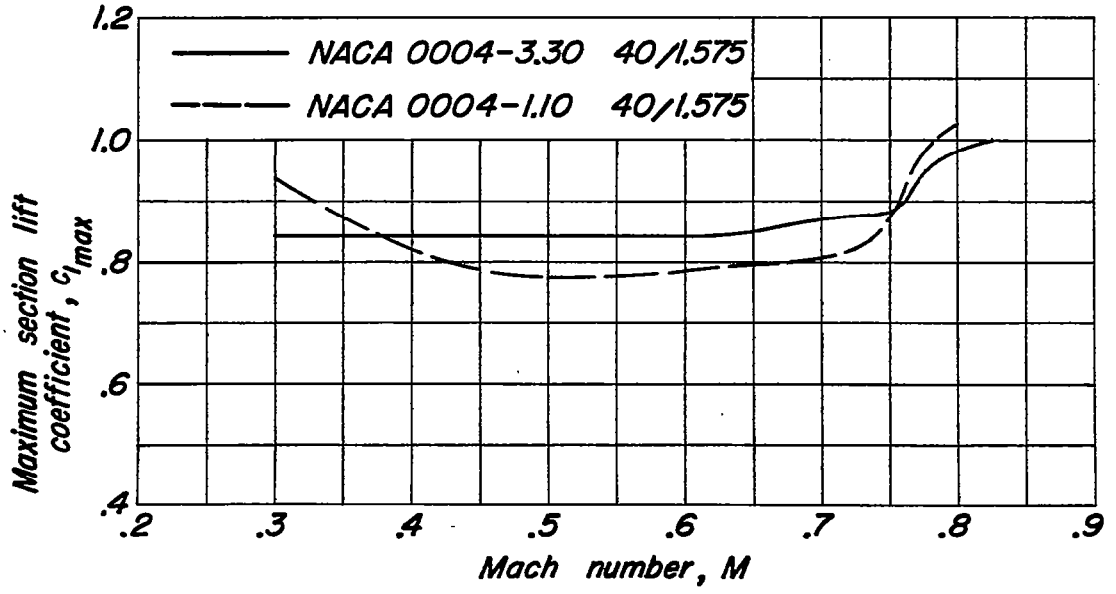

(a) Maximum thickness-chord ratio of 0.04.

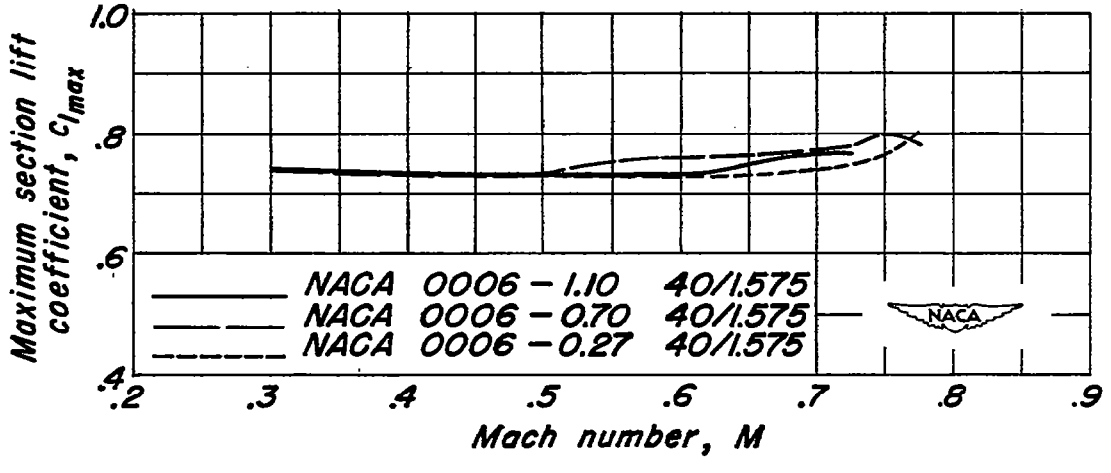

(b) Maximum thickness-chord ratio of 0.06.

Figure 7.- Effect of change of leading-edge radius on the variation of maximum section lift coefficient with Mach number.

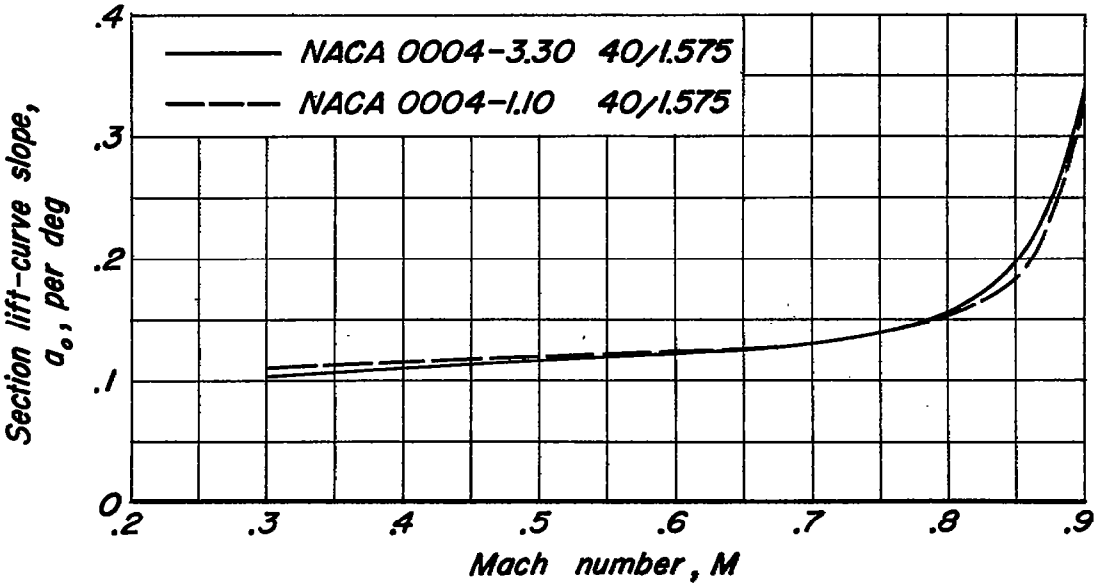

(a) Maximum thickness-chord ratio of 0.04.

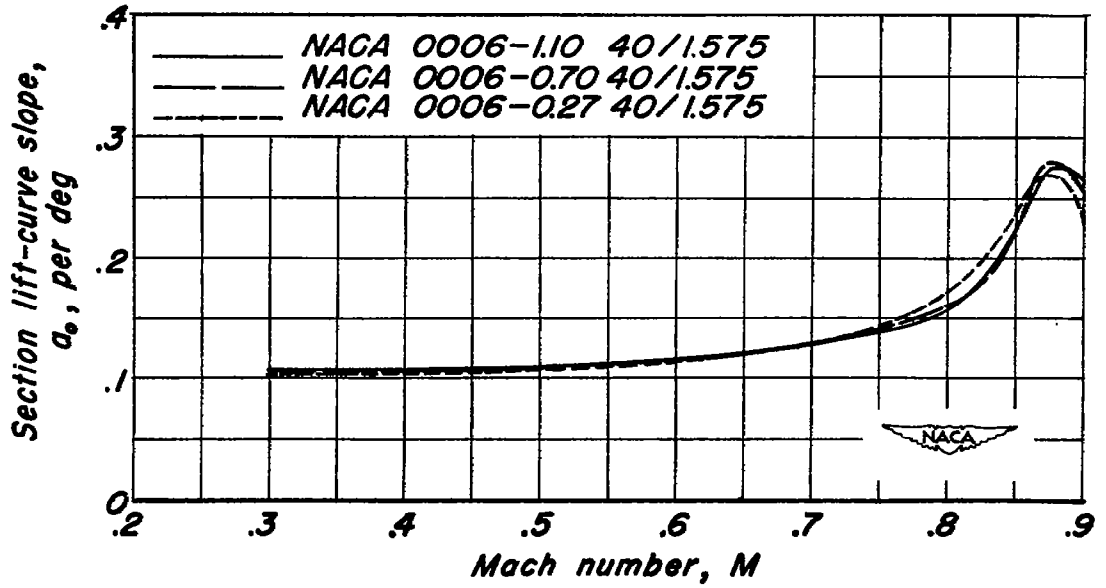

(b) Maximum thickness-chord ratio of 0.06.

Figure 8.- Effect of change of leading-edge radius on the variation of section lift-curve slope with Mach number.

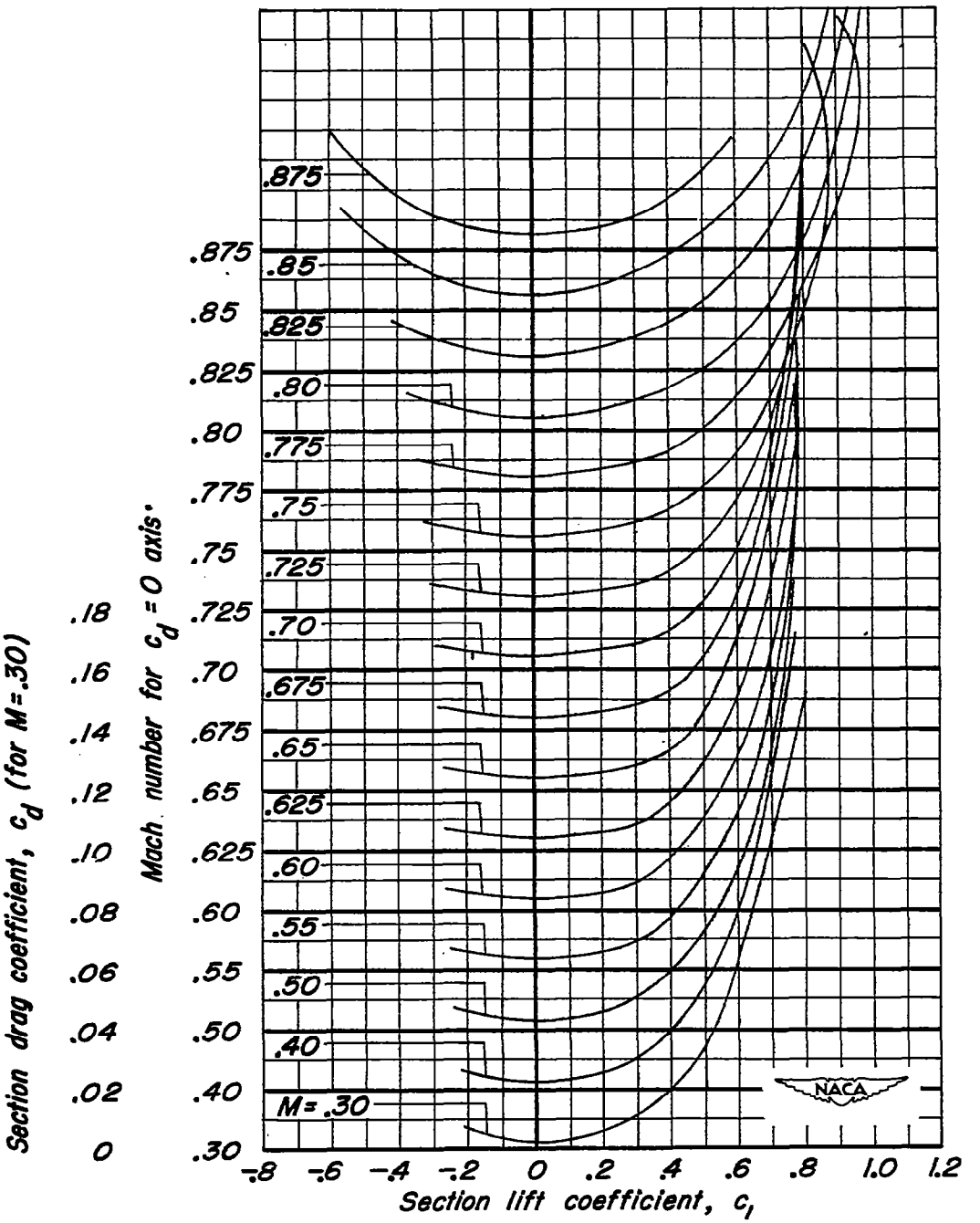

(a) NACA 0004-1.10 40/1.575 Airfoil.

Figure 9.- Variation of section drag coefficient with section lift coefficient at constant Mach numbers.

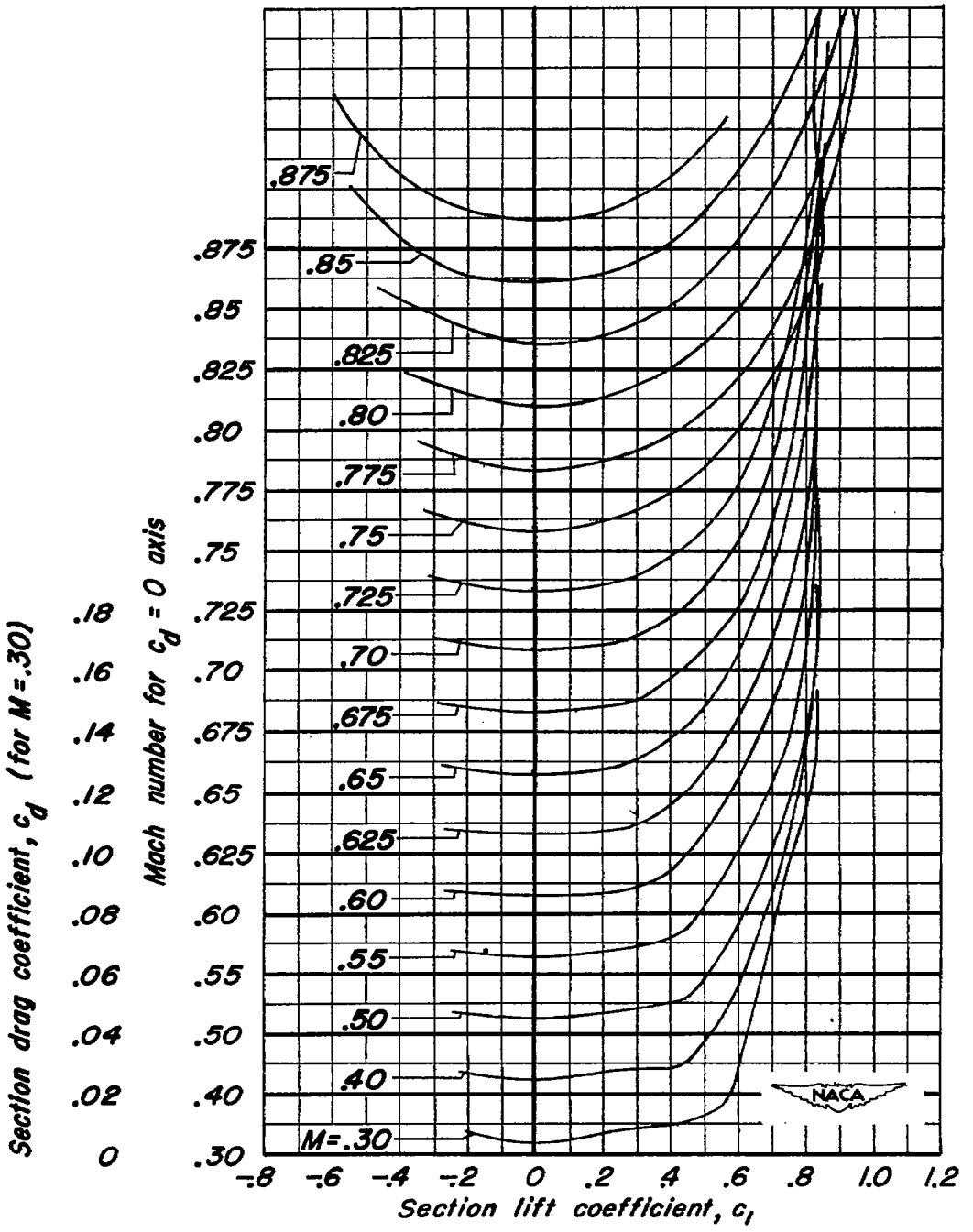

(b) NACA 0004-3.30 40/1.575 Airfoil.

Figure 9.- Continued.

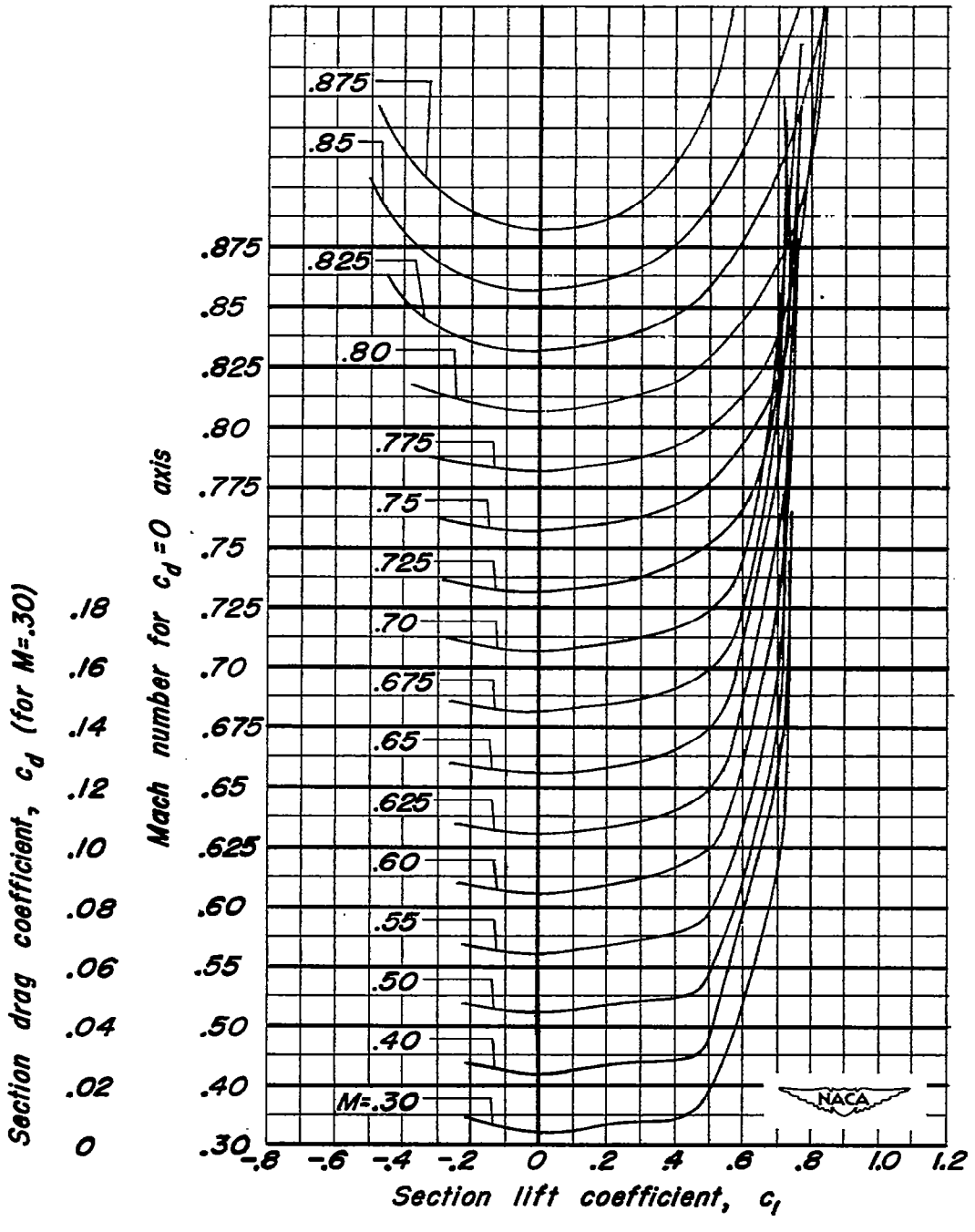

(c) NACA 0006-1.10 40/1.575 Airfoil.

Figure 9.- Continued.

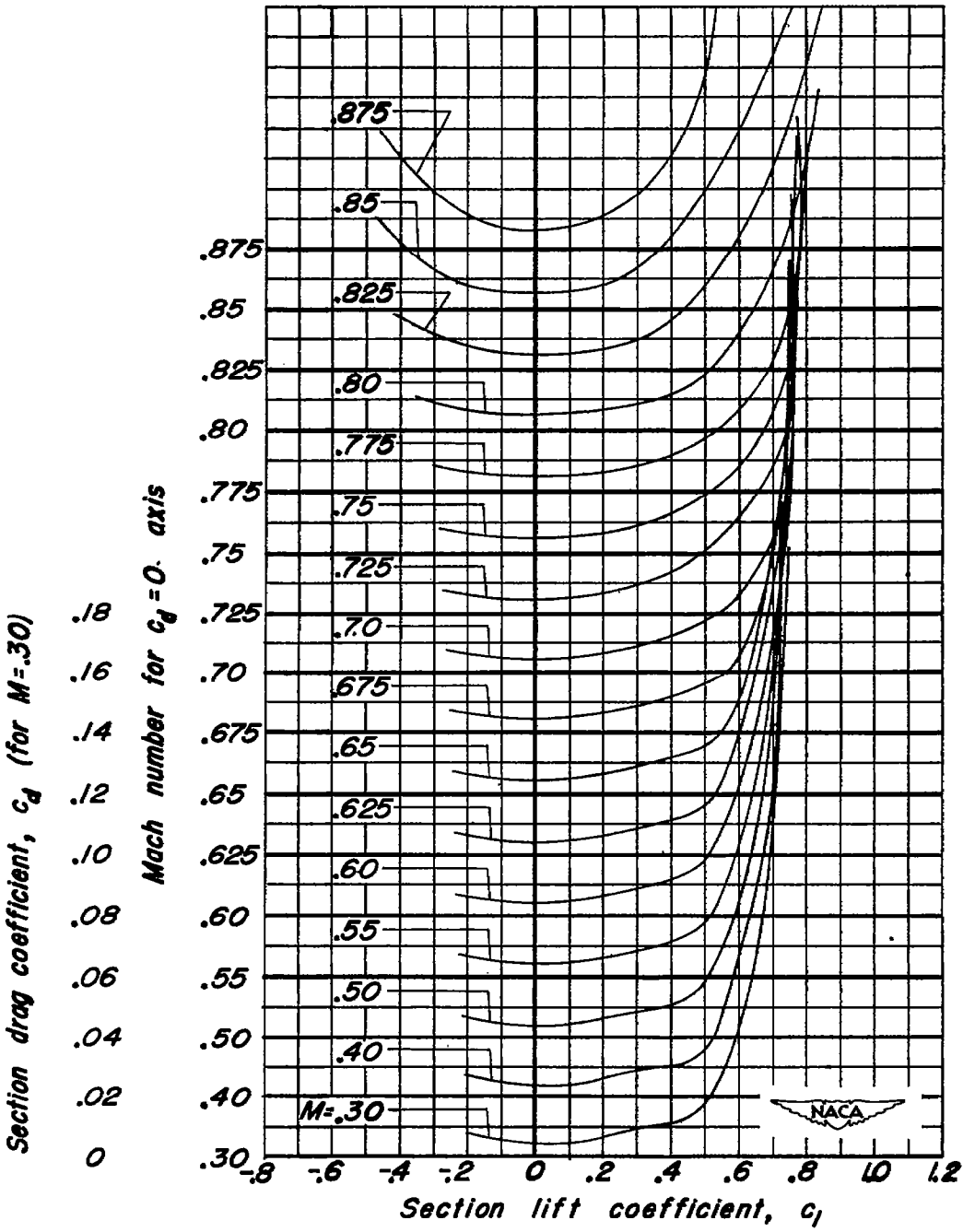

(d) NACA 0006-0.70 40/1.575 Airfoil.

Figure 9.- Continued.

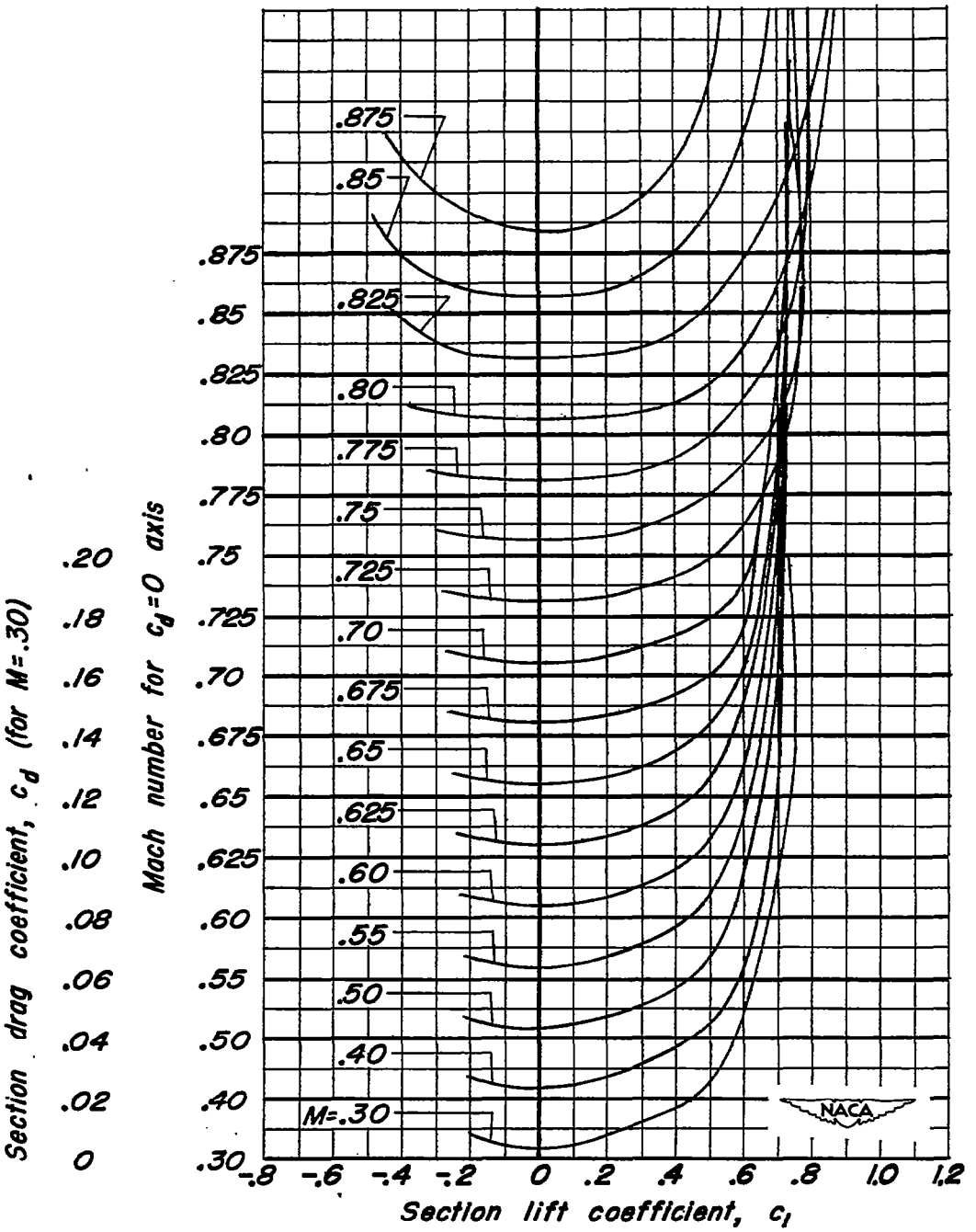

(e) NACA 0006-0.27 40/1.575 Airfoil.

Figure 9.- Continued.

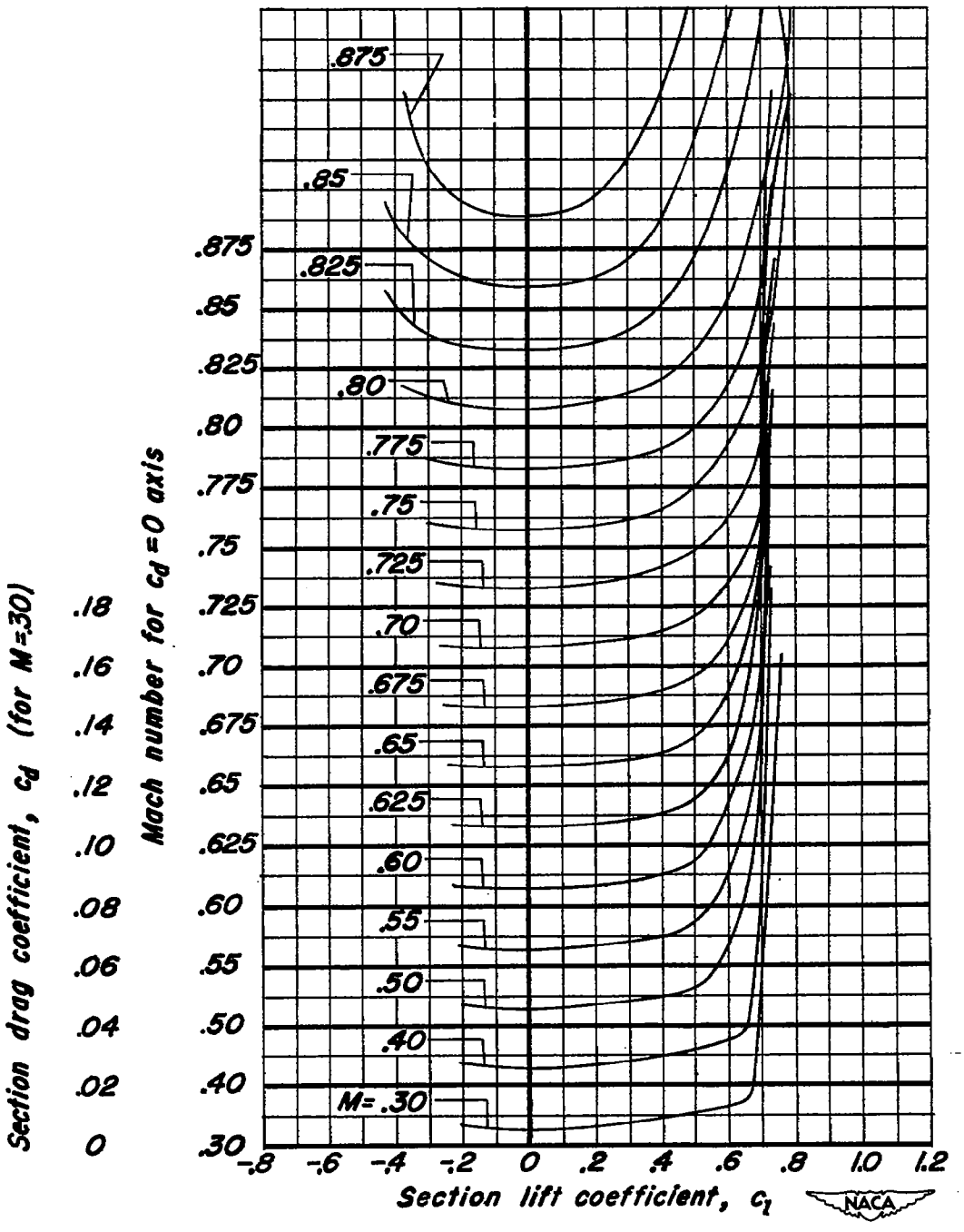

(f) NACA 0008-1.10 40/1.575 Airfoil.

Figure 9.– Continued.

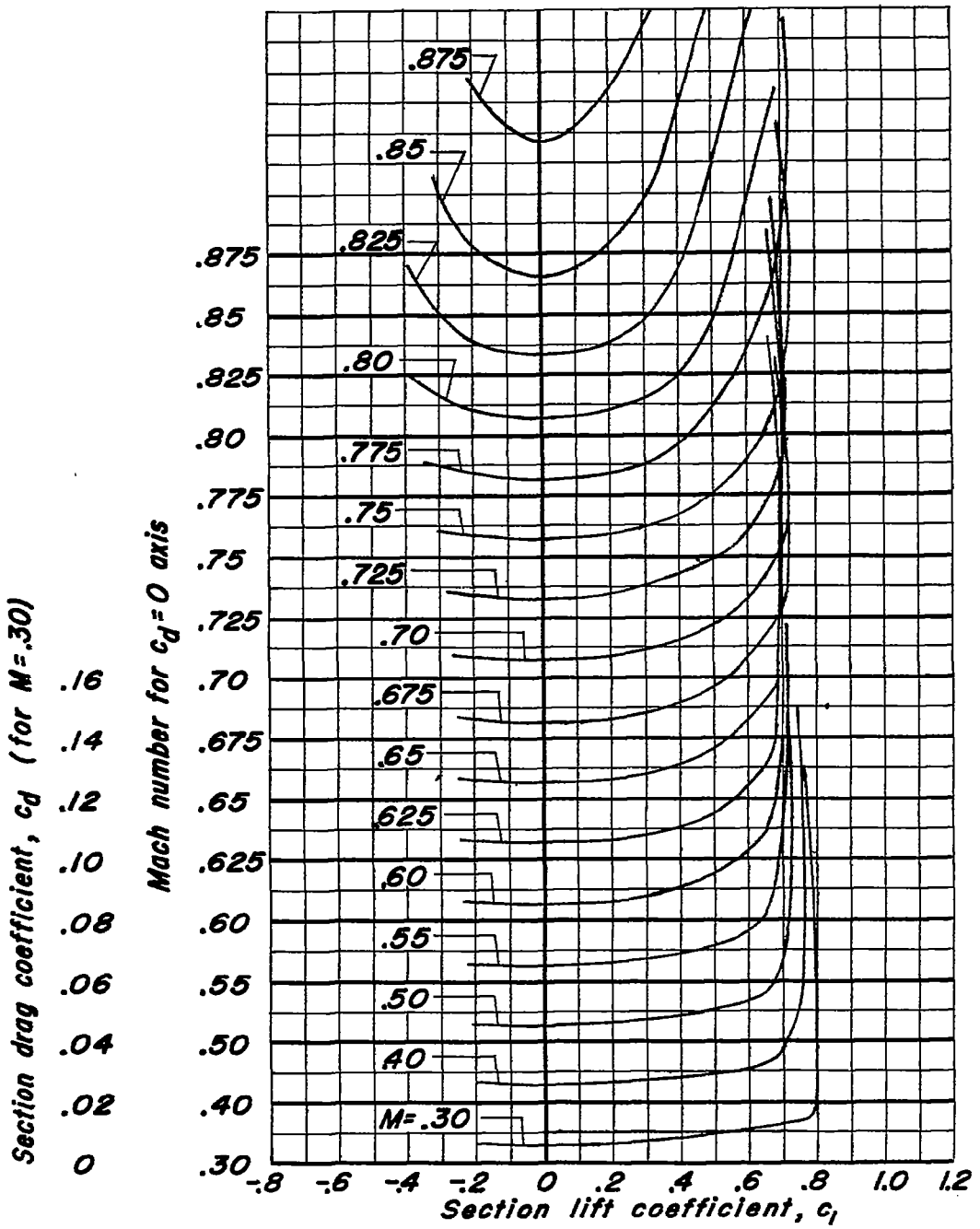

(g) NACA 0010-1.10 40/1.575 airfoil.

Figure 9.- Concluded.

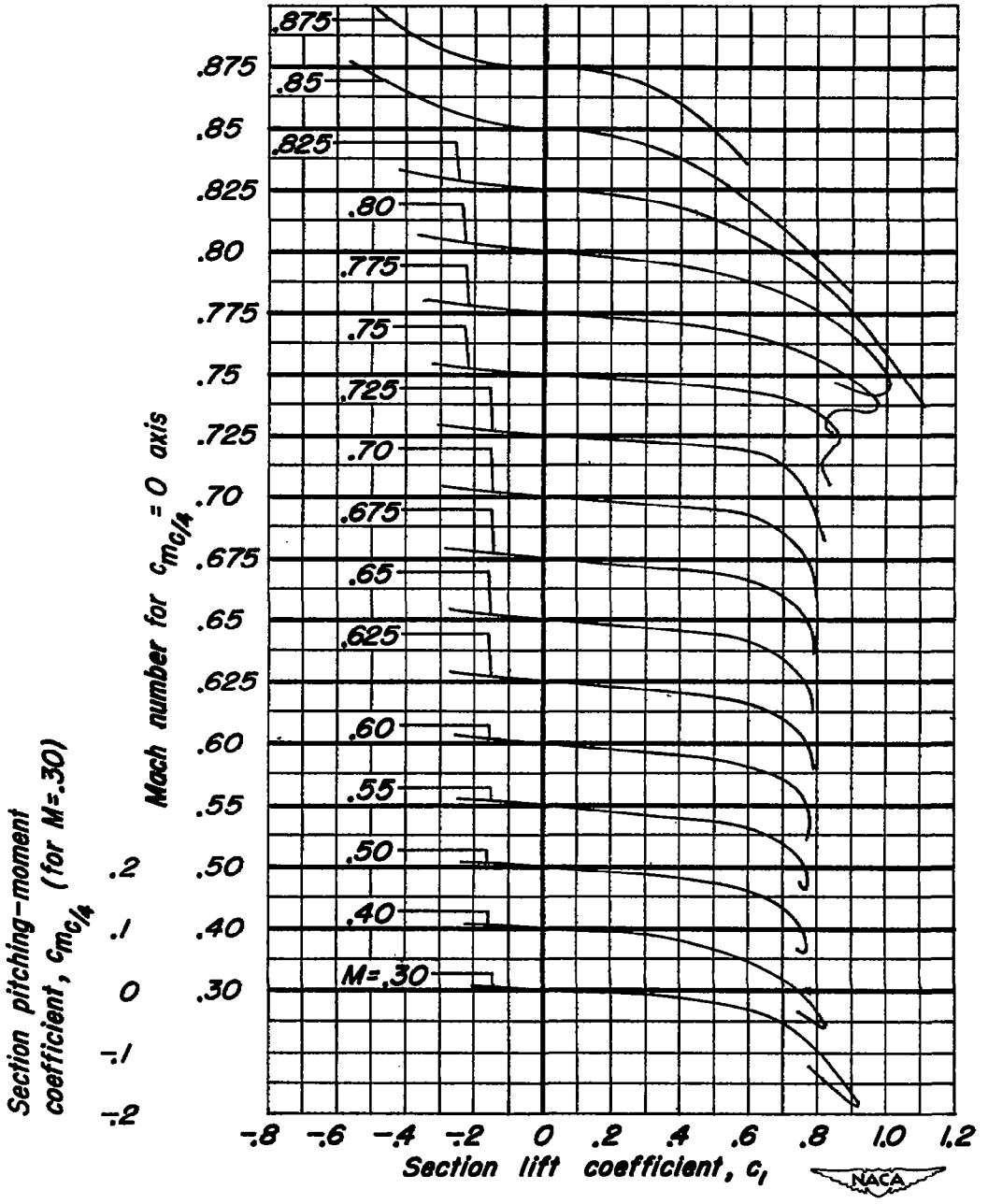

(a) NACA 0004-1.10 40/1.575 Airfoil.

Figure 10.- Variation of section pitching-moment coefficient with section lift coefficient at constant Mach numbers.

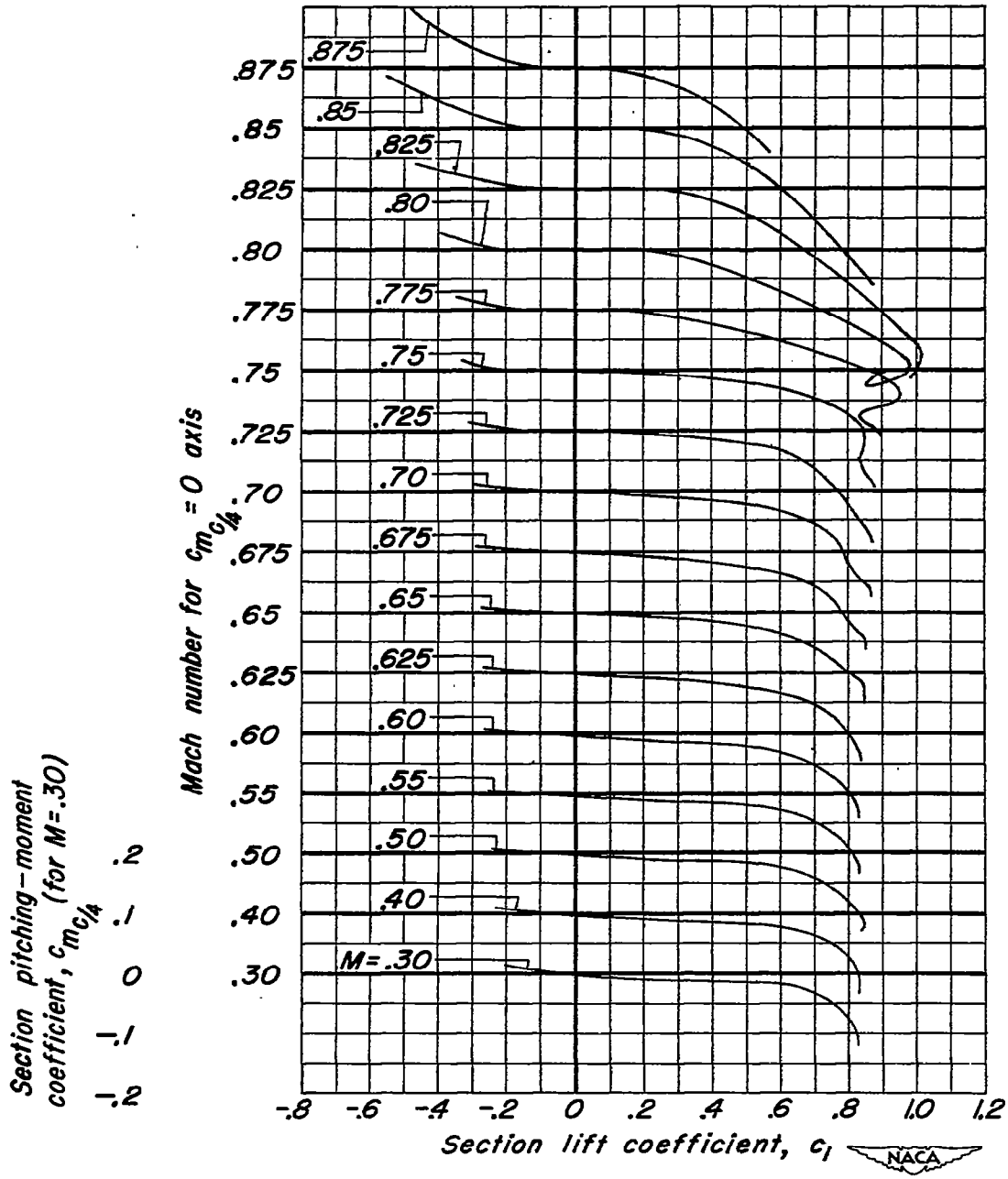

(b) NACA 0004-3.30 40/1.575 Airfoil.

Figure 10.- Continued.

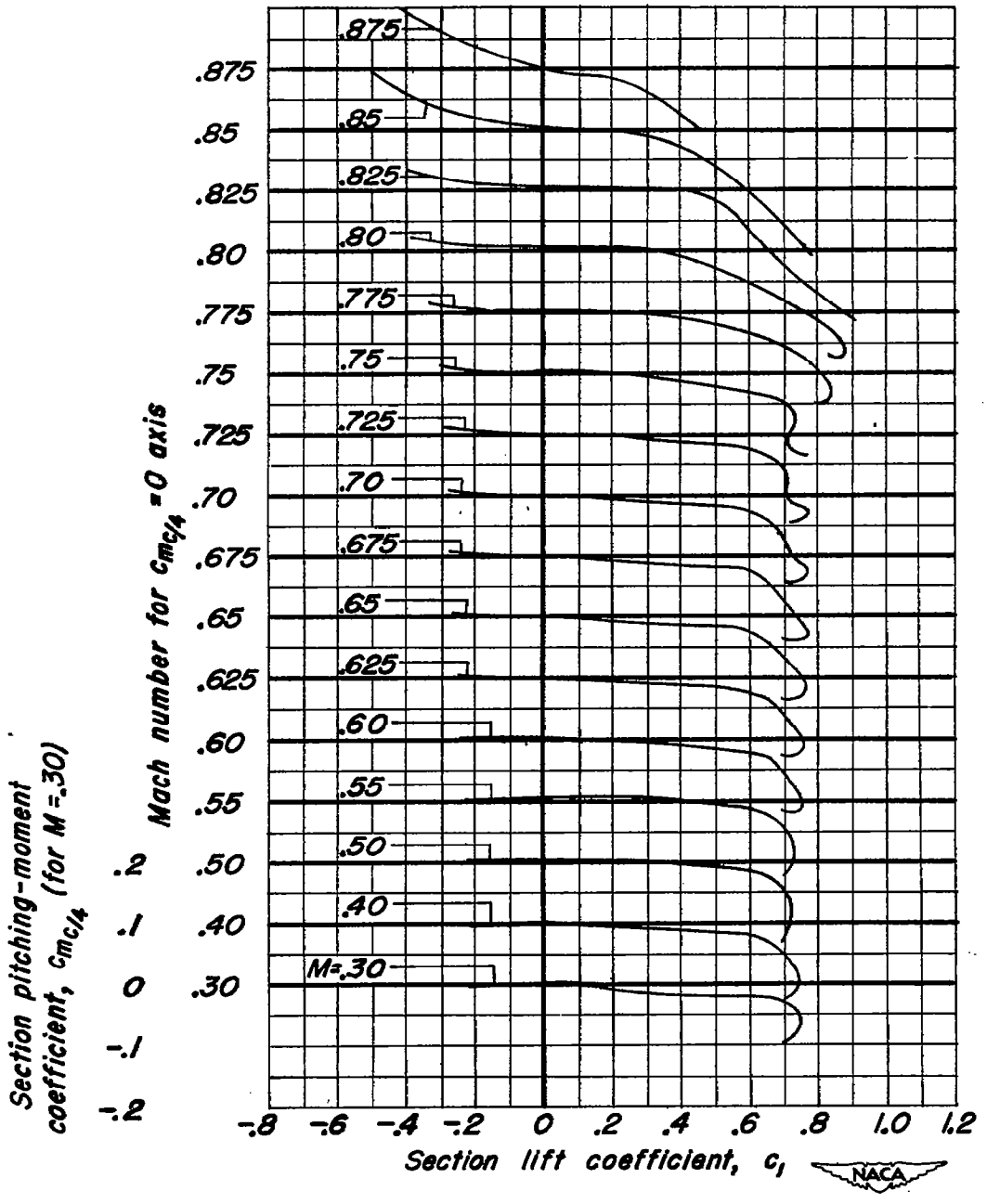

(c) NACA 0006-1.10 40/1.575 Airfoil.

Figure 10.- Continued.

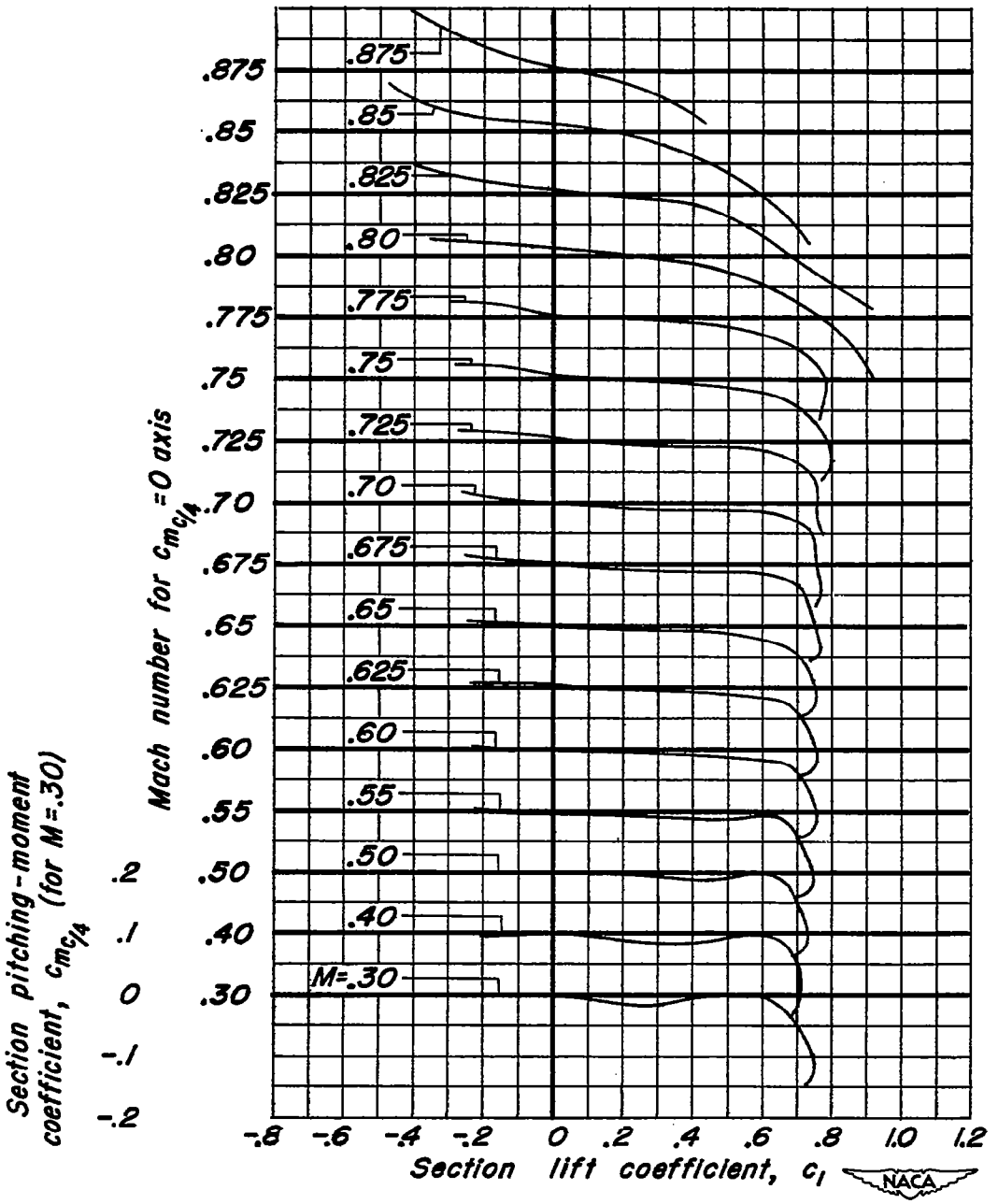

(d) NACA 0006-0.70 40/1.575 Airfoil.

Figure 10.- Continued.

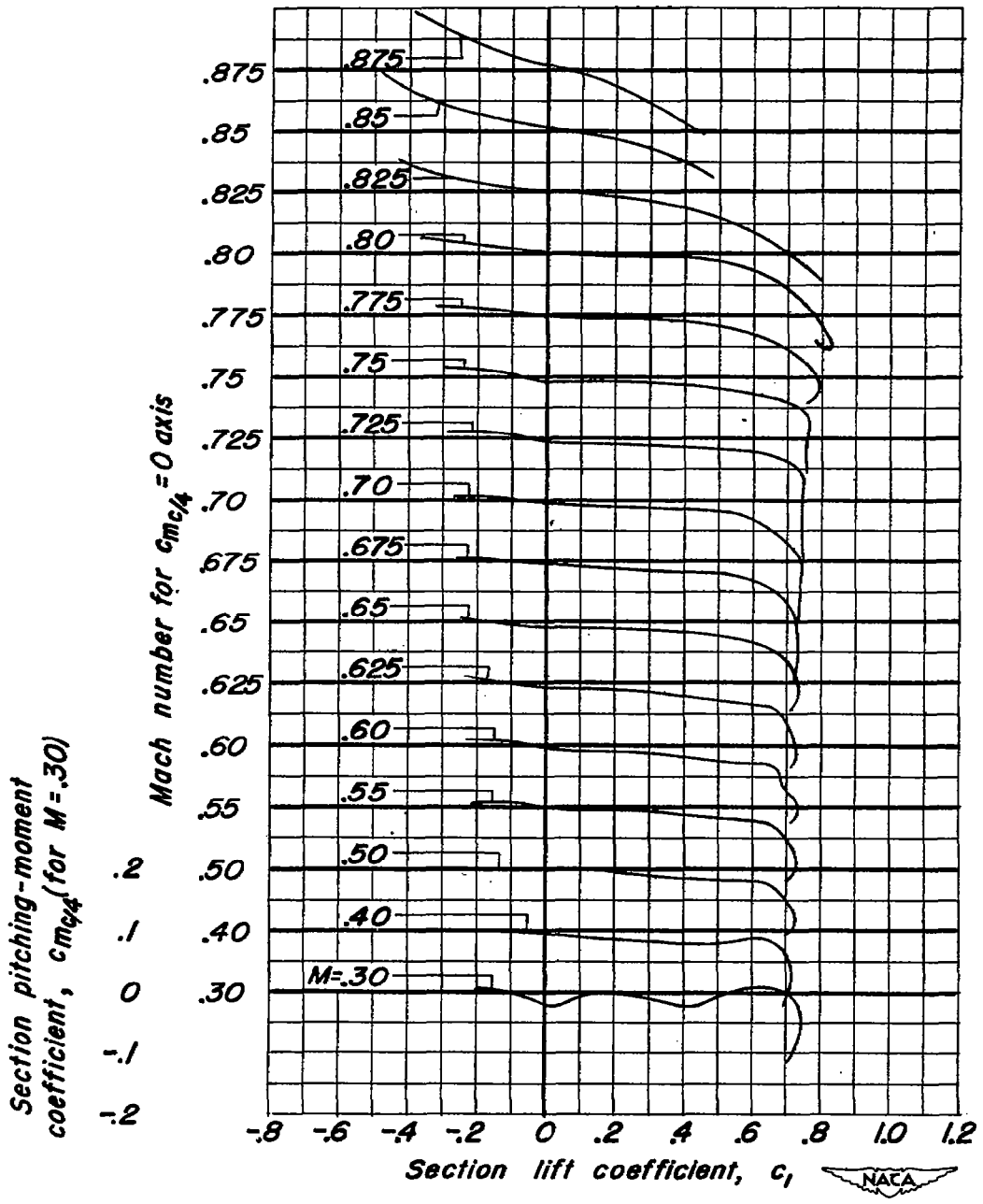

(e) NACA 0006-0.27 40/1.575 Airfoil.

Figure 10.- Continued.

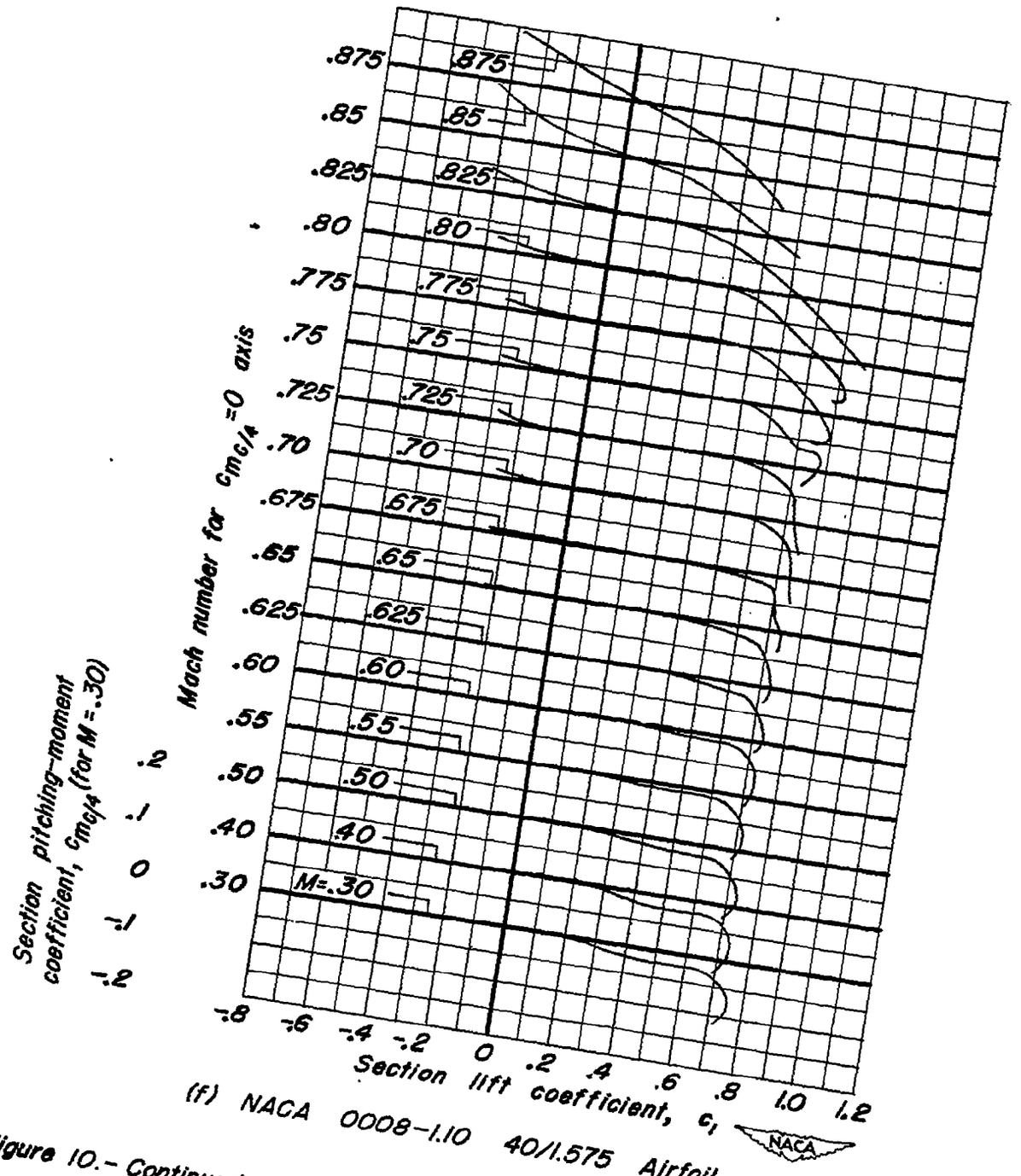

(f) NACA 0008-1.10 40/1.575 Airfoil.

Figure 10.- Continued.

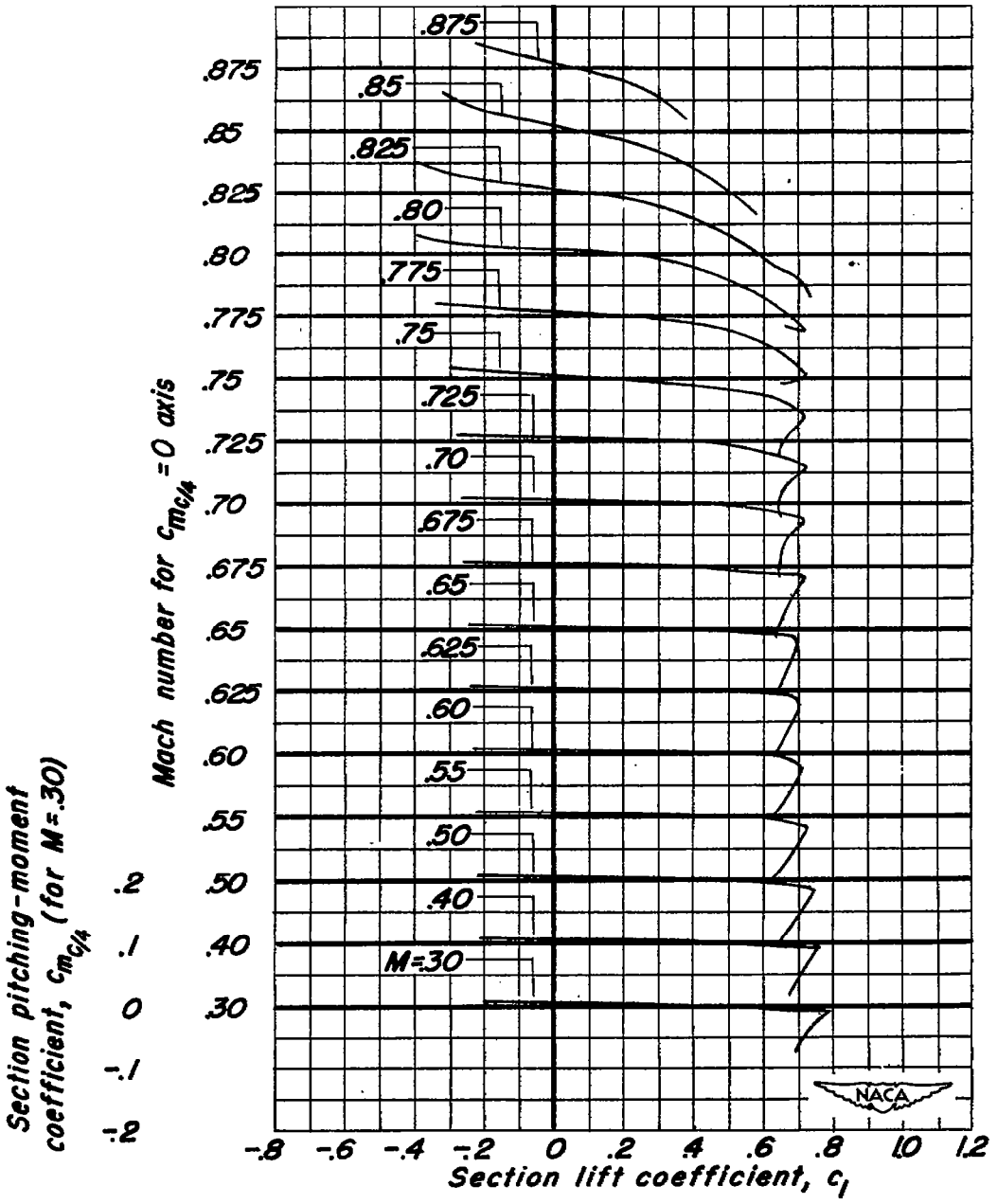

(g) NACA 0010-1.10 40/1.575 airfoil.

Figure 10.- Concluded.

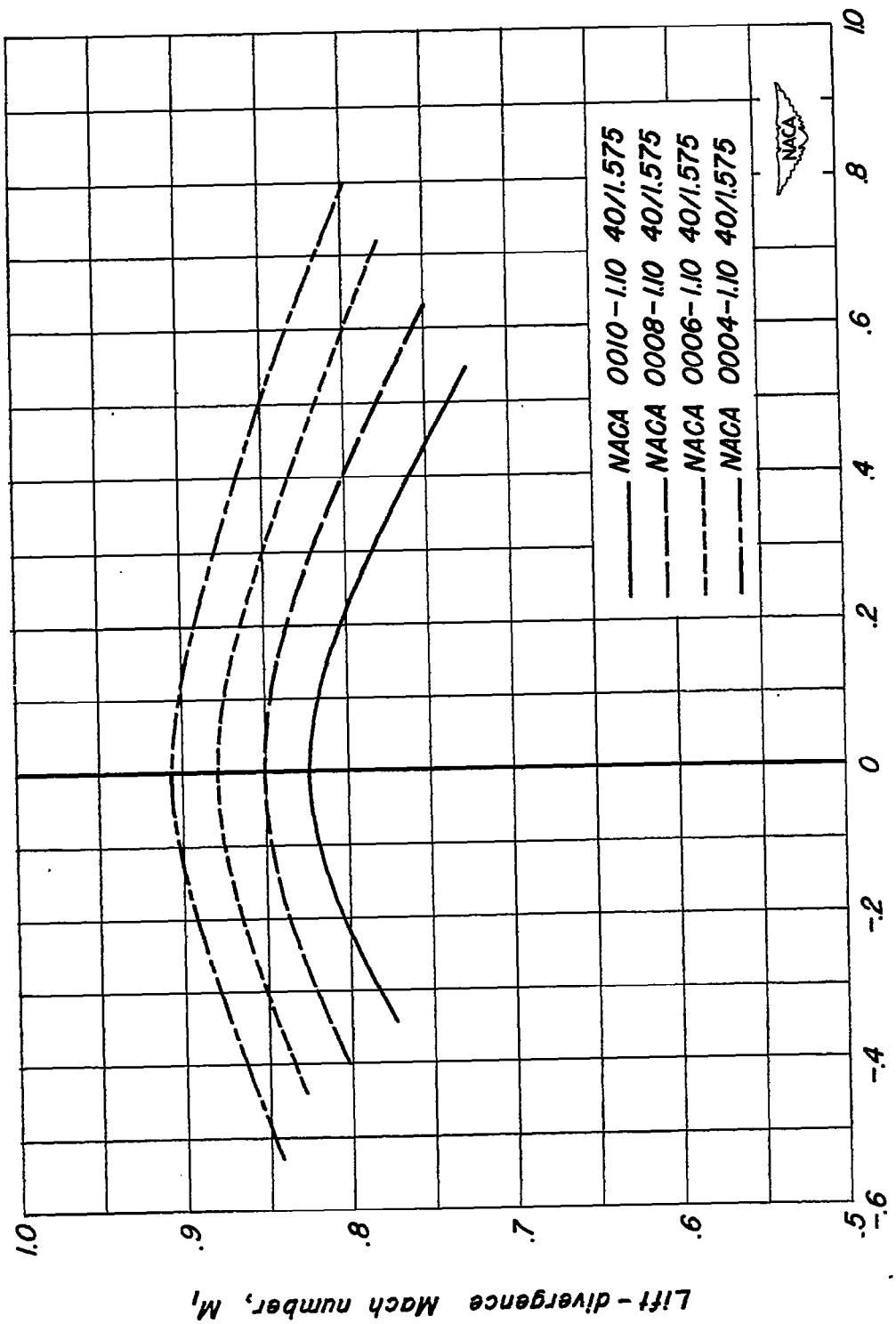

Figure 11.- Effect of change of maximum thickness-chord ratio on the variation of lift-divergence Mach number with section lift coefficient.

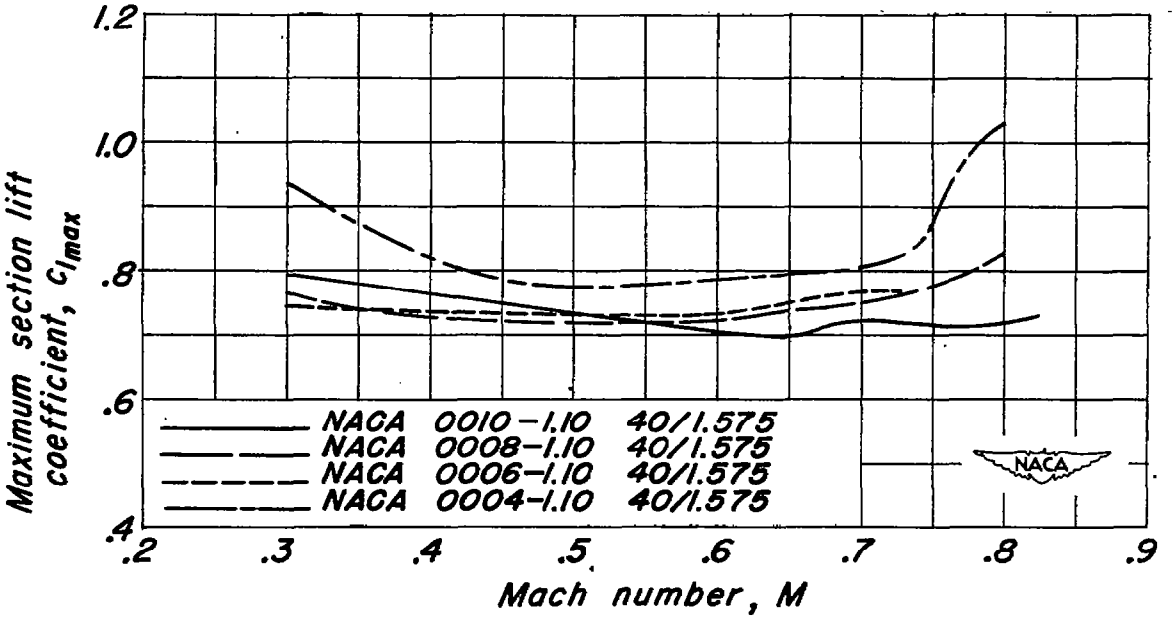

Figure 12.- Effect of change of maximum thickness-chord ratio on the variation of maximum section lift coefficient with Mach number.

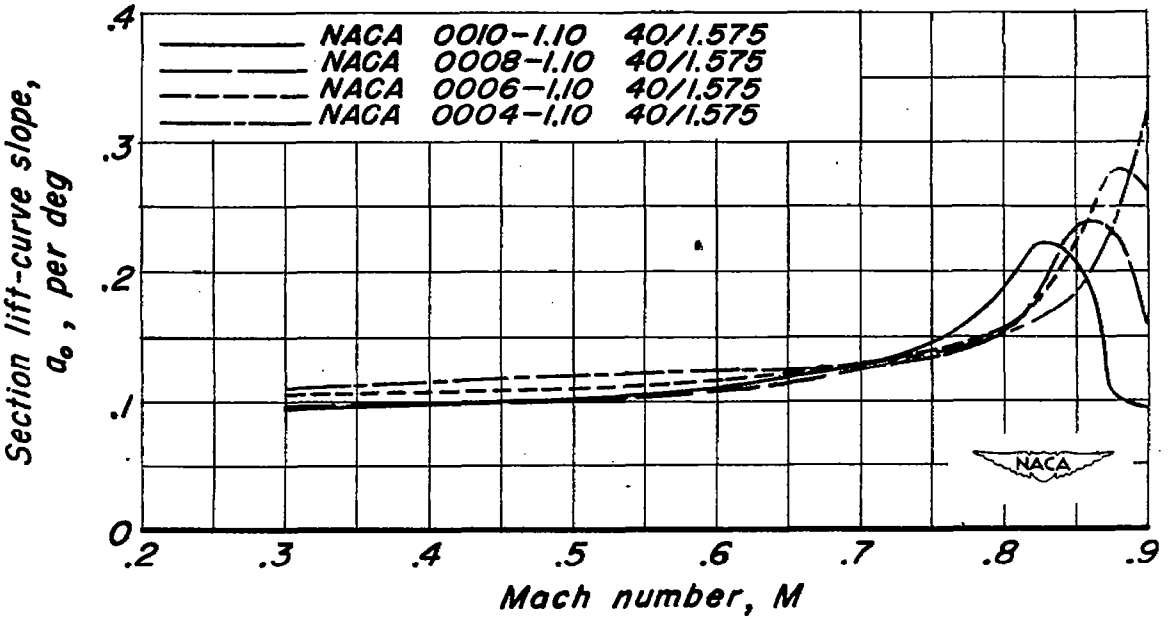

Figure 13.- Effect of change of maximum thickness-chord ratio on the variation of section lift-curve slope with Mach number.

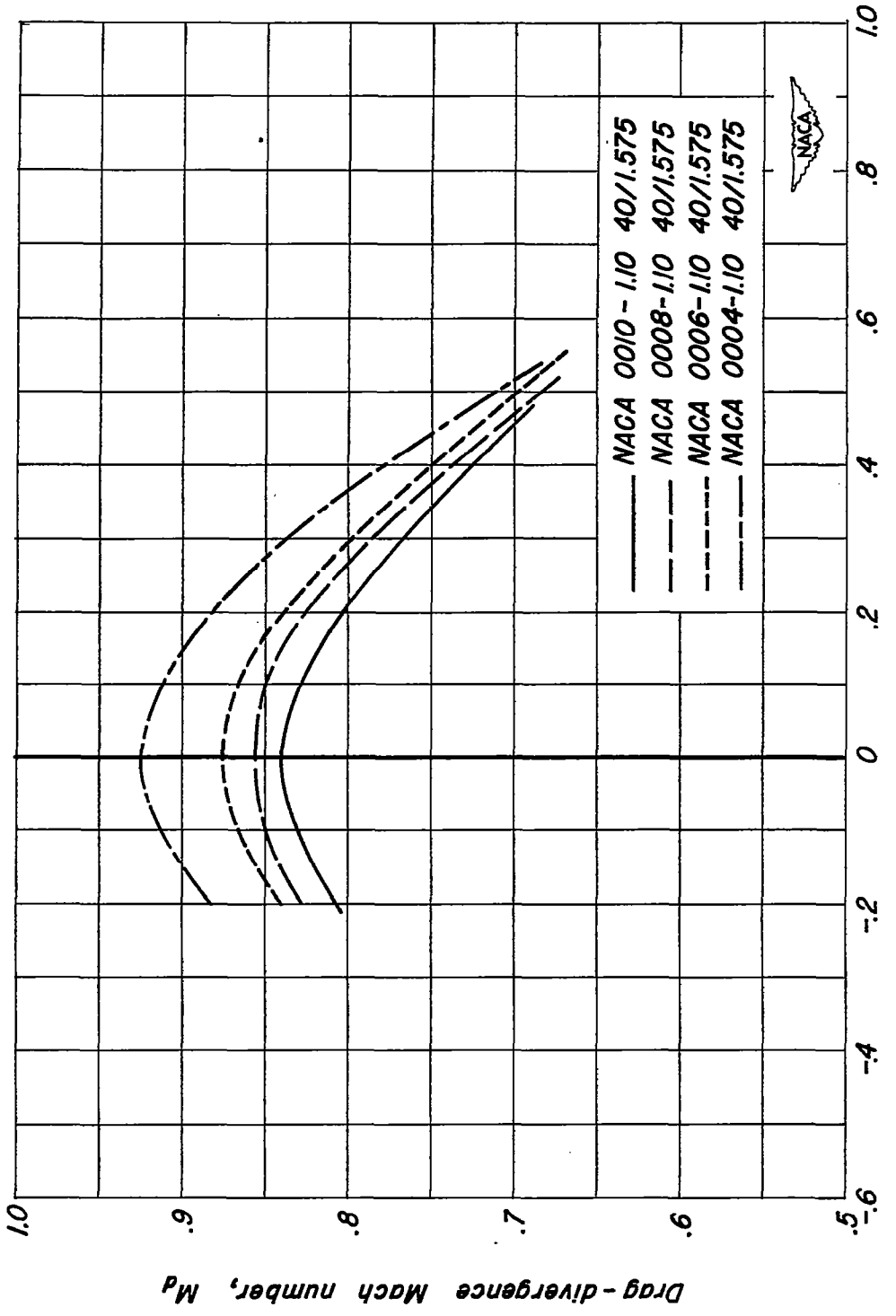

Figure 14.- Effect of change of maximum thickness-chord ratio on the variation of drag-divergence Mach number with section lift coefficient.